IMPACT OF PROCESS CONDITIONS ON METHANE PRODUCTION IN ANAEROBIC DIGESTION AND MICROBIAL ELECTROLYSIS CELL (AD-MEC) INTEGRATED SYSTEMS

A THESIS SUBMITTED TO
THE GRADUATE SCHOOL OF NATURAL AND APPLIED SCIENCES
OF
MIDDLE EAST TECHNICAL UNIVERSITY

BY

MERT ŞANLI

IN PARTIAL FULFILLMENT OF THE REQUIREMENTS
FOR
THE DEGREE OF MASTER OF SCIENCE
IN
ENVIRONMENTAL ENGINEERING

NOVEMBER 2022

Approval of the thesis:

IMPACT OF PROCESS CONDITIONS ON METHANE PRODUCTION IN ANAEROBIC DIGESTION AND MICROBIAL ELECTROLYSIS CELL (AD-MEC) INTEGRATED SYSTEMS

submitted by **MERT ŞANLI** in partial fulfillment of the requirements for the degree of **Master of Science** i**n Environmental Engineering, Middle East Technical University** by,

Prof. Dr. Halil Kalıpçılar
Dean, Graduate School of **Natural and Applied Sciences** _____

Prof. Dr. Bülent İçgen
Head of the Department, **Environmental Engineering** _____

Assist. Prof. Dr. Yasemin Dilşad Yılmazel Tokel
Supervisor, **Environmental Engineering, METU** _____

Examining Committee Members:

Prof. Dr. İpek İmamoğlu
Environmental Engineering, METU _____

Assist. Prof. Dr. Yasemin Dilşad Yılmazel Tokel
Environmental Engineering, METU _____

Prof. Dr. Bülent İçgen
Environmental Engineering, METU _____

Prof. Dr. Tuba Hande Ergüder Bayramoğlu
Environmental Engineering, METU _____

Assist. Prof. Dr. Bilgin Taşkın
Agricultural Biotechnology, Van Yüzüncü Yıl Üni.. _____

Date: 28.11.2022

I hereby declare that all information in this document has been obtained and presented in accordance with academic rules and ethical conduct. I also declare that, as required by these rules and conduct, I have fully cited and referenced all material and results that are not original to this work.

Name Last name: Mert Şanlı

Signature:

ABSTRACT

IMPACT OF PROCESS CONDITIONS ON METHANE PRODUCTION IN ANAEROBIC DIGESTION AND MICROBIAL ELECTROLYSIS CELL (AD-MEC) INTEGRATED SYSTEMS

Şanlı, Mert
Master of Science, Environmental Engineering
Supervisor: Assoc. Dr. Yasemin Dilşad Yılmazel Tokel

November 2022, 133 pages

Anaerobic digestion (AD) is a common method used for treatment of complex wastes with additional benefit of biogas production. Yet, the process has several limitations such as slow kinetics, long start-up periods and low methane (CH_4) production yield. With the integration of microbial electrolysis cells (MECs) into AD, it is anticipated that these limitations of AD will be reduced. The reasons of such improvements in the AD-MEC integrated systems may stem from the enhanced electron transfer in microbial consortium involved in AD and promotion of an additional methane production pathway. In this study, important process conditions of the AD-MEC integrated system were tested on two different experimental sets. Firstly, the impact of external voltage on methane production performance of two different complex wastes, namely cattle manure (C) and wastewater biosolids (WBS) were studied in batch AD-MEC reactors. The wastes were provided in four different mixtures (based on COD) as 100C:0WBS, 70C:30WBS, 30C:70WBS and 0C:100WBS and three different voltages of 0.3 V, 0.7 V and 0.9 V were tested in AD-MECs. Results showed that, there was not a significant impact of applied voltage on methane production in the WBS reactors, yet, in C added reactors applied voltage showed a significant enhancement. Among C dominant reactors the highest improvement was

recorded at 0.9 V application. Net methane yield of 100C:0WBS reactors at an applied voltage of 0.9 V were 128.3 mL CH_4/g volatile solids (VS) added which corresponds to a 70% increase in comparison to the conventional AD reactors (75.5 mL CH_4/g VS_{added}) operated as control. The highest improvement at around 40% were attained with 0.3 V application in WBS added reactors. Yet, this increase may not be linked to a bioelectrochemical process based on significantly low current production in these reactors. Further, the impact of using biofilm attached electrodes, *i.e.* bioelectrodes were assessed in a sequential experimental part. The results showed that using bioelectrodes from the first part, increased the maximum methane potential and methane production rate based on Gompertz fitting to the cumulative methane production data. In the second experimental set of this thesis, the impact of autoclave pretreatment and application of lower voltages in the range of 0.3 – 0.7 V were tested on the anaerobic treatability of WBS in AD-MEC systems. AD-MEC integrated systems showed similar performance enhancement compared to corresponding AD controls, regardless of the feed pretreatment. Additionally, the impact of using bioelectrodes were investigated and experiments were designed to compare methane production performance of bioelectrode and bare electrode AD-MECs, yet no significant difference was recorded in the case of WBS feed.

Keywords: microbial electrolysis cell, AD-MEC, methane, cattle manure, wastewater biosolids

ÖZ

ANAEROBİK ÇÜRÜTME VE MİKROBİAL ELEKTROLİZ HÜCRE (AÇ-MEH) ENTEGRE SİSTEMLERİNDE PROSES KOŞULLARININ METAN ÜRETİMİ ÜZERİNE ETKİSİ

Şanlı, Mert
Yüksek Lisans, Çevre Mühendisliği
Tez Yöneticisi: Dr. Öğr. Üyesi Yasemin Dilşad Yılmazel Tokel

Kasım 2022, 133 sayfa

Anaerobik çürütme (AÇ), biyogaz üretimine ek olarak kompleks atıkların arıtılması için kullanılan yaygın bir yöntemdir. Bununla birlikte, AÇ prosesinin yavaş kinetiği, uzun başlama süresi ve düşük metan (CH_4) üretim verimi gibi çeşitli sınırlamaları vardır. Mikrobiyal elektroliz hücrelerinin (MEH'ler) AÇ'ye entegrasyonu ile AÇ'nin bu sınırlamalarının azaltılacağı öngörülmektedir. AÇ-MEH entegre sistemlerinin performans iyileştirmesinin nedeni, AÇ'de yer alan mikrobiyal konsorsiyumdaki hızlanmış elektron transferinden ve ek bir metan üretim yolağının teşvik edilmesinden kaynaklanmaktadır. Bu çalışmada, AÇ-MEH entegre sistemine etki eden önemli proses koşulları iki farklı deney seti ile test edilmiştir. İlk olarak, harici voltajın iki farklı kompleks atığın, yani sığır gübresi (SG) ve atıksu arıtma çamuru (ATÇ) metan üretim performansına etkisi kesikli AÇ-MEH reaktörleri kurularak incelenmiştir. Atıklar 100SG:0ATÇ, 70SG:30ATÇ, 30SG:70ATÇ ve 0SG:100ATÇ olmak üzere dört farklı karışımda (KOİ bazında) reaktörlere beslenmiş ve AÇ-MEH'lerde 0,3 V, 0,7 V ve 0,9 V olmak üzere üç farklı voltaj test edilmiştir. Sonuçlar, ATÇ reaktörlerinde uygulanan voltajın metan üretimi üzerinde önemli bir etkisi olmadığını, ancak SG katkılı reaktörlerde uygulanan voltajın önemli bir artış gösterdiğini ortaya koymuştur. SG baskın reaktörler arasında en yüksek artış 0,9 V

uygulamasında kaydedilmiştir. Uygulanan 0,9 V voltajda 100SG:0ATÇ reaktörlerinin net metan verimi 128,3 mL CH_4/g $UKM_{eklenen}$ olup, bu değer kontrol olarak işletilen geleneksel AÇ reaktörlerine (75,5 mL CH_4/g $UKM_{eklenen}$) kıyasla %70'lik bir artışa karşılık gelmektedir. ATÇ eklenmiş reaktörlerde yaklaşık %40'lık oranda artış ile en yüksek iyileşme 0,3 V uygulaması ile elde edilmiştir. Ancak bu artış, bu reaktörlerdeki önemli ölçüde düşük akım üretimi ile birlikte değerlendirildiğinde bir biyoelektrokimyasal süreçle bağlantılı olmayabilir. Ayrıca, üzerinde biyofilm oluşmuş elektrotlar, yani biyoelektrotları kullanmanın etkisi ilk deneyleri takip eden farklı bir deneysel çalışma ile incelenmiştir. Deneysel Set 1 çalışma sonuçlarına göre, SG baskın reaktörlerde biyoelektrotların kullanılmasının, kümülatif metan üretim verilerine Gompertz modeline uyarlanmasıyla elde edilen maksimum metan potansiyelini ve metan üretim oranını artırdığını göstermiştir. Bu tezin ikinci deney setinde, otoklav ön işleminin ve 0,3 - 0,7 V aralığında değiştirilen daha düşük harici voltaj uygulanmasının AÇ-MEH sistemlerinde ATÇ'nin anaerobik arıtılabilirliği üzerindeki etkisi test edilmiştir. AÇ-MEH entegre sistemleri, ATÇ beslendiğinde atığın ön işleminden bağımsız olarak, ilgili AÇ kontrollerine kıyasla benzer performans artışı göstermiştir. Ayrıca, biyoelektrot kullanımının etkisi araştırılmış ve biyoelektrot ve bakir elektrot AÇ-MEH'lerin metan üretim performansını karşılaştırmak için deneyler tasarlanmıştır, ancak biyoelektrot kullanımının reaktörlerin ATÇ ile beslenmesi durumunda önemli bir fayda sağlamamıştır.

Anahtar Kelimeler: mikrobiyal elektroliz hücresi, AÇ-MEH, metan, sığır gübresi, atıksu arıtma çamuru

Dedication

To my family..

ACKNOWLEDGMENTS

Firstly, I wish to express my sincere gratitude to my supervisor Assist. Prof. Dr. Yasemin Dilşad Yılmazel Tokel for her guidance and everlasting support through the research. I would like to thank Examining Committee Members for their comments to this thesis. I also gratefully acknowledge the financial support provided to this research by the; Scientific and Technological Research Council of Turkey (TÜBİTAK) grant number 218M854. I would like to express my gratefulness to Prof. Dr. Bülent İçgen and Prof. Dr. İpek İmamoğlu for allowing me to use the facilities of their laboratories.

I am deeply indebted to the members of our research group BIOERG; Amin Ghaderi Kia, Ece Kutlar, Aykut Kaş, Berivan Tunca and Yasin Odabaş, for their comments, friendship and support. I want to exclusively thank my parents and my brother who have supported me throughout this journey.

TABLE OF CONTENTS

LIST OF TABLES

TABLES

LIST OF FIGURES

FIGURES

LIST OF ABBREVIATIONS

ABBREVIATIONS

AD: Anaerobic digestion

BES: Bioelectrochemical system

C: Cattle manure

CO_2 : Carbon dioxide

COD: Chemical oxygen demand

CoV: Coefficient of variation

CV: Cyclic voltammetry

DIET: Direct interspecies electron transfer

GC: Gas chromatography

MEC: Microbial electrolysis cell

MET: Mediated electron transfer

MFC: Microbial fuel cell

N_2: Nitrogen

NHE: Normal Hydrogen Electrode

OC: Open circuit

PS: Primary sludge

PBS: Phosphate buffer saline

SHE: Standard hydrogen electrode

SS: Stainless steel

sCOD: Soluble chemical oxygen demand

T: Temperature

TCD: Thermal conductivity detector

TKN: Total Kjeldahl nitrogen

TP: Total Phosphorous

TS: Total solids

VFA: Volatile fatty acids

VS: Volatile solids

WAS: Waste activated sludge

WBS: Wastewater biosolids

WW: Wastewater

CHAPTER 1

INTRODUCTION

1.1 Background Information

Rapidly rising energy needs throughout the world are depleting fossil fuel reserves at an enormous rate. As a result, experts all around the world have been attempting to develop alternative energy sources that have a low environmental impact. The biological synthesis of biogas from waste organic matter by anaerobic digestion (AD) is widely regarded as a promising technology for generating sustainable energy, which may be produced from a variety of industrial and agricultural feedstocks (Baek et al., 2020). Biogas that is generated via AD process typically contains 55-75 % methane (CH_4) and 45-25 % carbon dioxide (CO_2) and because of its high methane content, it is a valuable fuel that can be converted to power and used for heating purposes (Gray, 2004). However, there are some drawbacks of AD such as limited waste processing capacity, low methane production yield, long start-up times and low process stability (Bao et al., 2020; Kargi et al., 2011)

Bioelectrochemical systems (BES) are emerging energy efficient technologies that are used for energy generation from organic wastes, that can be combined with conventional waste to energy systems. A novel bioelectrochemical reactor known as microbial electrolysis cell (MEC) has been designed as a potentially efficient technique to support energy production from a wide spectrum of organics. In an MEC, in the anode compartment organic matter is oxidized by microorganisms, named exoelectrogens, and hydrogen is reduced on the surface of an abiotic cathode. For hydrogen production in an MEC a low external applied voltage (E_{app} = 0.114 V in theory) must be applied to the cell. However, because of the losses in the system, in practice higher voltages are required (typically $E_{app} > 0.5$ V) (Call & Logan, 2008). Nonetheless, because microbial activity is involved and microorganisms serve as

catalysts, the required external electrical input is much lower than the external voltage input necessary for water electrolysis (1.8–2.0 V), which is currently used for large scale hydrogen production. Therefore, MECs offer a sustainable way for efficiently generating hydrogen from renewable biomass (Wagner et al., 2009). This process of hydrogen production is known as electrohydrogenesis. However it should be noted that in most MEC systems, hydrogen production is accompanied with unintentional cathode-induced methane generation, due to the presence of methane-producing microorganisms (J. Liu et al., 2016; Rozendal et al., 2006; Wagner et al., 2009). Single-chamber MECs that are used for electrohydrogenesis, later appears to have given a possibility to accelerate the development of hydrogenotropic methanogens on the cathode, where they convert the abiotically produced hydrogen to methane (Villano et al., 2010). Along with hydrogenotrophic methanogens, there are also other electrotrophic microorganisms that colonize on the cathode and reduce carbon dioxide to methane via direct electron transfer (Villano et al., 2010).

This process of methane production in MECs is named as electromethanogenesis and it was first studied in Penn State University laboratories (Cheng et al., 2009a). In an MEC, methane production can take place in two ways: (i) indirectly through the production of intermediates such as hydrogen, formate, and acetate, which are then consumed by methanogens, (ii) directly via the activity of electrotrophic methanogens, which take up electrons directly from the cathode and reduce carbon dioxide to methane (Blasco-Gómez et al., 2017; Cheng et al., 2009a). Both processes need an external voltage addition. Methane formation through an intermediate is common to AD process. Yet, because electrotrophic methane synthesis offers as an additional route, the combination of MEC and AD may increase methane output, while simultaneously increasing the speed of the organic matter breakdown (Guo et al., 2013). Further, the integration of MEC to AD may rapidly reduce inhibitory factors while maintaining the system's anaerobic state. Removal of metal ions from various substrates along with electrochemical effect has also been reported in the literature. (Luo et al., 2014; Nancharaiah et al., 2015).

In AD process different types of wastes can be processed. For example, wastewater sludge, agro-industrial wastes such as animal manure and food wastes are among the most common feeds of AD process. Several studies compared the performances of conventional AD to AD-MEC integrated systems and most of them used wastewater sludge as feed. For example, in a recent study where wastewater sludge was used as a feed, methane production rate in the AD-MEC system (0.15 m^3 CH_4/m^3 reactor/d) was reported as three times higher than conventional AD reactor (0.05 m^3 CH_4/m^3 reactor/d) (Bao et al., 2020). Additionally in the same study, AD-MEC reactor around 29% higher COD removal was achieved (Bao et al., 2020). Similarly, in another work with AD-MEC integrated system around three times higher methane production rate (138 mL CH_4/L reactor/day) in comparison to control reactor (46 mL CH_4/L reactor/day) was recorded with waste activated sludge feed (W. Liu et al., 2016). Additional to the waste sludge, animal wastes are generated in huge quantities and can be used as feedstock in AD processes, because of their high organic content. In the literature, there is a limited number of studies, which investigates the integration of AD and MEC systems for enhanced biogas production from animal wastes such as cattle manure (Hassanein et al., 2020; Tartakovsky et al., 2014). In their study, Hassanein (2020) investigated the impact of using AD-MEC integrated system for methane production from dairy manure. Results showed that, integrated system increased the biogas production by 137% in comparison to the conventional AD (Hassanein et al., 2020).

Although various studies have showed increased methane generation in AD-MEC systems, there has been limited investigation of AD-MEC systems for co-digestion of complex wastes under a variety of applied potentials. Also, it is still unclear how the external voltage and electrode materials influences methane generation. Therefore, in this thesis the impact of different process conditions on the methane production performance of different complex wastes will be investigated in AD-MEC integrated systems.

1.2 Aim of the Study

Aim of this thesis study is to investigate the effects of process conditions, such as applied voltage, electrode material and substrate type on the performance of AD-MEC integrated systems. It is anticipated that waste organic matters will be utilized more in the eventual scaling-up and widespread application of BESs (Logan & Rabaey, 2012), as compared to simple substrates that are often used in laboratory research. This is simply because waste organic matters are abundant, inexpensive and pose a threat to environment if not managed properly. To this purpose, in this thesis two different complex wastes, namely cattle manure (C) and wastewater biosolids (WBS) were used as feed to AD-MEC reactors and. In total two different experimental sets were designed. In the first set, a mixture of the two feeds at varying ratios were used as feed, and based on the results of the first set, a second set of experiments were conducted to further study the WBS feed.

1.2.1 Specific Objectives and Scope of Experimental Set 1

The objective of the first experimental set (Set 1) was to investigate the impact of external voltage on the methane production performance of AD-MEC systems, where co-digestion of C and WBS (a mixture of primary sludge (PS) and waste activated sludge (WAS) taken from a municipal wastewater plant) was taking place. To this purpose, in the experimental design, three external voltages (0.3 V, 0.7 V and 0.9 V) and varying substrate mixing ratios of C and WBS were adjusted in single chamber AD-MEC reactors. The set consisted of AD-MEC reactors with different C to WBS mixing ratios (on COD basis) of 100C:0WBS, 70C:30WBS, 30C:70WBS and 0C:100WBS. Following the first run, a second experimental run was conducted to determine the impact of using pre-colonized electrodes, named as bioelectrodes, collected from the first run, in new AD-MEC reactors to determine the effect of bioelectrodes on methane generation.

1.2.2 Specific Objectives and Scope of Experimental Set 2

The objective of second experimental set (Set 2) was to investigate the impacts of feed pretreatment and bioelectrodes on methane generation from WBS in AD-MEC systems. In this set, the focus was solely on WBS digestion because in the AD-MEC systems of Set 1 in comparison to C relatively low enhancement in WBS digestion was observed. Therefore, to further investigate the utilization of WBS in AD-MEC systems, a number of AD-MEC reactors were operated under different conditions: with bare electrodes and bioelectrodes, with different applied voltages of (0.3, 0.5 and 0.7 V) and in the presence and absence of autoclave pretreatment of the WBS.

CHAPTER 2

LITERATURE REVIEW

2.1 Anaerobic Digestion

Anerobic digestion (AD) is the degradation of organic matters facilitated by microorganisms in oxygen-free environment. Hydrolysis, acidogenesis, acetogenesis, and methanogenesis are the four primary processes that are involved in conventional AD which is a method that was designed for the purpose of treating waste (Z. Yu et al., 2018). It is a multi-stage process that involves the interdependencies and interrelationships of numerous microbial consortiums with one another (Angelidaki et al., 2011). This process takes place in the absence of oxygen. In the process of AD, a wide variety of bacteria work together to reproduce and gather energy for metabolic processes by decomposing organic compounds in the absence of oxygen. At the conclusion of the anaerobic process, biogas is created as a result of the actions described.

The four stages of anaerobic digestion are broken down into their essential components and summarized in Figure 2.1. During the process of AD, each phase is carried out by a distinct type of microbial consortium under very particular environmental circumstances. These groups of microorganisms cooperate to achieve their goals. The kinetics of individual processes are nonlinear with respect to the concentration of substrates and inhibitors; nonetheless, the processes that are most likely to be rate-limiting are hydrolysis and aceticlastic methanogenesis, depending on the specific conditions (Angelidaki et al., 2011). Nonlinear kinetics can cause the fermentation of complex organics to produce intermediates (mostly short-chain fatty acids) that build up in the digester and cause process instability and decreased methane output (Zakaria & Dhar, 2019). The final result of a complex organic matter has the potential to become a new substrate for the subsequent consortium in the

food chain. Certain bacteria are unable to breakdown substrates in the absence of their symbiotic partners and need their presence.

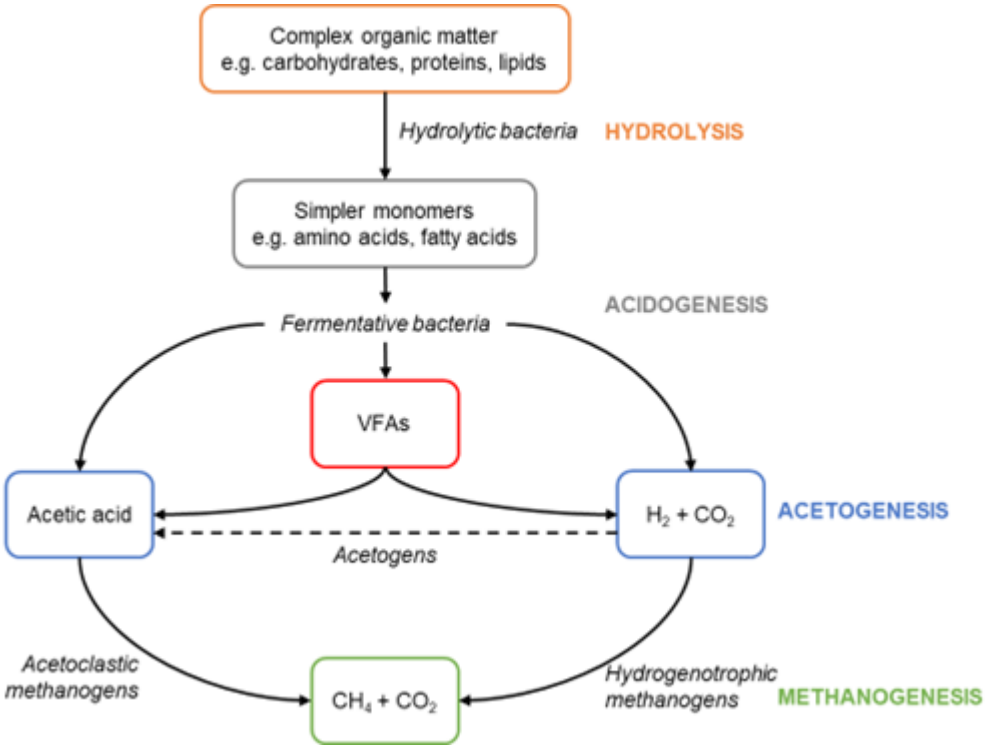

Figure 2.1 Stages of conventional AD

The use of AD to degrade organic pollutants and create biogas has achieved a great deal of success, but it still has limits, such as instability, poor decomposition of substrates, and limited biogas generation.

2.1.1 Hydrolysis

The initial and typically the rate-limiting stage in AD is hydrolysis (Kamusoko et al., 2022). Hydrolytic bacteria release extracellular enzymes (cellulases, lipases, proteases, and amylases) that breakdown complex organic polymers such as lipids, carbohydrates, proteins into long-chain fatty acids, simple sugars, and amino acids (Jain et al.,2015; Nagarajan et al.,2022). Equation (2.1) depicts the total reaction associated with the hydrolysis stage (Anukam et al., 2019).

$$(C_6H_{10}O_5)n + nH_2O \rightarrow n(C_6H_{12}O_6) + nH_2 \quad \text{(Eq. 2.1)}$$

2.1.2 Acidogenesis

Acidogenesis is the step of fermentation in which the products of hydrolysis (soluble organic monomers of sugars and amino acids) are degraded by acidogenic bacteria to create alcohols, aldehydes, volatile fatty acids (VFAs), and acetate, along with H_2 and CO_2 (Kamusoko et al., 2022). Acetic acid (CH_3COOH) is the most major organic acid used as a substrate by CH_4 forming microorganisms and is thus the most important acid at this stage. The majority of acidogenesis happens via the acetic acid pathway (Eq 2.2) and the butyric acid (C_3H_7COOH) pathway (Eq 2.4), as hydrogen being the end-product of this process. Propionic acid (CH_3CH_2COOH), on the other hand, is a further prevalent VFA that is created in the AD of organic wastes, and this process is one that consumes hydrogen (2.3) (Kamusoko et al., 2022).

$$C_6H_{12}O_6 + 2H_2O \rightarrow 2CH_3COOH + 4H_2 + 2CO_2 \quad \text{(Eq. 2.2)}$$

$$C_6H_{12}O_6 + 2H_2O \rightarrow 2CH_3CH_2COOH + 2H_2O \quad \text{(Eq. 2.3)}$$

$$C_6H_{12}O_6 + 2H_2O \rightarrow C_3H_7COOH + 2H_2O + 2CO_2 \quad \text{(Eq. 2.4)}$$

The generation of acetic acid is the preferred growth pathway for acetogenic bacteria because it offers the greatest potential energy yield for the growth.

2.1.3 Acetogenesis

Before being turned into biogas for good, the products of acidogenesis go through a few further transformations. These include acetogenesis and dehydrogenation. The byproducts of acidification and the leftovers of hydrolysis are used in the acetogenesis process, which results in the formation of acetic acid, carbon dioxide, and hydrogen. The acetate that is produced by acetogenic bacteria may either be directly consumed by aceticlastic methanogens, or it can be destroyed by syntrophic

associations of bacteria (syntrophic acetate oxidizers) and hydrogen-consuming methanogenic archaea (Angelidaki et al., 2011).

2.1.4 Methanogenesis

The AD process comes to a close with the methanogenesis stage, which is the fourth and final step. At this step, archaea convert CH_3COOH and H_2 into CO_2 and CH_4; the archaea that are responsible for this conversion often referred as methanogens, and they are strictly anaerobes that are extremely sensitive to even trace levels of oxygen. The acetoclastic methanogens consume acetic acid to produce CH_4 and CO_2 (Eq 2.5), whereas the hydrogenotrophic methanogens use CO_2 and H_2 to produce CH_4 and H_2O (Eq 2.6).

$$CH_3COOH \rightarrow CH_4 + CO_2 \quad \text{(Eq. 2.5)}$$

$$CO_2 + 4H_2 \rightarrow CH_4 + 2H_2O \quad \text{(Eq. 2.6)}$$

In most cases, acetoclastic and hydrogenotrophic methanogens may be found coexisting in AD populations. (Kirkegaard et al., 2017). Because of their sluggish growth rate and severe sensitivity to environmental changes, the methanogens play an incredibly significant role in the AD processes (Anukam et al., 2019). Because methanogenic archaea are particularly sensitive to a decrease in pH, which might create a buildup of volatile fatty acids leading to fast acidification, the rate of methanogenesis is the stage in the AD that is the rate limiting step (Arelli et al., 2022).

2.2 Bioelectrochemical Systems (BESs)

Over the course of the past three decades, the world has witnessed a massive extension of evolution with the goal of enhancing the well-being of humans at the expense of the natural environment. As a result, a large number of researchers and experts carry out millions of studies each year in an effort to reduce environmental

harm and boost environmental adaptability (Dattatraya Saratale et al., 2022). With increased industrialization, population growth, and economic expansion, 85 percent of the world's energy demand is met by fossil fuels (Raj et al., 2022). BESs, are a potential hybrid approach that can simultaneously overcome several obstacles to human-environment compatibility. This is accomplished through the production of energy and valuable chemicals, as well as the degradation of organic and inorganic substrates (Kokko et al., 2018; W. Wang et al., 2022). BESs make use of electro-active microorganisms, which are organisms that are capable of participating in the redox processes that take place between chemicals and conducting electron transfer to and from an electrode (Logan et al., 2019).

Dependent on the aim, BESs differ one from another greatly in reactor configurations, utilized substrates, bacterial communities present in the reactor, etc. Despite the differences, BESs can be divided into 2 mainly according to their application, all the other versions are came out as modifications to these 2 main types (Figure 2.2) as Microbial Fuel cells (MFC), Microbial Electrolysis Cells (MEC).

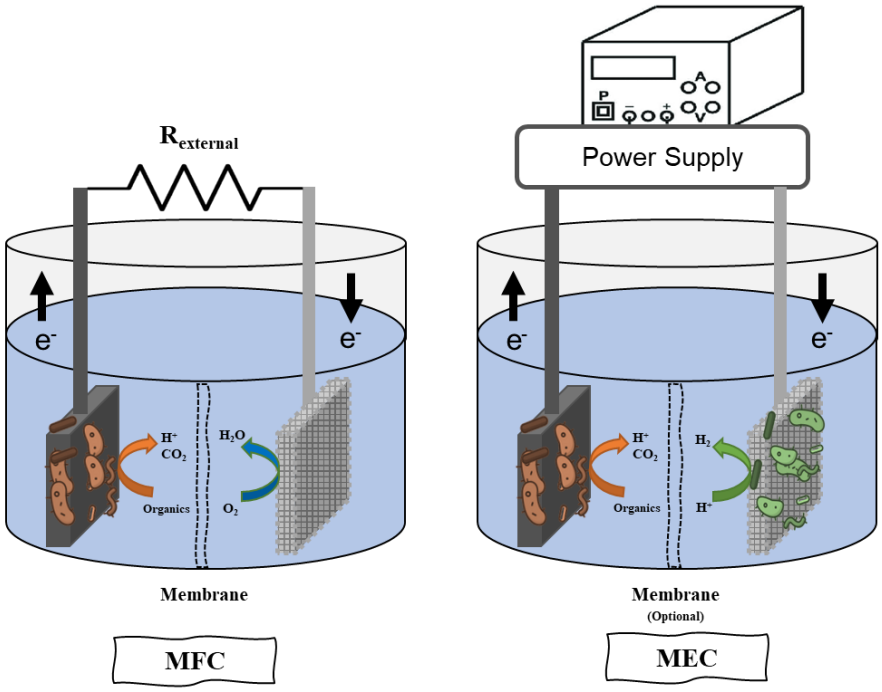

Figure 2.2 Schemes of different MFC and MEC systems

2.2.1 Microbial Fuel Cells (MFCs)

MFCs are developed to generate electricity from the process of degradation of organic materials in the system. Exoelectrogenic microorganisms may oxidize either organic or inorganic materials, and MFCs make use of these organisms. During this oxidation process, electrons are transferred from the anode to the cathode via conductive wire. The electrons are donated to the anode by exoelectrogens. When a resistor is connected to this conductive wiring in the series configuration, an electric current will be generated (Logan et al., 2006). Since MFCs convert organic substances directly into electricity using oxygen as the terminal electron acceptor at the cathode chamber, they are predicted to offer better conversion efficiency compared to conventional bioconversion techniques. Cation exchange membranes, also known as CEMs, are often installed in the middle of double chamber fuel cells (also known as H-Cells) during the manufacturing process. This membrane stops oxygen from escaping into the anode chamber while allowing protons to travel into

the cathode chamber, where they combine with oxygen to form water. The anode chamber remains oxygen-free as a result (Logan et al., 2006).

2.2.2 Microbial Electrolysis Cells (MECs)

Microbial Electrolysis Cells, also known as MECs, are modified versions of MFCs that are used to produce hydrogen gas (Logan et al., 2008). In MECs, neither compartment contains oxygen, which allows anaerobic microorganisms to thrive and proliferate. The production of biofuels, either in the form of hydrogen gas or methane gas, is the primary objective of MECs (Figure 2.3).

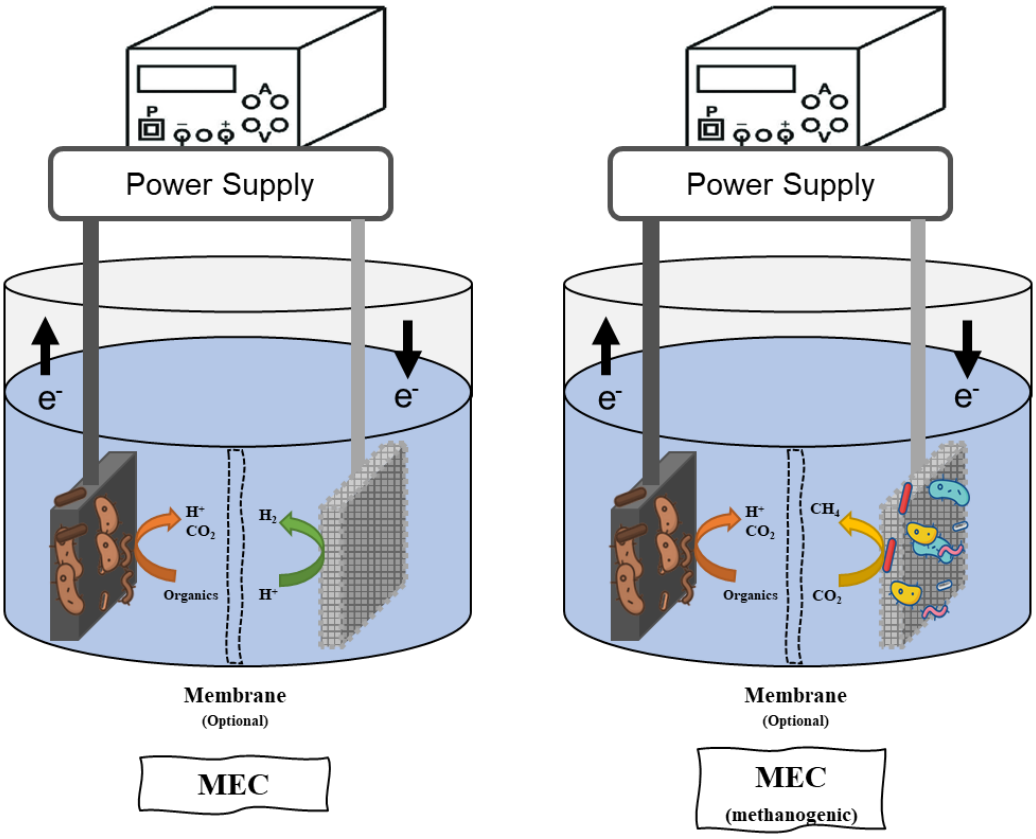

Figure 2.3 Hydrogen producing MEC and mehtanogenic MEC

2.2.2.1 Methane production in MECs: Electromethanogenesis

Methane production at the cathode can occur by two different electrochemical mechanisms. These mechanisms are not thermodynamically favorable and require some energy to drive the reaction. The energy needed (given as Normal depends on the pathway in which methane production occurs. In the direct electron transfer pathway, electrotrophic methanogens on the cathode surface directly utilize the electrons and protons and reduce the carbon dioxide (Eq 2.7) (Cheng et al., 2009; Villano et al., 2010).

$CO_2 + 8H^+ + 8e^- \rightarrow CH_4 + 2H_2O$ (E_{cat}=-0.24V vs. Normal Hydrogen Electrode (NHE)) Eq (2.7)

The other path is indirect electron transfer, in which hydrogen evolution happens on the cathode (Eq 2.8) then hydrogenotrophic methanogens utilize the produced hydrogen and convert it to the methane shown on Eq 2.9 (Cheng et al., 2009).

$(2H^+ + 2e^- \rightarrow H_2)$ (E_{cat} =-0.41V vs.NHE) Eq (2.8)

$(CO_2 + 4H_2 \rightarrow CH_4 + H_2O)$ Eq (2.9)

When the energy necessary to drive the reactions is compared, methane generation via direct electron transfer is more energy-efficient since the energy required for the hydrogen evolution process has a lower potential (E_{cat} = -0.41V vs. NHE). In the cathode chamber of a MEC, the suggested paths for the formation of methane are depicted in Figure 2.4.

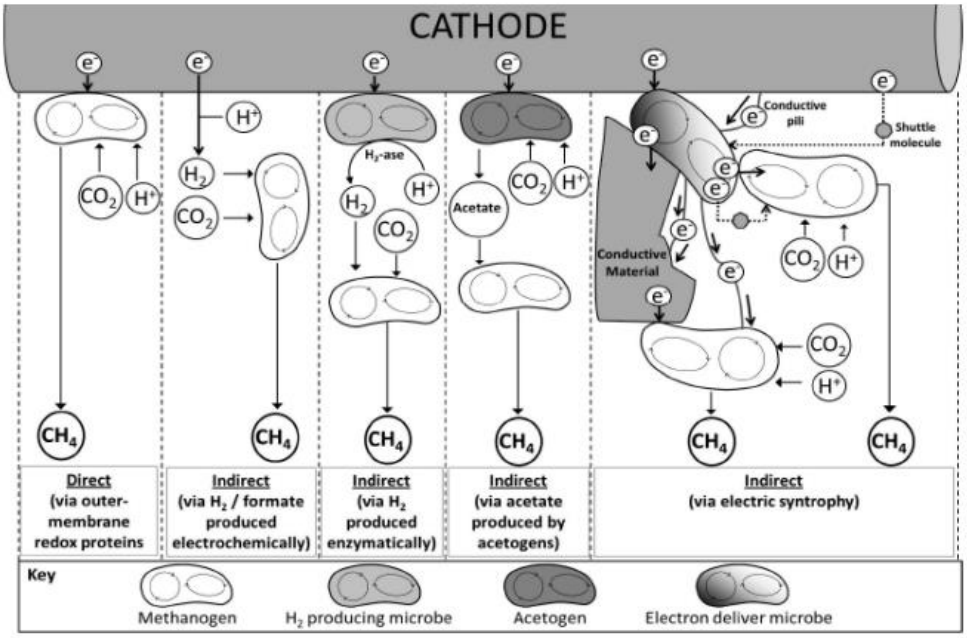

Figure 2.4 Electron transfer mechanisms within cathode (Blasco-Gómez et al., 2017)

2.3 AD-MEC coupled systems

Despite bottlenecks such as long start-up periods, decreased methane concentrations, and vulnerability to environmental change, AD has been the primary technique for bioenergy generation till now. The possibility of methane production in MECs with waste/wastewater treatment was originally brought up by preliminary studies (Cheng et al., 2009a; Clauwaert et al., 2008).Since the electrotrophic methane production is involved as an additional pathway, the combination of MEC and AD can boost methane generation while also speeding up the organic matter breakdown process (Guo et al., 2013). Simultaneously, the coupling of MEC processes can rapidly reduce inhibitory factors while maintaining the system's anaerobic state. The electrochemical effect can also remove heavy metal toxicity in the systems of different bacteria (Luo et al., 2014; Nancharaiah et al., 2015). The findings of methane production focused MEC research have been demonstrated using a wide range of reactors, operating parameters, and substrates. There were a variety of reactor types employed for MEC technology, including single- and dual-chamber

MECs, combined MEC and AD reactors, and others. These experiments employed a range of applied voltages, from 0.1 V (J. Yu et al., 2019) to 3.5 V (Tartakovsky et al., 2014), to determine the impact of the voltage. The operational parameters are extremely important to the outputs of the processes that are carried out by the integrated AD-MEC systems, and they have a significant impact on those outcomes. In this scenario, the pace, performance, and consequences of the combined AD-MEC process are all determined by the parameters in question.

2.3.1 Reactor Type

In terms of optimization, process performance, and the generation of biogas, reactor types of the MEC systems is very significant. The initial MEC design consisted of two chambers, and one of those chambers was equipped with a proton exchange membrane (PEM). In two chamber MECs, anode and cathode chambers are separated from each other by proton exchange membrane to allow H^+ flow from anode to cathode (Logan et al., 2019). In single chamber MECs, anode and cathode are placed in the same chamber.

2.3.1.1 Double chamber MECs

The anode chamber and the cathode chamber of a two-chamber MEC system are separated from one another by a selective membrane in order to maintain their individual functions (Figure 2.5). Because only certain ions are able to pass through the membrane, the chemical and physical characteristics of the electrolytes in each chamber of a two-chamber MEC can be distinct from one another. These parameters include pH, alkalinity, and the biology of the electrolytes. On the other hand, membranes impose an internal resistance, which might potentially slow down the MEC's pace of methane generation (Kadier et al., 2016; Karthikeyan et al., 2017). Despite the fact that double chamber MECs have a number of benefits, they also have a number of disadvantages, such as increased complexity, increased difficulties

in operations and scale-up issues, increased voltage losses, and an increase in the cost of manufacturing membranes.

Figure 2.5 Double chamber MEC configuration

2.3.1.2 Single chamber MECs

Single chamber MECs were developed both to enhance the generation of biogas and to make the construction of reactors more straightforward. In addition, in contrast to MFCs, MECs operate in an anaerobic environment; hence, splitting the membrane would not result in the introduction of oxygen to the anode and would not have a detrimental impact on the efficiency of MEC. Single-chamber MECs contain a cathode, anode, and a mutual electrolyte between the two electrodes. The removal of the membrane from the MEC reactor reduce the potential loss that takes place as a result of the membrane resistance, which ultimately results in increased current density and an increased rate of biogas production (Logan, 2008). This is just one of the many benefits that can be gained from using a single chamber MEC. Methane is created in the MEC because of the lack of a membrane, and the methanogenic bacteria use the biohydrogen that generated (Zhang & Angelidaki, 2014).

2.3.2 Important Factors of MECs

2.3.2.1 Electrode Material

The electrode offers space for biofilm colonization and acts as a baffle to strengthen the hydrodynamic behavior in reactor, which might influence MEC performance (De Vrieze et al., 2018). Recent research into the influence of electrode materials on AD performance shows that carbon and metals are the most common electrode materials utilized in AD-MEC. Figure 2.6 shows electrodes made of various materials used in our laboratory.

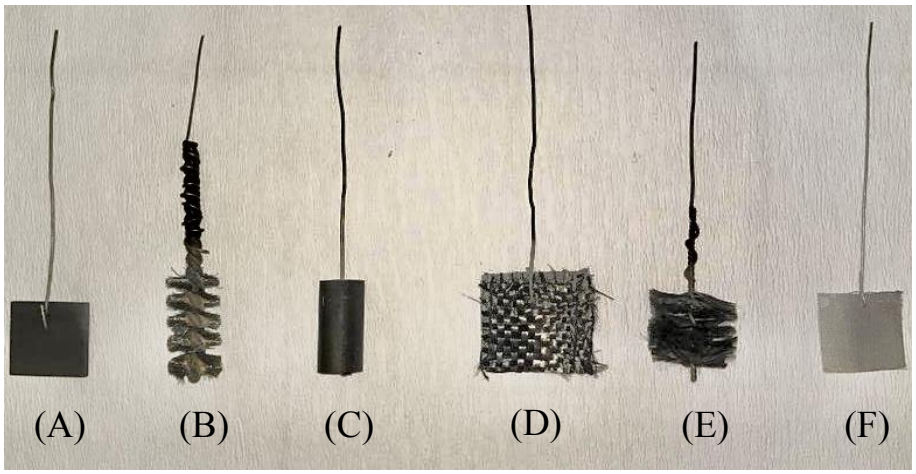

Figure 2.6 Various electrode materials used in MEC reactors (A) Graphite plate, (B) SS Brush, (C) Graphite rod, (D) Carbon cloth, (E) Carbon fiber brush and (F) SS mesh

Anode Materials

The electroactive microorganisms transfer electrons from the anode to the cathode, making the anode a crucial part of the MEC. For a material to be considered as an excellent anode, it has to possess important qualities such as biocompatibility, chemical stability, non-corrosiveness, high conductivity of electricity, low resistance, affordability, and porosity (Bora et al., 2022). In more recently, many

kinds of anode materials have been employed in MECs. Among them, carbon-based anodic materials are the most common form of MEC anode material due to the chemical stability they exhibit under anaerobic anodic circumstances (Escapa et al., 2016; Kadier et al., 2016).

Cathode Materials

In the cathode of MECs, hydrogen gas and a variety of additional compounds with added value are generated. Because it is the location where hydrogen evolution takes place, the cathode material selection is the most important aspect of the MECs. Electrodes serve not just as conductors but also as a habitat for the bacteria that live on them (Zhang & Angelidaki, 2014). An ideal electrode material must be biocompatible, have a high surface area and a rough surface, and transmit electrons effectively between bacteria and electrodes (Wei et al., 2011). As with anodes, cathode electrodes and materials may be made from readily available and inexpensive carbon-based substances. Catalysts are being employed on carbon-based electrodes to speed up the process. Platinum and palladium, because their stability and exquisite catalytic characteristics, are known as the most utilized metals to date. However, nickel, cobalt-molybdenum, stainless steel, and their alloys have been demonstrated to be suitable cathode materials as well. They are convenient to go to, inexpensive, stable, and offer modest upsides (Escapa et al., 2016; Kadier et al., 2016; Bora et al., 2022).

2.3.2.2 Applied Voltage

One of the necessary physical criteria for the operation of the MECs to produce methane is the applied voltage or external voltage. Changes in the applied voltage significantly affect the development and distribution of electroactive organisms, which in turn affects methane production (Ding et al., 2015; Villano et al., 2016). The bulk of previous studies used voltages ranging from 0.3 to 1.8 V, however the proposed voltage varied greatly. It is essential to keep in mind the possibility that the

microorganism may be negatively affected by the high levels of electric potential that have been applied. In the presence of high potentials, Wang and colleagues (K. Wang et al., 2017) found that cell metabolism was reduced, and the cells themselves ruptured. It has been shown via a variety of studies that Gram-positive bacteria are utilized most frequently as electro active organisms in MECs when paired with the anaerobic digestion process in order to produce methane. Because of the thick peptidoglycan cell wall that is characteristic of these organisms, having a three-dimensional structure gives great resistance to external disruptions (Yu et al., 2018). Consequently, in order to obtain a high rate of methane generation, it is necessary to take into consideration the appropriate external voltage, which should be different for each kind of substrate.

2.3.2.3 Substrate Type

Various substrates given as a feed into the system of AD-MEC integrated systems for increased methane generation (Yu et al., 2018). In a simplified way, the substrates used in AD-MEC systems can be divided into two main categories: simple and complex substrates.

Simple Substrates

In the early investigations of MEC, readily available substrates for exoelectrogens such as acetate, glucose, and volatile fatty acids were used. These substrates are also known as fermentation end products. According to the literature review, simple substrates have been used in the early stages of MEC systems, but in general, the use of complex substrates dominates studies in the field (Figure 2.7).

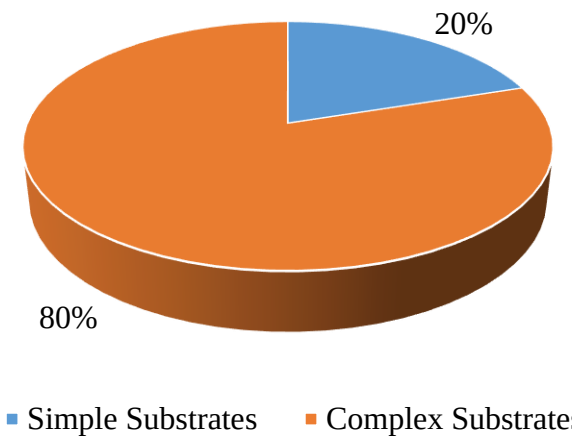

Figure 2.7 Distribution of studies in Table 2.1 and Table 2.2, based on substrate complexity

Table 2.1 lists the simple substrate used studies within information of operating parameters, anode materials, and cathode materials used in the summarized works, as well as the reactor volumes and anode and cathode materials used in their construction. The increases expressed in the Table 2.1 indicate the increase of each set compared to its control reactor.

Table 2.1 Studies focusing on methane production in AD-MECs with simple substrate

Substrate	Reactor Type	Operation	T (°C)	Volume (L)	Applied Voltage (V)	Anode Material	Cathode Material	CH_4 Production	Ref
Acetate	DC	Continuous	22	0.225	0.6	Graphite Granules, Graphite Rod	Graphite woven web with Pt fixed to a graphite rod	0.41 mole CH_4/mole acetate	(Clauwaert et al., 2008)
Acetate	SC	Batch	35	0.27	0.5,1 and 1.5	Carbon brush	Carbon brush	0.351 L CH_4/g COD at 1V	(Flores-Rodriguez et al., 2019)
Acetate	SC	Batch	30	0.13	0.8	Graphite brush	Carbon cloth coated with Pt	84-93 L/m^3/d CH_4	(X. Li et al., 2019)
Acetate	DC	Batch	36	0.6 anode, 0.7 cathode chamber	Cathode potential at -0.8V vs SHE	Carbon felt	Carbon felt coateed with Pt	0.91 m^3 CH_4/m^3 reactor	(Yuan et al., 2020)
Acetate	SC	Continuous	30	2.4	0.9	Preacclimated graphite brushes	SS mesh	0.0118 L CH_4/L/d	(Rader & Logan, 2010)
Acetate	SC	Batch	25	0.23	1	Carbon felt	SS	360.2 mL/g COD	(Q. Yin et al., 2016)
Acetate	DC	Batch	30	0.3 each chamber	Cathode potential between -0.7V and -1.2V vs Ag/AgCl	Graphite fiber brush	Carbon cloth	656 mmol CH_4/d/m^2) at -1.2V set potential	(Cheng et al., 2009)

Substrate	Reactor Type	Operation	T(°C)	Volume (L)	Applied Voltage (V)	Anode Material	Cathode Material	CH_4 Production	Ref
Glucose	SC	Batch	35	0.27	0.5, 0.7, 1 and 1.5	Carbon fiber brush winded with SS wire	Carbon fiber brush winded with SS wire	Cumulative 219 mL CH_4 at 1V	(Choi et al., 2017)
Glucose	SC	Fed-batch	21	0.36	Anode potential -0.4V vs Ag/AgCl	Stainless steel frame with carbon fiber	Stainless steel mesh	179.5 ml CH_4	(Zakaria & Dhar, 2021)

DC: Double chamber; SC: Single Chamber

Complex Substrates

Since wastewater sludge was mainly used in AD systems that is why most of the AD-MEC research was focusing on the wastewater sludge nowadays. In the literature, there is a limited number of studies, which investigates the integration of AD and MEC systems for enhanced biogas production from real wastes such as cattle manure (Hassanein et al., 2020; Tartakovsky et al., 2014) (Figure 2.8).

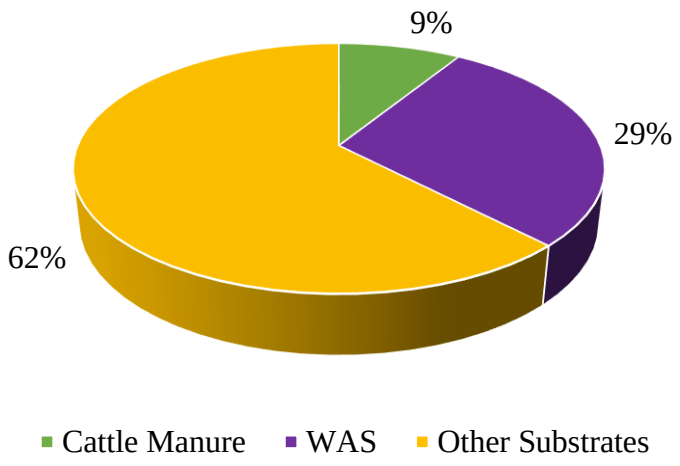

Figure 2.8 Feed distribution among the studies summarized in Table 2.2

The vast majority of studies on AD-MEC use complex substrates. Table 2.2 shows the studies using various waste types (complex substrates) and varying operational conditions.

Table 2.2 Studies focusing on methane production in AD-MEC systems with complex substrate usage

Substrate	Reactor Type	Operation	T(°C)	Volume (L)	Applied Voltage (V)	Anode Material	Cathode Material	CH_4 Production	Ref
Acetate+Domestic WW	TC	Batch	22	0.2	1.2	Carbon brush	Ti wowen wire mesh coated with Pt	CH_4 composition of biogas increased from 60 to 88-98%	(Jin et al., 2017)
Acetate+Domestic WW	SC	Batch	25	0.5	0.7 to 1.3	Carbon cloth	Nickel foam	0.08 to 0.17 L/L/d	(Y. Hou et al., 2015)
Cattle Manure	SC	Batch	35	0.35	3.5	IrO_2 covered titanium mesh	SS	0.57 L/L/d	(Tartakovsky et al., 2014)
Cattle Manure + Aloe Peel Waste	SC	Batch	36	0.3	0.6	Graphite rod	Graphite rod	226.84 NmL/gVS	(Xing et al., 2021)
CO_2	DC	Batch	35	0.2 each	Cathode potential at -0.7V vs SHE	Graphite felt	Graphite felt	384 mmol $CH_4/m^2.d$	(Baek et al., 2017)
Cow Dung	SC	Batch	20	0.6	1	Graphite	SS	39 and 133 % increase compared with AD	(Jiao et al., 2022)

Substrate	Reactor Type	Operation	T (°C)	Volume (L)	Applied Voltage (V)	Anode Material	Cathode Material	CH_4 Production	Ref
Dairy Manure	SC	Continuous	35	8	1.2	Graphite plate	SS cylinder	23.6 L on MEC and 10.9 L CH_4 on AD	(Hassanein et al., 2020)
Dextrin/ peptone	SC	Batch	22	2.1	0.5,1.1 and 2	Carbon felt	Carbon felt	0.88 L CH_4 at 2V	(Dou et al., 2018)
Domestic WW, Synthetic WW	SC	Continuous	21	3	1	Carbon felt	SS	0.061 L CH_4/L/d for synthetic WW	(Moreno et al., 2016)
Food Waste	SC	Batch	35	0.9	0.9	Graphite plates	Stainles steel	0.59 m^3/m^3/day (total gas)	(Hassanein et al., 2017)
Food Waste	SC	Sequencing batch (SBR)	35	20	0.3	Graphite carbon meshes coated with Ni	Ni,Cu, and Fe coated graphite carbon meshes	10-76 L/day with respect to changing OLR	(Park et al., 2019)
Food Waste	SC	SBR	35	15	0.3	Graphite carbon mesh coated with Ni	Ni,Cu, and Fe coated graphite carbon meshes	0.56 L CH_4/g VS_{rem}	(Lee et al., 2017)

Substrate	Reactor Type	Operation	T(°C)	Volume (L)	Applied Voltage (V)	Anode Material	Cathode Material	CH_4 Production	Ref
Leachate	SC	Batch	35	0.5	0.7	Graphite rod	Graphite rod	>33 mmol CH_4 for 15.9 gCOD/L feed	(Gao et al., 2017)
Pig Slurry	DC	Continuous	23	0.5 anode, 0.265 cathode chamber	Cathode potential at -0.8V vs SHE	Carbon felt	Granular graphite	79L $CH_4/m^3/d$	(Cerrillo et al., 2018)
Sewage Sludge	SC	Batch	37	0.15	1.4 and 1.8	Ti/Ru mesh plates	Ti/Ru mesh plates	130-165 mL cumulative methane	(Guo et al., 2013)
Sewage Sludge	SC	Batch	30,35 and 40	2.5	0.3	Graphite felt	Graphite felt	1.11 L CH_4/L at 35°C	(Ahn et al., 2017)
Sewage Sludge	SC	SBR	25	12	0.3,0.5 and 0.7	Graphite fiber fabric	Graphite fiber fabric	370 mL/L/d and 346 mL/L/d CH_4 for 0.3 and 0.5V respectively	(Q. Feng et al., 2016)
Sludge	SC	Batch	37	0.18	0.6, 0.8, 1.3, 1.8 and 2.3	Ti/Ru mesh plates	Ti/Ru mesh plates	0.26 L in total	(Xiao et al., 2018)

Substrate	Reactor Type	Operation	T(°C)	Volume (L)	Applied Voltage (V)	Anode Material	Cathode Material	CH_4 Production	Ref
Sludge	SC	Batch	35	2	0.3 and 0.6	Fe tube	Graphite pillar located in Fe tube	170.2 L/kg VS at 0.3V	(Y. Feng et al., 2015)
Sludge	SC	Batch	10	0.02	Cathode potential at -0.9V vs Ag/AgCl	Granular activated carbon (GAC)	Granular activated carbon (GAC)	20.30 mg CH_4-COD/gVSS	(D. Liu et al., 2016)
Sludge	SC	Batch	35	0.5	0.1, 0.3, 0.5, 0.7 and 0.9	Graphite felt	Graphite felt	2.92 L CH_4/L for 0.7V	(J. Yu et al., 2019)
Swine Manure	SC	Batch	38	0.8	2.5	Carbon felt	Ti mesh	22m^3/t dry swine manure	(Y. Liu et al., 2020)
Synthetic WW	SC	Continuous	35	1	1	Graphtite	Graphite	248.5 mL/h	(Y. Li et al., 2016)
Synthetic WW	DC	Batch	35	0.4 each chamber	0.4, 0.6, 0.8, 1 and 2	Carbon felt	Carbon felt	62.8 mL at 0.8V	(Ding et al., 2015)
Synthetic WW	SC	Batch	38	0.4	0.8	Carbon cloth	SS mesh	152 mL CH4/g VS	(Hagos et al., 2018)

Substrate	Reactor Type	Operation	T(°C)	Volume (L)	Applied Voltage (V)	Anode Material	Cathode Material	CH_4 Production	Ref
Synthetic WW	DC	Batch	35	0.2	Cathode potential at -0.9V vs Ag/AgCl	Platinum	5 different carbon stick	74.7 mL/L/d for CS wrapped in felt	(Zhen et al., 2018)
WAS	SC	Fed-Batch	22	0.18	1.2	Carbon fiber	SS mesh	5.6 to 14.0 mL/d	(Asztalos & Kim, 2015)
WAS	SC	Batch	22	33	0.75, 1.5 and 2	Reticulated vitreous carbon	Nickel steel	5.3 L biogas	(Sugnaux et al., 2017)
WAS	SC	Batch	20	0.55	0.8	Graphite brush	Carbon cloth	56.4 mL CH_4/L/d	(Cai et al., 2016)
WAS	SC	Batch	30	0.17	0.4 and 1	Carbon felt	SS	293 mL for 0.4 and 340 mL for 1V	(Bo et al., 2014)
WAS	SC	Batch	20-25	0.5	0.8	Graphite brush	Carbon cloth	138 mL CH_4/Lreactor /d	(W. Liu et al., 2016)
WAS	SC	Batch	35	1	0.6	Activated carbon fiber textile	Activated carbon fiber textile	1541 mL cumulative methane	(Chen et al., 2016)

Substrate	Reactor Type	Operation	T(°C)	Volume (L)	Applied Voltage (V)	Anode Material	Cathode Material	CH_4 Production	Ref
WAS	SC	Batch	35	0.5	0.3, 0.6, 0.9, 1.2	GFF with multi-wall Carbon Nanotube and nickel ion coatings	GFF with multi-wall Carbon Nanotube and nickel ion coatings	175.42 mL CH_4 at 0.9V	(Joicy et al., 2022)
WAS	SC	Batch	55	1	0.6	Carbon felt	Carbon felt	~ 110 mL/gVS_{added}	(C. Yin et al., 2019)
WAS	SC	Batch	25	0.52	1	Carbon brush	SS mesh	WAS-Fenton-AD had 162 mL $CH_4/L/d$	(H. Hou et al., 2020)
Winery Waste	SC	Continuous	31	1100	0.9	Graphite fiber brush	Graphite fiber brush	Biogas production 0.15-0.28 L/day (%86 percent CH_4)	(Cusick et al., 2011)

SC: Single Chamber; DC: Double Chamber, TC: Three Chamber

Pretreatment of substrate

While the hydrolysis reaction is often the step in AD on lignocellulosic biomass that determines the pace of the process, pretreatment can enhance the efficiency with which biomass is hydrolyzed, which in turn improves the performance of the AD-MEC system. Ultrasound (Hu et al., 2019), freezing-thawing (F/T) (Hu et al., 2020), alkaline (Xu et al., 2020), and different combinations like ultrasound-alkali, heat-alkaline or combination of all are typical pretreatment treatments (Bao et al., 2020). After receiving pretreatment, AD-MEC was found to have effects that were synergistic. According to Vu and Min (2019), the CH_4 yield from AD-MEC with thermal pretreatment was 47.7% and 33% greater than that of conventional AD and AD-MEC, respectively. A deterioration of the sludge cell that releases intracellular biopolymer as a result of thermal pretreatment might lead to an increase in the concentration of COD and VFA (Bao et al., 2020). In recent investigations, pretreatment was mostly performed to AD-MEC that was fed with easily degradable substrates as wastewater, sludge, or food waste (Table 2.1 and 2.2)

CHAPTER 3

MATERIALS AND METHODS

3.1 Inoculum and Waste Characteristics

3.1.1 Set 1: Inoculum and Waste Characteristics

Anaerobic sludge from anaerobic digester at a municipal wastewater treatment plant in Eskişehir, Turkey was taken and used as the inoculum. The inoculum had a chemical oxygen demand (COD) of 32,204 ± 1827 mg/L, total solids (TS) of 3.72 ± 0.01%, and a volatile solid (VS) of 2.00 ± 0.02% (54% of TS). It was stored at 4^{o}C until the experiment.

PS and WAS were obtained from the primary and secondary sedimentation tanks of the same treatment plant in Eskişehir, Turkey. PS and WAS were mixed at 1:1 ratio (v:v), and the mixture is labeled as WBS. C was taken from the feed tank of a biogas plant located in Polatlı, Turkey. Collected manure was blended for 15 minutes to have more homogenous composition before the utilization. The sludge and manure samples were stored at -20°C before use. The characteristics of WBS and C are given in Table 3.1.

Table 3.1 The characteristics of WBS and C used in Set 1

Parameter	WBS	C
pH	6.35	7.46
Total Solids (TS) (%)	4.8 ± 0.05	10.1± 0.08
Volatile Solids (VS) (%)	3.2 ± 0.04	8 ± 0.07
COD (mg/L)	51,118 ± 2,895	107,792 ± 4,525
TKN (mg NH_4-N/L)	1,134 ± 36	1,859 ± 16
TP (mg PO_4^{3-}/L)	350 ± 28	267 ± 1.4
Alkalinity (mg $CaCO_3$/L)	2,467 ± 115	5,222 ± 385

3.1.2 Set 2: Inoculum and Waste Characteristics

Similar to the Set 1, anaerobic sludge from anaerobic digester at a municipal wastewater treatment plant in Eskişehir, Turkey was taken and used as the inoculum. It was stored at 4^{o}C until the experiment. The characteristics of WBS sample and inoculum used in experimental Run 1 is provided in Table 3.2.

Table 3.2 Characteristics of WBS and inoculum in Run 1

Parameter	WBS	Inoculum
pH	6.5	7.48
TS (%)	4.38 ± 0.005	3.4 ± 0.005
VS (%)	1.9 ± 0.002	1.9 ± 0.002
VS (% of TS)	0.56 ± 0.005	0.56 ± 0.001
COD (mg/L)	57,894 ± 1,285	nd

nd: not determined

Same WBS and inoculum used within first run used in Run 2 as well. Due to the waiting period between the two experimental runs, before setting up Run 2 another set of characterization analysis was conducted (Table 3.3).

Table 3.3 Characteristics of WBS and inoculum at Run 2

Parameter	WBS	Inoculum
pH	6.39	7.55
TS (%)	3.6 ± 0.003	2.4 ± 0.02
VS (%)	2.1 ± 0.02	1.4 ± 0.01
VS (% of TS)	0.58 ± 0.01	0.58 ± 0.02
COD (mg/L)	54,118 ± 2,948	nd

nd: not determined

Specific Methanogenic Activity (SMA) Test

Specific Methanogenic Activity (SMA) assay was conducted to observe the methanogenic activity of the inoculum used in reactors. Briefly, serum bottles with 110 mL of total volume were divided into two as control and test. All reactors were operated as duplicate. Into the test reactors, 33.5 mL of inoculum culture, 10 mL of reactor media containing phosphate buffer that is prepared for the integrated system, a known amount of acetic acid (HAc: CH_3COOH) to reach a COD concentration of 3000 mg/L and finally deionized water to complete the active volume to 65 mL were added. In the control reactors, deionized water was added instead of acetic acid and all others were kept the same to reach the same active volume. The activity is calculated based on the comparison of actual (measured) methane production and theoretical (calculated) methane production. If the activity of the inoculum is higher than 70%, the seed was considered suitable for use in the reactors. Before starting a reactor set, SMA test was performed. An example calculation and results are provided in Appendix A.

3.1.2.1 Pretreatment of Wastewater Biosolids

In order to determine the rate limiting step on methane production from WBS via the use of AD-MEC systems, feed pretreatment was performed. There are a number of other pretreatment methods used in the literature such as microwave and ultrasonication ((Bao et al., 2020; H. Hou et al., 2020)). In this study, relatively milder pretreatment methods to avoid the release of any inhibitory compounds to the electro-active microorgansisms was applied for comparison. For pretreatment three different methods were selected, the conditions of each is summarized in Table 3.4.

Table 3.4 Pretreatment methods applied to the WBS feed

Pretreatment	Method	Conditions
1	Autoclave	Autoclaved for 60 min in 15 psi at 121^{o}C
2	Alkali	0.1M NaOH was used to get pH to 10. Half an hour after the pH was set to 10. Same procedure applied for 1 hour
3	Heat	Mixture of WBS was stayed in the 90^{o}C for 30 minutes and 1 hour.

Among these pretreatment methods the method which provides highest soluble COD(sCOD) increase in comparison to raw WBS was used in the experiments.

3.2 Reactor Medium

3.2.1 Medium Used in Set 1 Reactors

The medium used in all reactors was the mixture of phosphate buffered saline (PBS), sodium bicarbonate, vitamin and trace element solution. PBS (50mM, pH=7) was prepared as stock solution and contained $NaH_2PO_4 \times H_2O$ 9.94 g/L, $Na_2HPO_4 \times H_2O$ 5.5 g/L, NH_4Cl 310 mg/L, KCl 130 mg/L (Cheng et al., 2009b). 2.5 g/L $NaHCO_3$ was separately prepared into an autoclaved,anaerobic empty bottle. Trace element solution was prepared according to the composition stated in Table 3.5, after the preparation of the solution it was sterilized with autoclave and purged with pure nitrogen ($N_{2)}$ gas for 10 minutes and it was added to the medium as 10 mL/L.

Table 3.5 Trace element solution composition

Chemical composition	**g/L**
Nitrilotriacetic acid	1.5
$MgSO_4.7H_2O$	3
NaCl	1
$MnSO_4.H_2O$	0.5
$NiCl_2.6H_2O$	0.2
$CoCl_2$	0.1
$CaCl_2.2H_2O$	0.1
$FeSO_4.7H_2O$	0.1
$ZnSO_4$	0.1
$AlK[SO_4]_2$	0.01
$CuSO_4.5H_2O$	0.01
$Na_2MoO_4.2H_2O$	0.01
H_3BO_3	0.01

Vitamin solution contained the given ingredients in Table 3.6 and added to the medium with the same dosage of trace element solution. PBS and trace element solution were mixed on aerobic conditions, after that mixture was autoclaved and purged with pure N_2 for 10 minutes. Steril and anaerobic vitamin and bicarbonate solutions were transferred into the PBS-trace element mixture through syringe.

Table 3.6 Vitamin solution chemical composition

Chemical composition	**mg/L**
Pyridoxine HCl	10
Thiamin HCl	5
Riboflavin	5
Nicotinic acid	5
Calcium pantothenate	5
Vitamin B12	5
p-aminobenzoic acid	5
Thioctic acid	5
Biotin	2
Folic acid	2

3.2.2 Medium Used in Set 2 Reactors

The medium used in Set 1 was used with several changes in Set 2. The reason for changing the medium was due to the potential inhibitory effects of PBS solution due to high P content (R. Wang et al., 2015). In this set, PBS concentration was decreased to 5mM by adjusting $NaH_2PO_4 \times 2H_2O$ 0.6 g/L, $Na_2HPO_4 \times 2H_2O$ 0.25 g/L, NH_4Cl 310 mg/L, and KCl 130 mg/L, upon preparation it was autoclaved for sterilization and made anaerobic via purging with ultra-pure N_2 gas. $NaHCO_3$ concentration was also increased from 2.5 g/L to 5 g/L. Both trace element solution and vitamin solution were kept the same as in Set 1 (See Table 3.5 and Table 3.6 for their composition). All solutions were prepared separately, sterilized via autoclave or filtration, made anaerobic via purging with ultra-pure N_2 gas for 10 minutes and then added to the PBS.

3.3 Analytical Methods

3.3.1 Characterization Experiments

TS (Method 2540 B), VS (Method 2540 E), COD (Method 5220 B), total Kjeldahl nitrogen (TKN) (Method 4500N) and total phosphorus (TP) (Method 4500 P) were determined according to the standard methods (APHA 1999). Orthophosphate (PO_4^{-3}) and ammonium (NH_4-N) was performed according to the amino acid colorimetric method (Hach Method 8178) and Nessler colorimetric method (Hach Method 8038) using a spectrophotometer (Hach Company, DR9200, USA), respectively.

3.3.2 Determination of Biogas Production and the Content of Biogas

Produced biogas amount was quantified using a water displacement device and its composition was determined using a gas chromatography (Thermo Scientific, TRACE GC Ultra, USA) equipped with a thermal conductivity detector (TCD) and two columns connected in series (CP-Moliseve 5A and CP-Porabond Q). Oven, injector, and detector temperatures were set as 35℃, 50℃ and 80℃, respectively. Helium was used as carrier gas at a constant pressure of 75 kPa. Biomethane production in the reactors were calculated using methane percentage and total biogas production as described elsewhere (Alkaya and Demirer 2011). For manual injections, a glass GC syringe (Part number: 050051-LL, VICI AG, USA) was used. The injection volume was 100 μL. Calibration equation was developed by the utilization of 4 point duplicate injections of calibration gas with volumes ranging from 50 μL to 200 μL. The calibration gas was a mixture of hydrogen, N_2, CO_2 and CH_4. The composition of mixture was, 50% hydrogen, 30% CO_2, 10% N_2, and 10% CH_4. An example calibration for methane was given in Table 3.7 and Figure 3.1.

Table 3.7 Methane gas calibration for GC-TCD

Injection Volume(ul)	Trial	Peak Area	Mean	Standard Dev.	Coefficient of Variation (CoV) (%)
50	1	104083	102159.50	2720.24	2.7
	2	100236			
100	1	210225	208712.50	2139.00	1.0
	2	207200			
150	1	343001	341336.50	2353.96	0.7
	2	339672			
200	1	441426	440037.50	1963.64	0.4
	2	438649			

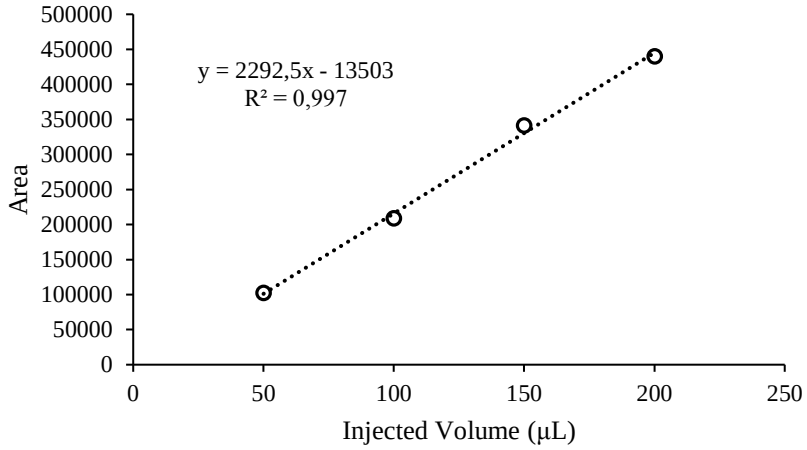

Figure 3.1 Methane gas calibration curve and equation

3.3.3 Determination of Acetic Acid

Acetic acid content was determined with a gas chromatograph (TRACE GC Ultra, Thermo Scientific) housing a flame ionization detector (FID) and a free carboxylic acids analysis column (Nukol-25326, Supelco) as described elsewhere (Kas and Yilmazel 2022).

In order to get an accurate reading of the acetic acid content in the samples, 0.22 uM pore-sized PES syringe filters were used. In order to guarantee that free forms of the organic acids were present, the pH of the samples was lowered to below 2.5 by diluting the samples to 5:6 ratios with 1 N HCl. This was done so that the samples could be analyzed. Injections of 2 μL were administered manually using a liquid GC syringe with a capacity of 10 μL. In order to verify that the results were correct, the needle was cleaned with acetone before each injection, and the GC column was purged with methanol after every two injections. Calibration equation was developed by the utilization of 4 point triplicate injections with concentrations ranging from 1mM to 10 mM of VFA Mix solution (Sigma-Aldrich). An example calibration for methane was given in Table 3.8 and Figure 3.2.

Table 3.8 Calibration injections for acetic acid

Concentration (mM)	Area	Mean	Standard Dev.	CoV (%)
1	16948722	15613343	1232376.9	7.9
	13975756			
	15915552			
2.5	27314596	30516743	2266812.5	7.4
	31986107			
	32249527			
5	60382948	66669464	4710423.8	7.1
	67904339			
	71721105			
10	143244737	139175910	6200425.1	4.5
	143868412			
	130414581			

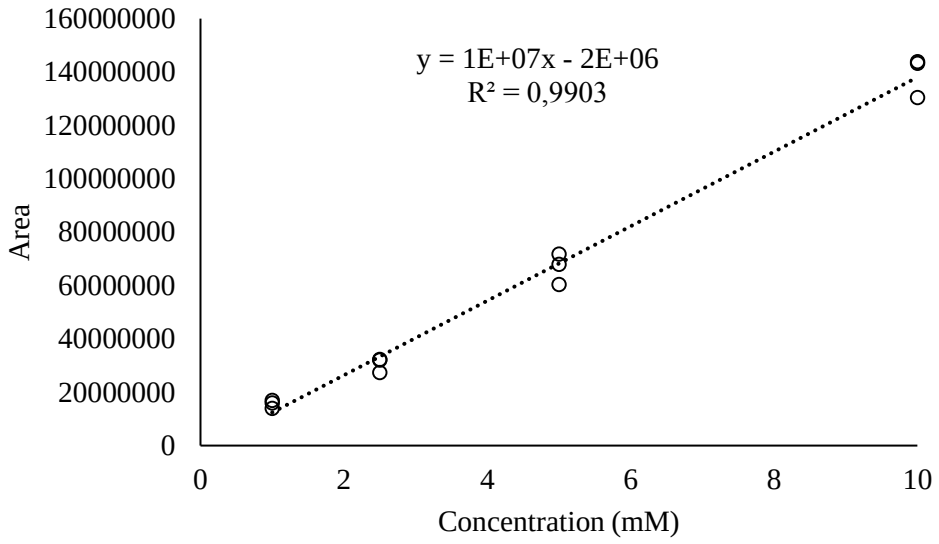

Figure 3.2 Acetic acid calibration curve and equation

3.4 Cyclic Voltammetry

In order to identify the biofilm formation over the cathodes, an analysis has been made. Electrochemical activity over the bioelectrodes was measured using cyclic voltammetry (CV) analysis with a scan range of 0.7 to 0 V vs. Ag/AgCl and a scan rate of 1 mV/s using a potensiostat (Gamry, Interface 1010B, USA). Reference electrode used in the CV was Ag/AgCl filled with 3 M NaCl (Ag/AgCl +200 mV vs standard hydrogen electrode (SHE); model RE-5B, BASi).

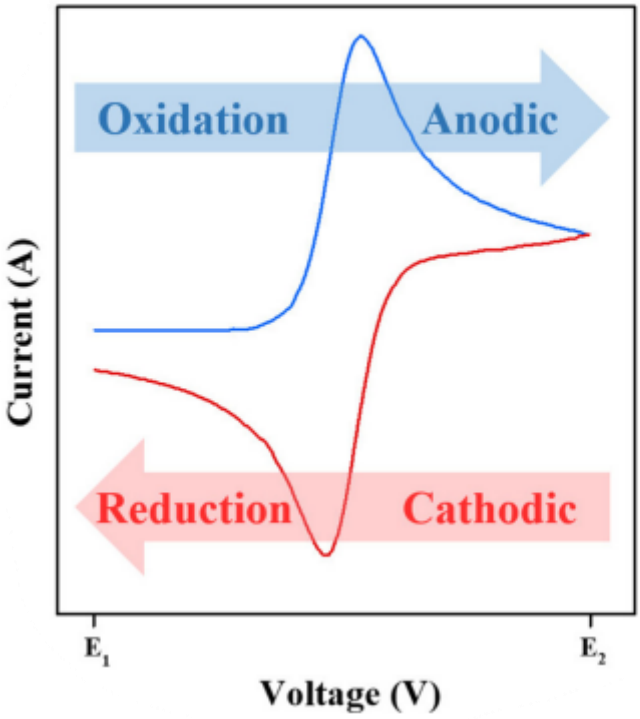

Figure 3.3 An example cyclic voltammogram of a theoretical electrochemical activity plotting anodic and cathodic peak (Kim et al., 2020)

(Elgrishi et al., 2018)For both sets, CV was carried out initially at the beginning of the test period and then again at the conclusion of the test period. To prepare a reactor for CV analysis, the reference electrode was placed into the reactor inside an anaerobic chamber (Plas Labs 818-GB, MI, USA) from the side port.

3.5 Calculations

3.5.1 Current Production

To monitor current production due to oxidation of organics, the voltage across the external resistor (R_{ex}: 10 Ω) connected to the anode electrode is continuously monitored using the data acquisition unit and calculated as given in Eq. 3.1.

$$I = \frac{V}{R_{ex}}$$ (Equation 3.1)

3.5.2 Determination of Current Density

The produced current was normalized by dividing it into anode total surface area (A) immersed in the reactor electrolyte. This normalized current is called current density (J) and is calculated using Eq. 3.2. (Kas & Yilmazel, 2022)

$$j\left(\frac{A}{m^2}\right) = \frac{I}{A}$$ (Equation 3.2)

3.5.3 Biomethane Production Data Analysis: Gompertz Fitting

Produced cumulative methane of reactors was fit by the changed version of Gompertz which is known as modified Gompertz equation (Eq.3.3) (P. Li et al., 2019) to interpret the methane production rate and other relevant parameters for different reactors.

$$P = P_{\infty} \times exp\left\{-exp\left[\frac{R_m \times e}{P_{\infty}}(\lambda - t) + 1\right]\right\}$$ (Equation 3.3)

P is representing the cumulative methane production (mL) within the reactors, P∞ is potential of methane production (mL), Rm is the maximum specific methane production rates (mL/d), and λ is the lag phase duration for methane production (days), while t is the time and e is equivalent to 2.718282.

3.5.4 Change in Energy Efficiency

Change in energy recovery efficiency calculated as given in Eq. 3.4.

$$Change\ in\ energy\ \text{recovery}\ efficiency = \frac{W_{CH_{4(AD-MEC)}} - W_E}{W_{CH_{4(AD)}}}$$ (Equation 3.4)

where, W_E is representing the electrical energy input for AD-MEC integrated system throughout the operation time, $W_{CH4(AD\text{-}MEC)}$ is the energy recovery as methane from the AD-MEC and $W_{CH4(AD)}$ is the energy recovery as methane from the conventional AD system (Huang et al., 2022).

3.6 Experimental Design and Procedures

The purpose of the research presented in this thesis is to investigate the factors that influence the generation of methane in AD-MEC integrated systems. These factors include applied voltage, electrode material, and the kind of substrate that is employed. First experimental set was operated to observe methane generation from C and WBS under different external voltages. The results of Set 1 showed that, WBS dominated reactors (0C:100W) showed lower performance in comparison to C dominant reactors. Therefore, aim of the Set 2 was to investigate the effect of biofilm formation and pretreatment performance of WBS fed AD-MEC integrated systems. A schematic representation of Set 1 and 2 is given in Figure 3.3. This is a schematic representation of all the experimental studies conducted in this thesis. The experimental design and reactor operation of each set will be explained in the following sections.

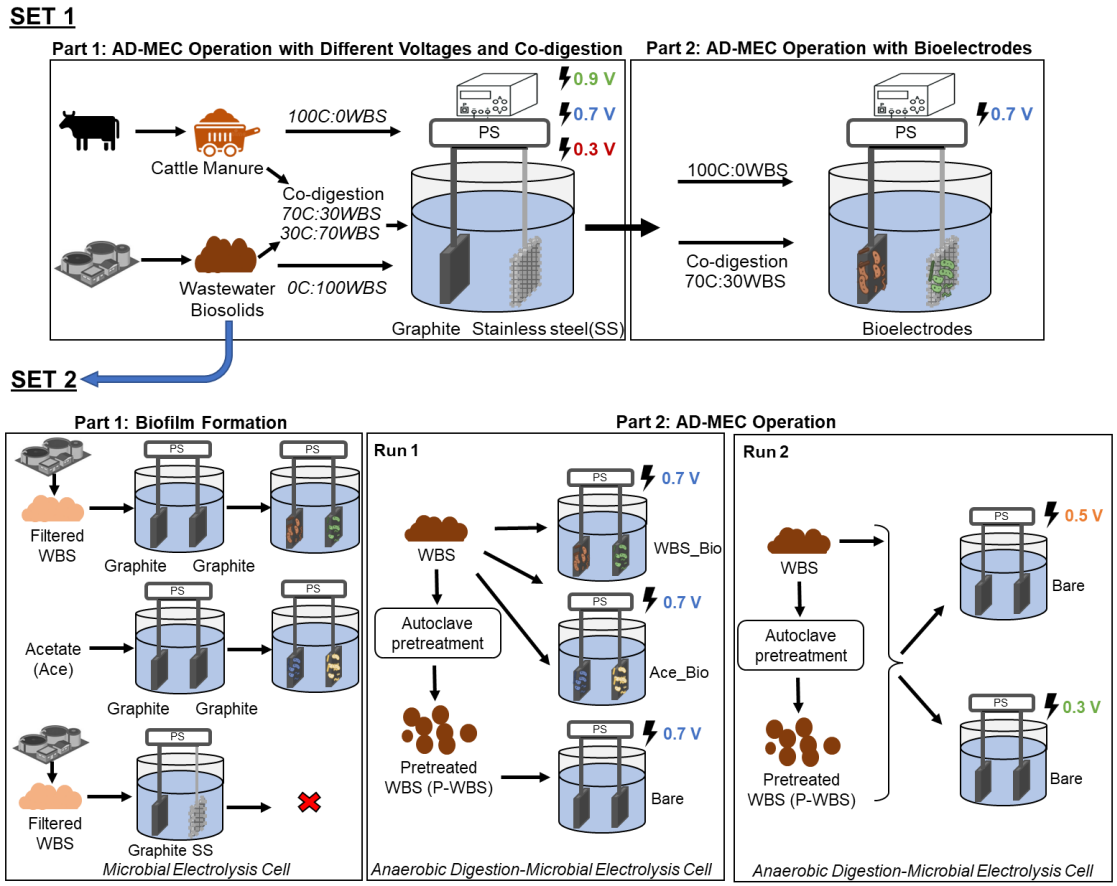

Figure 3.4 Schematic representation of this thesis (Set 1 and Set 2)

3.6.1 Reactor construction, operation and experimental design of Set 1

Reactor construction and operation in Set 1

The single-chamber membrane-free reactors were fabricated by opening two side ports on 100 ml borosilicate bottles with a total volume of 130 mL (Figure 3.4). Graphite plates (Eren Karbon Grafit San. Tic. Ltd. Sti, Istanbul, Turkey) with the dimensions of 2.5 cm (L), 2.5 cm (W) and 0.3 cm (D) were used as anode. Anodes were polished with sandpaper (first grit type 400 and after 1200), cleaned by staying on 1M HCl overnight and rinsed 4 times in Milli-Q deionized water. After that they were connected to the circuit with grade 2 titanium wires (Timed metal, Turkey) with an inner diameter of 0.08cm to provide a good contact (< 0.1 Ω) which were also cleaned with the sandpaper. The cathode was stainless steel (SS) mesh (Type 304, mesh size 60*60) were cut to get the same surface area with anodes (surface area of 15.5 cm2). SS mesh electrodes were connected to a SS wire (Type 304) to provide a good contact (< 0.1 Ω). SS meshes used in the reactors were polished with same sandpaper and rinsed with deionized water (Milli-Q). Electrodes were fixed in the thick butyl rubber stopper and then pushed into the boroslicate bottles. Sideports were crimp sealed in order to make sure that reactors stayed anaerobic throughout the experiment.

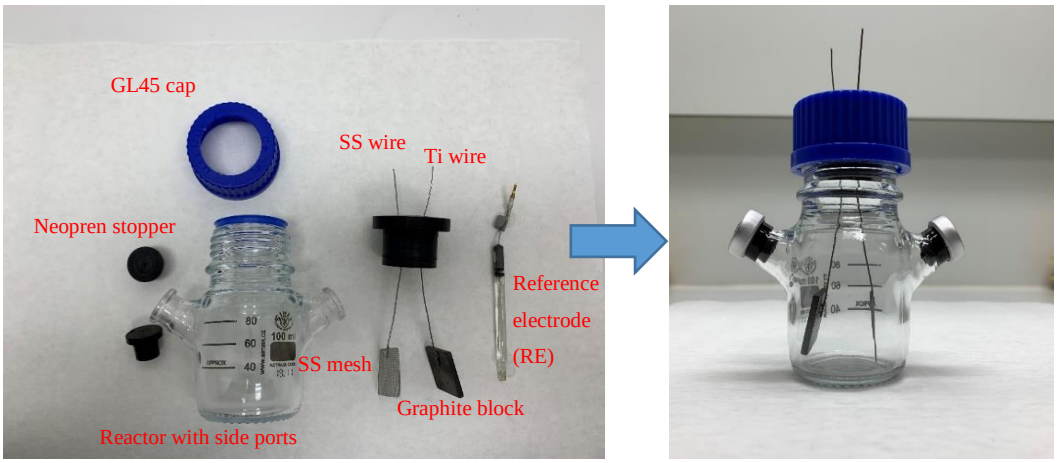

Figure 3.5 MEC reactor configuration on Set 1 (during CV reference electrode is placed in between electrodes)

AD-MEC reactors were operated at different fixed voltages (0.3 V, 0.7 V and 0.9 V) by adjustable power supplies (Marxlow, RXN-1502D, China) (Figure 3.6) under batch operation mode.

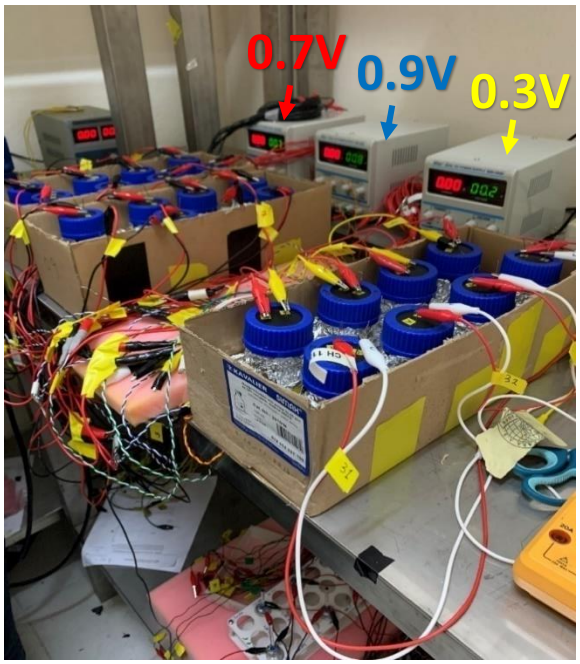

Figure 3.6 Reactors during Set 1 operation

For the operation of the reactors, test leads attached to the anodes were connected to the positive terminal and test leads attached to the cathodes were connected to the negative terminal of the power supply. Each test lead linked to the positive terminal has a series of ten ohm resistors connected to record the voltage required to compute current (Yilmazel et al., 2018). A data acquisition unit (Keysight Technologies, 34972A LXI Data Acquisition, USA) was used to record voltage at 10 min intervals and current was calculated using Ohm's law. The headspace of the reactors was purged with 20% CO_2 and 80% N_2 before the start of the experiment. Before autoclaving, purging and adding other nutrients, the pH of the medium was measured. All reactors were operated at incubated at 35℃ ± 2 in a controlled temperature room in duplicate without mixing (Kas & Yilmazel, 2022). Reactors operated as duplicates and when the increase in cumulative methane production between consecutive measurements dropped below 3% reactor operation was stopped.

Experimental Design of Set 1

There were two experimental sets in this study. In the first set, the objective was to determine biomethane production potential from co-digestion of C and WBS. The second set was a follow-up study and the objective was to determine the impact of inserting a bioelectrode on the methane production performance of an AD-MEC reactor (Figure 3.7).

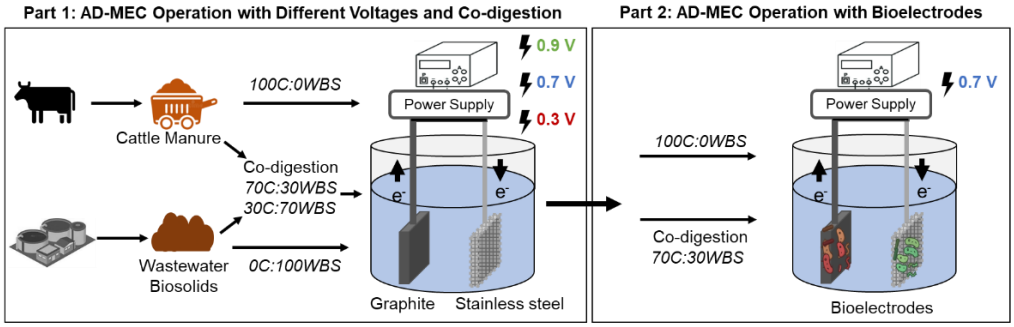

Figure 3.7 Schematic representation of Set 1

In each part AD-MEC reactors were prepared together with control reactors. Including the controls, in total four types of reactors were operated; seed control (Blank), conventional anaerobic digestion reactor (AD), open circuit control (OC) and the AD-MEC reactor. OC controls were prepared similar to AD-MEC reactors with electrodes inside the reactor, but no power was supplied to them. AD-MEC reactors were operated under three different applied voltages (Table 3.9). Experimental design is given in Table 3.9. Briefly, blank reactors were operated to determine the background methane formation from the inoculum and OC controls were operated to observe the effect of the electrode surface area on biomass attachment. Also, AD reactors were used to provide a benchmark for AD-MEC reactors and compare the performance of conventional system with the integrated AD-MEC reactors. The wastes added to the reactors as substrate were provided at varying mixing ratios (COD basis) as follows: 100% C and 0% WBS (100C:0WBS), 70% C and 30% WBS (70C:30WBS), 30% C and 70% WBS (30C:70WBS) and 0% C and 100% WBS (0C:100WBS).

Table 3.9 Experimental design of Part 1 (Bare electrodes were used)

Reactor Type	Feed*	Electrodes	Applied Voltage (V)
Blank	-	-	-
Conventional Anaerobic Digestion (AD)	+	-	-
Open Circuit (OC)	+	+	-
AD-MEC (0.3)	+	+	0.3
AD-MEC (0.7)	+	+	0.7
AD-MEC (0.9)	+	+	0.9

*4 types of feed were added to the reactors as 0C:100WBS, 30C:70WBS, 70C:30WBS, 100C:0WBS

C: cattle manure; WBS: wastewater biosolids

After Part 1 experiments were stopped, Part 2 was started to investigate the impact of using now colonized electrode, *i.e.*, bioelectrode, inside an AD-MEC reactor (Figure 3.4). The objective in the second part was to have an understanding of the lifetime of the bioelectrodes. In Part 2 only two reactors were selected for further investigation: 100C:0WBS_0.7 and 70C:30WBS_0.7. When the bioelectrode formation period (Part 1) is over their data was analyzed and are summarized as follows i) daily methane production together with current density, ii) CV peaks (cathodic peaks for duplicate reactors), iii) cumulative methane production. In Part 2, 0.7 V applied AD-MECs were chosen for further study since the replication of reactors were quite well especially in CV analysis. The electrodes that were present in the reactors of Part 1 were stored in the fridge at 4 ^{o}C. For Part 2, these so-called "bioelectrodes" were used in a new AD-MEC set. Before testing the bioelectrodes (in Part 2), to revive the biofilm on the stored electrodes, MECs were fed with sterile acetate for a few cycles without adding any new inoculum. During this revival period, current was monitored (Current density profiles given in Appendix D). Then, similar to Part 1, another 45 days of AD-MEC operation was started by inserting these bioelectrodes to the new reactors. Also, their respective OC reactors were operated in the same manner.

The revival protocol details were as follows: the bioelectrode pair previously belonging to 100C:0WBS_0.7 of Part 1 was carefully removed from the reactors inside the anaerobic chamber without touching the surface, placed into a glass bottle and submersed into PBS solution (50 mM) and kept in dark at 4℃ for around 40 days. After 40 days, they were inserted into new MEC reactors of the same configuration as in AD-MECs. These reactors were filled with the same PBS media and fed with 20 mM acetate when current density (mA/cm^2) drops below 0.01 for about 2 cycles of operation. Here there was no addition of any inoculum as the aim was to revive the attached biomass by feeding acetate. After two cycles (~ 9 days), the reactors were emptied and then to operate as AD-MEC they were filled with the same feed of 100C:0WBS as in Part 1 and inoculated with AD seed. These AD-MEC reactors were operated similar to Part 1 at an applied potential of 0.7 V. The same electrode removal and replacement protocol was followed for the corresponding OC controls of feed 100C:0W. The electrodes from OC controls were also placed into new OC controls and operated similar to Part 1 with no applied voltage.

3.6.2 Reactor construction, operation and experimental design of Set 2

Reactor construction and operation in Set 2

Same reactors used in the Set 1 were used in Set 2. In this set there were again two parts. Part 1 is named as biofilm formation, and Part 2 is named as AD-MEC reactor operation (Figure 3.8). In Part 1 of Set 2, graphite block anodes were used similar to Set 1. Yet, two different cathodes were tested: SS mesh electrodes and graphite blocks. SS mesh electrodes Type 304, (mesh size 60*60) were connected to a SS wire (Type 304) to provide a good contact (< 0.1 Ω). SS meshes used in the reactors were polished with same sandpaper and rinsed with deionized water (Milli-Q). However, based on the results of the biofilm formation part, SS mesh cathodes were not used in Part 2 reactors. In the reactors, graphite blocks (Eren Karbon Grafit San. Tic. Ltd. Sti, Istanbul, Turkey) with the dimensions of 2.5 cm (L), 2.5 cm (W) and 0.3 cm (D) were used. Electrodes polished with sandpaper (first grit type 400 and

after 1200), cleaned by staying on 1M HCl overnight and rinsed 4 times in Milli-Q deionized water. After that they were connected to the circuit with grade 2 titanium wires (Timed metal, Turkey) with an inner diameter of 0.08 cm to provide a good contact (< 0.1 Ω) which were also cleaned with the sandpaper. Electrodes were fixed in the thick butyl rubber stopper and then pushed into the boroslicate bottles. Sideports were crimp sealed in order to make sure that reactors stayed anaerobic throughout the experiment.

During Part 1, reactors were operated by injecting the substrate into the reactor (fed-batch) for multiple cycles without removing any liquid. The objective here was to form biofilm attached electrodes, named as bioelectrodes. During Part 2, AD-MEC reactors were operated to compare the bioelectrodes and bare electrodes under batch operation mode. Similar set-up for Set 1 is used in Set 2. Current was monitored continuously, and methane measurements were done periodically. All reactors were incubated at 35℃ in a controlled temperature room in duplicate without mixing. Reactors operated as duplicate and when the increase in cumulative methane production between consecutive measurements dropped below 3% reactor operation was ended.

Experimental Design in Set 2

The experiments consisted of two parts: (1) biofilm formation, and (2) AD-MEC operation (Figure 3.8).

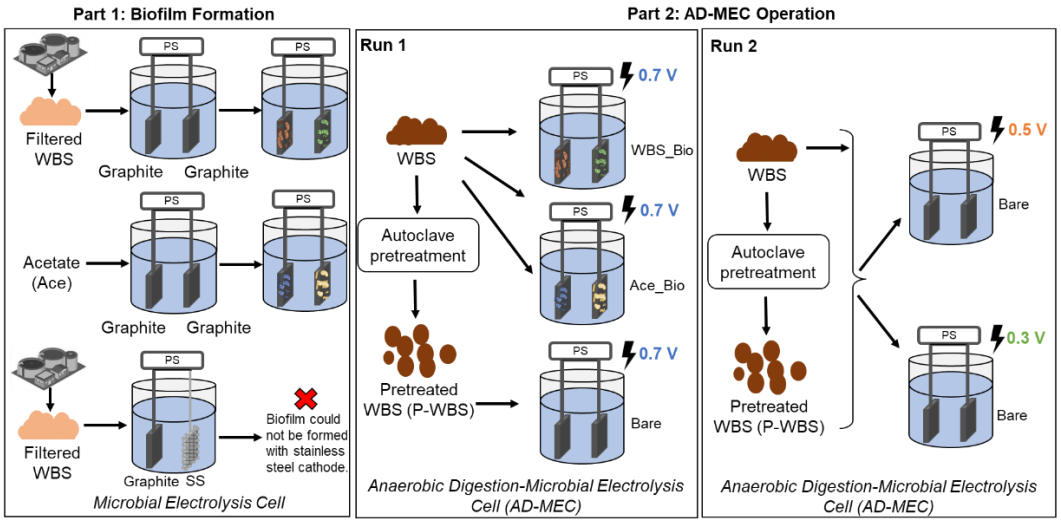

Figure 3.8 Schematic representation of Set 2

The objective of the biofilm formation part was to determine whether colonization of electrodes, *i.e.*, biofilm formation is possible with the SS mesh electrode when WBS is used as substrate. For this purpose, WBS was used as a substrate and 0.7 V external whole cell potential is applied to the reactors. To understand whether the cathode material used has an inhibitory effect on the biofilm formation with WBS substrate, two different reactors were included in the experimental design with different electrodes. The reason for changing the cathode material was because there was not significant current production with SS mesh cathode in the Set 1 experiments of this thesis work. Therefore, in this set at first the impact of SS mesh and graphite were compared. The experimental design of Part 1 is given in Table 3.10. There were three groups of reactors, in all of which anode was kept as graphite and applied voltage was also the same.

Table 3.10 Experimental design of biofilm formation part

Reactor	Feed	Anode	Cathode	Applied Voltage (V)
SS_WBS	WBS	Graphite Plate	SS Mesh	0.7
Gr_WBS	WBS	Graphite Plate	Graphite Plate	0.7
Gr_Ace	Acetate	Graphite Plate	Graphite Plate	0.7

In the first group (SS_WBS), SS mesh was used as the cathode, as in Set 1 and these reactors were fed with filtered WBS. In the second group (Gr_WBS), graphite plate was used as cathode and again the feed was filtered WBS. In third group, named Gr_Ace, graphite plate was used as cathode and the reactors were fed with acetate to determine the impact of feed (substrate) on the biofilm formation. All reactors were operated with an applied voltage of 0.7 V as 4 replicates, since 4 sets of cathode and anode needed for the AD-MEC operation (Figure 3.9). Two electrodes were needed for AD-MECs and two were needed for their corresponding OC controls.

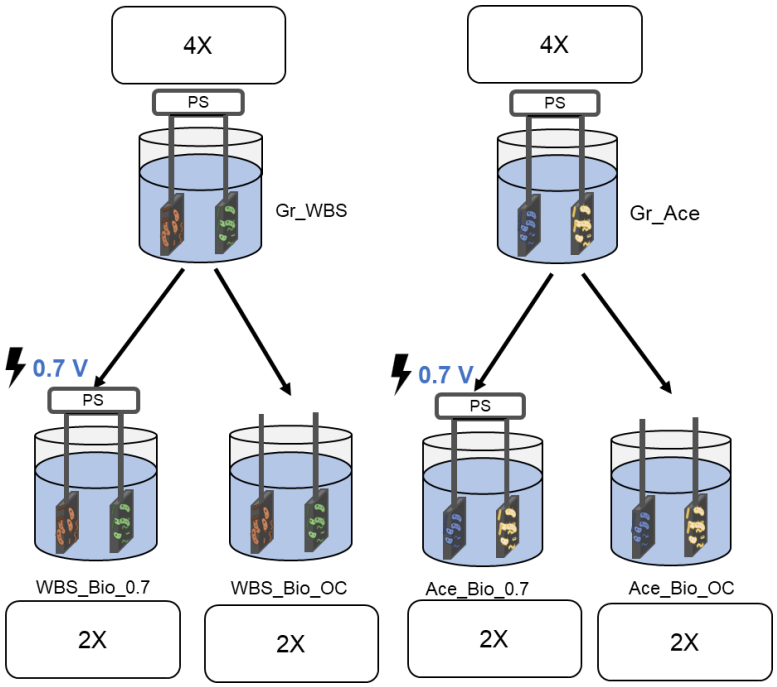

Figure 3.9 Distribution of bioelectrodes formed in Part 1 into the Part 2 reactors

During this part, when the current reached its highest point and then dropped below 0.05 mA, a new cycle was begun by injecting the corresponding substrate (Filtered WBS and acetate). After a number of cycles, when the level of current production in each reactor had reached a steady state, this part considered complete.

In Part 2, named as AD-MEC operation, there were in total of two experimental runs. In the first run, the objective was to determine the impact of feed pretreatment, and examine the impact of electrode acclimation on the anaerobic treatability of WBS in

AD-MEC system. Here, AD-MEC reactors were kept on 0.7 V. After Run 1 experiments were stopped, Run 2 was started to investigate the impact of using different voltages on AD-MEC integrated system. The objective of Run 2 was to determine the impact of applying different voltages (0.3 V and 0.5 V) on the methane production performance of AD-MECs. In each run AD-MEC reactors were operated together with control reactors similar to Set 1. Experimental design of both runs is given in Table 3.11. In this table AD-MEC reactors are shown in shaded rows and all others are control reactors. Additionally, reactors designated with "p" indicate that they were fed with pretreated feed.

Table 3.11 Experimental Design of AD-MEC Operation (Part 2)

Run	Reactor Name	Feed Pretreatment	Electrode	Biofilm Formation Substrate	Applied Voltage (V)
Run 1	Blank	-	-	-	-
	AD	-	-	-	-
	OC	-	Bare	-	-
	Ace_Bio_OC	-	Bio	Acetate	-
	WBS_Bio_OC	-	Bio	Filtered WBS	-
	Ace_Bio_0.7	-	Bio	Acetate	0.7
	WBS_Bio_0.7	-	Bio	Filtered WBS	0.7
	Bare_0.7	-	Bare	-	0.7
	pAD	+	-	-	-
	pOC	+	Bare	-	-
	pWBS_0.7	+	Bare	-	0.7
Run 2	Blank	-	-	-	-
	AD	-	-	-	-
	WBS_0.3	-	Bare	-	0.3
	WBS_ 0.5	-	Bare	-	0.5
	pAD	+	-	-	-
	pWBS_0.3	+	Bare	-	0.3
	pWBS_0.5	+	Bare	-	0.5

CHAPTER 4

RESULTS AND DISCUSSIONS

4.1 Set 1: The Impact of Applied Voltage on Co-Digestion of Cattle Manure and Wastewater Biosolids

The experimental design of Set 1 is provided in Table 3.9 and briefly described in Figure 3.7. In this set, the objective was to compare the methane production performance of AD-MEC reactors under 3 different applied voltages of co-digestion of C and WBS. There were in total two experimental parts in Set 1 and the results will be presented for each part separately.

4.1.1 Part 1: AD-MEC Operation with Different Voltages and Co-Digestion

Methane production and organic removal

The cumulative methane production of the reactors in Set 1 is given in Figure 4.1. In these reactors hydrogen was not detected in the biogas in any reactors which may be due to its fast consumption and transformation to methane by hydrogenotrophic methanogens (Lee et al. 2009). AD-MEC reactors which have a higher abundance of C in the feed showed a significant increase in comparison to the AD and OC controls. For instance, average cumulative methane production in 100C:0WBS_0.9 reactors were recorded as 184.62 ± 6.2 mL, while the production in AD and OC reactors of the same feed (100C:0WBS) were averaged at 133.97 ± 9.9 mL and 142.54 ± 3.2 mL, respectively (Figure 4.1B). This is corresponding to a 37.8% increase in methane production with respect to the conventional AD with 0.9 V application and 29.5% increase with respect to the OC controls. Despite the highest increase recorded at an applied voltage of 0.9 V, both 0.7 V (148.52 ± 7.9) and 0.3

V (157.06 ± 11.22) applied AD-MEC reactors produced more than AD and OC controls. In the case of sole manure feed, there was a positive correlation with the applied voltage; as the applied voltage increased methane production was increased. In OC controls, 6% higher methane with respect to AD was recorded, this is an indication that voltage application was the major factor enhancing methane production rather than providing a surface area for biomass attachment. In the case of 70C:30WBS, all AD-MEC reactors produced similar amount of methane around 183 mL, while AD and OC controls produced around 127 mL during the 40 days of reactor operation (Figure 4.1B). Again, there was a positive impact of AD-MEC reactor operation and around 44% higher methane was produced with a bioelectrochemical system as opposed to conventional system. The fact that in both AD and OC reactors similar methane productions were attained can be interpreted as low impact of providing a surface area for biomass attachment in methane production in these reactors.

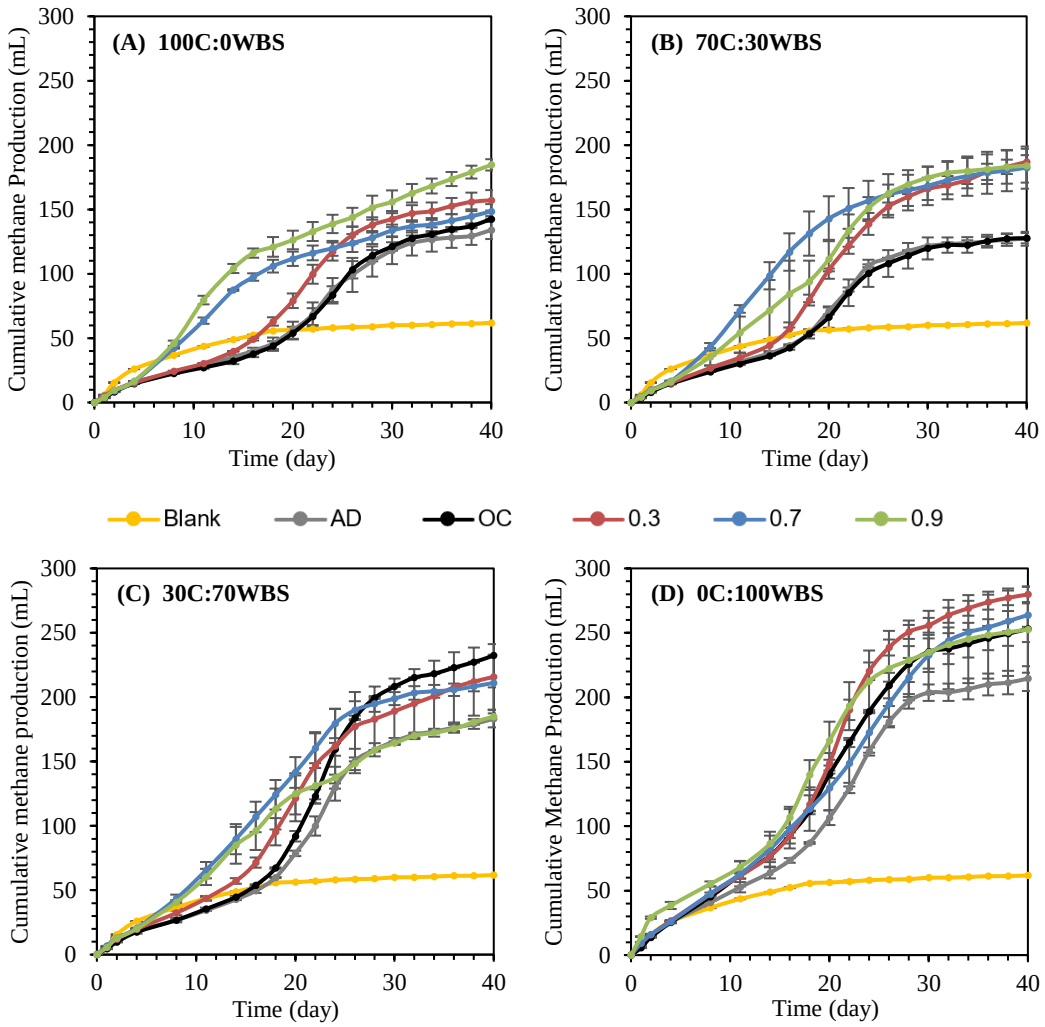

Figure 4.1 Cumulative methane production in A) 100C:0W, B) 70C:30W, C) 30C:70W and D) 0C:100W reactors

When WBS served as main substrate (with 0C:100WBS and 30C:70WBS feed), the impact of AD-MEC operation was relatively lower in comparison to manure dominant feeds, especially at higher applied voltages. For instance, with 0C:100WBS feed the highest enhancement was recorded with 0.3 V application, and 30% higher amount of methane was produced in comparison to AD. In the case of 0.7 V there was around 23% increase and with 0.9 V the increase was around 17% with respect to AD reactors.

As opposed to manure only reactors, there was a reverse relation with the voltage; as applied voltage was increased the enhancement in methane production was decreased. Further, OC reactors produced around 18% higher methane than AD reactors; indicating a positive impact of providing a surface area for biomass attachment. The impact of OC was even more significant with 30C:70WBS feed; and the highest amount of methane were produced in the case of OC. There was no enhancement with 0.9 V application, while there was more methane production with 0.3 V and 0.7 V in comparison to AD. However, as OC controls produced the highest amount of methane (27% higher than AD) with 30C:70WBS feed, the enhancement in methane production the 0.3 V and 0.7 V reactors could not be attributed to applied voltage (Figure 4.1C).

The modified Gompertz equation (Eq.3.3) was used to fit the methane production data in each reactor (Table 4.1). All Gompertz fitting graphs are provided in the Appendix E. Based on Gompertz fitting the lag times (λ) and the rates (R_m) in the reactors can be compared. When C was used as a (co-)substrate, there was always an improvement in the lag phase at applied voltages of 0.7 V and 0.9 V (Table 4.1). For example, when AD-MEC reactors were used with 100C:0WBS feed there was a significant decrease in the lag time (λ) averaging around 70% with an applied voltage of 0.7 V and 0.9 V. Further, the methane production rate (R_m) was also significantly enhanced; around 63% increase was recorded in 0.9 V applied reactors while 46% increase was recorded in 0.3 V and 0.7 V applied reactors. Also, for the feed of 70C:30WBS there was a considerable increase in the rate at all applied voltages, and a considerable decrease in lag phase was recorded for 0.7 V and 0.9 V applied reactors. The fact that there was a decrease in the lag time may be explained by the consumption of more easily biodegradable components of C by the exoelectrogens. The enhancement of methane production can be explained by the presence of DIET between exoelectrogens and methanogens, and the reduced impact of inhibition in the AD-MEC reactors (Huang et al., 2022). It has been reported that hydrogenotrophic methanogens are more tolerant to some inhibitory factors such as high ammonia concentration (Florentino et al., 2019; Huang et al., 2022). Even

though no microbial community analysis was performed in our study, in the literature it has been proven that in MECs with stainless steel mesh cathodes hydrogenotrophic methanogens became dominant among archaea (Siegert et al., 2015). In the case of WBS dominant feed (30C:70WBS or 0C:100WBS) lower enhancement in the rates were recorded, except 0.3 V application with 100% WBS feed. A similar observation was made by Feng et al. (2016) when WAS was used as feed and in comparison, to 0.6 V, AD-MEC reactors with 0.3 V application performed better (Feng et al., 2016). Also, in most of OC controls a longer lag time was needed despite higher methane production potential when compared to the AD this may be due to the time requirement of the biomass for surface attachment.

Table 4.1 Kinetic parameters calculated from the fitting with the modified Gompertz model of Part 1 reactors

	Feed Mixing Ratio	Reactor	P_∞ (mL)	R_m (mL/d)	λ (d)	R^2
Part 1	100C:0WBS	AD	174.7	4.8	6.5	0.984
		OC	188.2 (8)	5.3 (10)	7.9 (-)	0.984
		0.3	177.1 (1)	7.0 (46)	7.6 (-)	0.988
		0.7	177.5 (2)	7.0 (46)	2.0 (69)	0.987
		0.9	178.1 (2)	7.8 (63)	1.8 (72)	0.989
	70C:30WBS	AD	145	5.6	6.1	0.979
		OC	147.4 (2)	5.4 (-)	6.3 (-)	0.984
		0.3	202.4 (40)	8.5 (52)	7.8 (-)	0.992
		0.7	182.6 (26)	9.4 (68)	3.3 (46)	0.999
		0.9	203.3 (40)	7.9 (41)	4.7 (23)	0.993
	30C:70WBS	AD	209.7	8.3	8.9	0.982
		OC	256.0 (22)	12.1 (46)	11.1 (-)	0.987
		0.3	236.2 (13)	9.3 (12)	6.8 (24)	0.992
		0.7	225.0 (7)	9.5 (14)	4.0 (55)	0.996
		0.9	193.6 (-)	7.2 (-)	2.6 (71)	0.999
	0C:100WBS	AD	256.2	8.5	5.8	0.981
		OC	289.6 (13)	10.3 (21)	5.7 (2)	0.991
		0.3	313.2 (22)	12.5 (47)	7.0 (-)	0.987
		0.7	332.8 (30)	9.2 (8)	4.9 (16)	0.994
		0.9	282.2 (10)	10.3 (21)	3.7 (3)	0.985

*The number in parenthesis indicates the percentage increase in P_∞ and, R_m and decrease in λ with respect to AD controls: (-) indicates no enhancement.

Based on the modified Gompertz model fitting, lag time of 100C:0WBS_0.7 (2 day) and 100C:0WBS_0.9 (1.8 day) were decreased in comparison to the lag time of 100C:0WBS_AD reactors, which was around 6.5 days. Likewise, lag time in 70C:30WBS_0.7 (3.3 day) and 70C:30WBS_0.9 (4.7 day) reactors were shorter than the lag time of 70C:30WBS_AD (6.1 day) reactors. For 100C reactors, implementation of voltage increases the methane production rate from 4.84 mL/day (AD) to 7 mL/day at 0.3 V, 7 mL/day at 0.7 V and 7.8 mL/day at 0.9 V. Increased methane production rates were also achieved with the voltage addition in 70C:30WBS reactors. Rate of 70C:100WBS increased from 5.6 mL/day to 8.5 mL/day at 0.3 V, 9.4 mL/day at 0.7 V and 7.9 mL/day at 0.9 V.

With the 100W reactors, lag time decreased with 0.7 V and 0.9V application. Lag time of the AD decreased from 5.8 days to 4.9 days with 0.7 V and to 3.7 days with 0.9 V. Methane production rate of the 100WBS reactors increased from 8.5 mL/day (AD) to 12.5 mL/day for 0.3V, 9.2 mL/day for 0.7V and 10.3 mL/day for 0.9 V. On 30C:70WBS reactors voltage addition also decreased the lag time for all three different voltages. Except 100WBS reactors, all OC reactors showed increased lag time.

The application of voltage (in AD-MEC reactors) or increased surface area due to placement of electrodes into reactors (in OC controls) has no significant impact on the VS removal efficiency amongst different reactors for various mixtures of feed. For example, among 0C:100WBS fed reactors, slightly higher VS removal was observed in 0C:100WBS_0.7 reactors. On the other hand, AD reactors of 100C:0WBS feed had the highest VS removal among others.

In general, when VS removals are compared depending on the substrate type, the VS removal increases with the ratio of W in the substrate. Hence, it can be concluded that VS removal is dependent on the type of substrate not the reactor operation conditions. The 0C:100WBS group had the highest average VS removal with 24 ± 1.7%, while the 100C:0WBS group had the lowest VS removal with an average of 17 ± 2.1%. The average VS removal of the 30C:70WBS and 70C:30WBS groups

was in between and averaged at 22 ± 2.4% and 19 ± 1.2%, respectively. The reported VS removals in this study are at the lower end of typical removal efficiencies reported in the literature. In another work 41.9% VS removal from cattle manure was reported using AD-MEC system (Hassanein et al., 2020). In another study, when researchers tested the co-digestion of cow manure and aloe peel in an AD-MEC reactor with 0.6 V voltage application for 35 days and reported 39.95 ± 0.19% VS removal with AD and 46.28 ± 0.15% VS removal with AD-MEC reactors (Xing et al., 2021). The low VS removal implies that there might be partial inhibition in the reactors. Hence, the effluent samples concentrations of VFA, ammonium (NH_4-N), and orthophosphate (PO_4-P) was examined to determine any potential inhibition factors (Table 4.2).

In the literature, for livestock manure digestion, inhibition related to nitrogen has been reported; and inhibition may start at total NH_4-N concentrations between 1500 mg/L – 2000 mg/L (Nielsen and Angelidaki, 2008). Since NH_4-N inhibition typically has an adverse impact on methanogens, it is usually accompanied by VFA accumulation in the reactors (Nielsen and Angelidaki, 2008 and Speece, 1999). In our reactors, the effluent NH_4-N concentrations ranged between 550 – 1100 mg/L and yet no significant acetic accumulation was detected.

On the other hand, effluent orthophosphate concentrations in the reactors ranged from 700 to 1,100 mg P/L (Table 4.2) and this is due to the PBS addition to the reactors. It has been reported for AD processes results in methane production are slowed down by orthophosphate concentrations greater than 414 mg-P/L (R. Wang et al., 2015). Therefore, high concentration of PO_4-P in reactors might be a possible source for the inhibition of the digestion process.

Initial pH measurements was affected with the type of feed in the reactors. With the solely C as feed reactors were in the range of 7.55 to 7.78. On 70C:30WBS reactors initial pH differs from 7.43 to 7.74. Differs from the C feed reactors, WBS reactors have the initial pH within the range of 7.40 to 7.48. Final pH levels are given in Table 4.2.

Table 4.2 VS removals, final pH and effluent VFA, PO_4-P and NH_4-N concentrations in the Part 1 reactors

Reactor		VS removal (%)	Total VFA (mg/L)	PO_4-P (mg/L)	NH_4-N (mg/L)	Final pH
100C:0WBS	AD	20 ± 0.7	172.5 ± 25.9	1073.2 ± 304.8	920 ± 452.5	8.25 ± 0.06
	OC	16 ± 0.7	320.5 ± 11.2	1102.2 ± 50.7	850.0 ± 23.6	8.32 ± 0.04
	0.3	17 ± 3.1	258.3 ± 31.7	1094.0 ± 20.8	666.7± 471	8.25 ± 0.07
	0.7	17 ± 2.0	112.3 ±6.4	984.8 ± 202.9	560.0 ± 84.9	8.21 ± 0.04
	0.9	15 ± 1.6	109.4 ± 16.6	924.5 ± 2.3	635.0 ± 21.2	8.72 ± 0.07
70C:30WBS	AD	18 ± 0.9	173.8 ± 4	705.0 ± 146.7	666.7 ± 47.1	8.45 ± 0.08
	OC	19 ± 0.7	225.3 ± 14.2	996.2 ± 163.7	733.3 ± 0.5	8.30 ± 0.13
	0.3	18 ± 0.2	190.9± 2.6	854.4 ± 92.2	550.0 ± 23.6	8.42 ± 0.03
	0.7	21 ± 1.3	120.7 ± 14.9	836.5 ± 6.9	605.0 ± 7.1	8.31 ± 0.13
	0.9	20 ± 0.1	96.2 ± 73.1	810.4 ± 186.8	665.0 ± 77.8	8.59 ± 0.03
30C:70WBS	AD	20 ± 0.5	234.6 ± 46.3	1009.3 ± 200.6	683.3 ± 70.7	8.35 ± 0.01
	OC	23 ± 0.9	205.6 ±26.1	1045.2 ± 16.1	750.0 ± 23.6	8.60 ± 0.37
	0.3	21± 1.3	169.7 ± 45.2	882.1 ± 34.6	566.7 ± 47.1	8.79 ± 0.07
	0.7	22 ± 5.8	73.7 ± 22.7	815.3 ± 27.7	610.2 ± 7.2	8.64 ± 0.02
	0.9	24 ± 0.1	167.2 ± 118.1	935.9 ± 83.0	710.0 ± 56.6	8.65 ± 0.06
0C:100WBS	AD	25 ± 0.7	42.0 ± 3.1	1161.2 ± 69.6	1,110 ± 391.3	8.41 ± 0.03
	OC	24 ± 2.3	114.5 ± 5.4	934.3 ± 103.8	816.7 ± 2117.9	8.5 ± 0.08
	0.3	24 ± 1.9	44.4 ± 8.6	986.5 ± 76.1	683.3 ± 117.9	8.79 ± 0.54
	0.7	26 ± 2.8	79.4 ± 9	694.6 ± 170.6	550.2 ± 169.7	8.58 ± 0.01
	0.9	24 ± 1.5	57.3 ± 0.7	844.6 ± 13.8	640.0 ± 56.6	8.7 ± 0.09

To provide a comparison between different feed compositions methane production in the reactors were normalized per net methane produced over added VS (Figure 4.2). The net methane yield was calculated by subtracting the methane produced in

the Blank reactors. Among 100C:0WBS fed reactors, the highest yield of 128.3 ± 4.66 mL net CH_4/g VS_{added} was attained in 0.9 V applied reactors corresponding to a 70% increase with respect to the yield (75.5 ± 7.3 mL net CH_4/g VS_{added}) attained in AD controls (Figure 4.2A). With 100C:0WBS even though the yields recorded in OC, 0.3 V and 0.7 V reactors were all higher than AD (at an average by 21%), they were similar to each other. Hence, the enhancement may be attributed to voltage application only in the case of 0.9 V and the enhancement in 0.3 V and 0.7 V applied reactors may only stem from the positive impact of biomass attachment. It is proven that the presence of the electrodes in anaerobic digesters provide enhancement in the performance of digestion. Yet this is unrelated to the electrochemical interaction with the electrodes, rather the electrodes are beneficial because they provide additional surface area for microbial adhesion and retention (Baek et al., 2021; de Vrieze et al. 2014). There was no measurable impact of current generation (applied voltages of 0.5 V and 1.0 V) on methane production compared to an OC control (de Vrieze et al., 2014). However, when the electrodes were removed from the OC controls methane production significantly decreased, indicating that a key factor in the AD-MEC configuration was the biomass retention in the electrodes (de Vrieze et al., 2014).

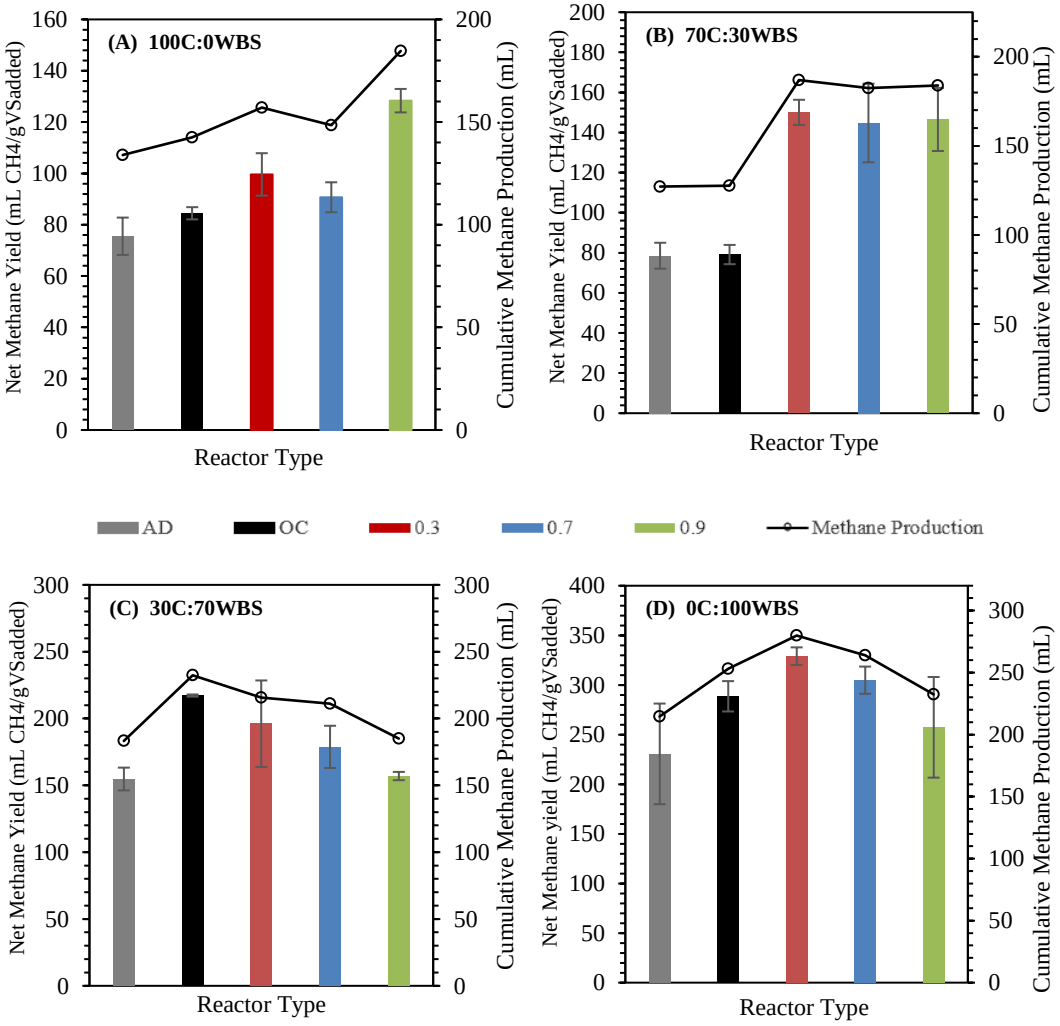

Figure 4.2 Methane yields in A) 100C:0W, B) 70C:30W, C) 30C:70W and D) 0C:100W reactors

Clearly, in terms of the yield of methane only 0.9 V provided a significant advantage. With 70C:30WBS, when yields were analyzed, it was clear that all AD-MEC reactors showed a higher biomethane yield than AD and OC controls. The highest yield with 70C:30WBS was 150.07 ± 6.3 mL net CH_4/g VS_{added} recorded in 0.3 reactors, corresponding to almost 91% increase with respect to AD. Similar to 70C:30WBS, the highest average yield was attained in 0.3 reactors with 30C:70WBS and 0C:100WBS reactors. Yet only the difference (~43%) between 0C:100WBS_0.3

and AD controls was considerable due to the variation in the replicate reactors (see the error bars in Figure 4.2.C and D).

On the other hand, as expected from the cumulative methane production data, there was no significant increase in yield of WBS dominant reactors except 0C:100WBS_0.3. Yield of 30C:70WBS_OC reactor has the highest yield over the 30C:70WBS reactors. There are a limited number of studies where complex wastes such as WAS and animal manure have been used as feed of AD-MEC reactors. In most of these studies, different units were used to provide methane yields such volume of methane per removed COD, volume of methane per removed VSS and volume of methane per removed VS which makes it difficult to compare (Table 4.3). Yet, in most of these studies a conventional AD reactor was also operated as a control and for comparison the yield enhancements are provided with respect to control in Table 4.3.

Clearly, direct comparison between the performances is not possible without the same reactor configuration, materials, and reactor operational conditions in AD-MEC systems The literature comparison shows that WBS combination has never been used in the field. The study is unique in this regard. Normalized improvement on yield basis can be utilized to assess AD-MEC system performance. Methane improved 70% on C fed 0.9 V applied reactors in Set 1. It had a better yield improvement with batch system at 0.9V than prior studies stated in Table 4.3. Similar studies found less improvement with higher voltages like 1.2 and 3.5. (Table 4.3).

Table 4.3 Comparison of the performance of AD-MEC integrated systems methane production yields from this study and literature

Substrate	Working volume (mL)	Reactor Type	T (°C)	Applied Voltage (V)	Anode Material	Cathode Material	CH_4 Improvement in Comparison to Control	Reference
Cattle Manure + Aloe Peel Waste	300	Batch	36	0.6	Graphite Rods	Graphite Rods	64% yield increase [a]	(Xing et al, 2021)
Cow Dung	600	Batch	20	1	Graphite	Stainless Steel	17-45% increase*	(Jiao et al 2022)
Cattle Manure	350	Batch	35	3.5	IrO_2-covered titanium mesh	Stainless Steel	32% increase*	(Tartakovsky et al., 2014)
Dairy Manure	8000	Continuous	35	1.2	Graphite Plate	Stainless Steel Cylinder	137% increase*	(Hassanein et al., 2020)
Cattle Manure	65	Batch	35	0.9	Graphite Plate	Stainles Steel Mesh	70% increase	This study
WAS	2000	Batch	35	0.3	Fe Tube	Graphite Pillar	22.4 % yield increase [b]	(Feng et al., 2015)
WAS	690	Batch	20	0.8	Carbon Brush	Carbon Cloth	97% increase*	(Bao et al., 2020)
WAS	800	Batch	35	0.3,0.6	Reticulated vitreouscarbon	Reticulated vitreouscarbon	9.4% yield increase on both voltage [c]	(Gajaraj et al., 2017)
WAS	1000	Batch	35	0.6	Activated Carbonfiber Textile	Activated Carbonfiber Textile	40% yield increase at 0.6V [a]	(Chen et al., 2016)
WBS	65	Batch	35	0.3	Graphite Plate	Stainless Steel Mesh	43% yield increase [a]	This study

* Improvement of methane stated as increase in cumulative methane production
[a]mL/gVS
[b]L/kgVSS
[c]mL/COD

Higher increase on cumulative methane production were stated with the continuous system at 1.2 V with much higher working volume and different electrode configuration. To the best of our knowledge, we report a nice point on methane increase within the literature.

With sludge-fed AD-MECs, different voltages (0.3–1.5 V) were applied to study the effect of electrical stimulation on WAS anaerobic digestion. 0.9 V inhibited methane production, whereas 0.6V produced the most (Feng et al., 2015). In our study, with the implementation of 0.3 V and relatively cheap materials on anode and cathode we acquired 37% percent increase on yield basis within WBS fed reactors.

Current production and electrochemical activity

Current production in AD-MEC reactors is associated with the oxidation organics and release of electrons to the anode via the activity of exoelectrogenic microorganisms forming (Kas and Yilmazel, 2022). Current density profiles of 100C:0WBS fed AD-MEC reactors are given in Figure 4.3A. There was a good replication between the duplicate reactors, and the highest peak current was attained at 100C:0WBS_0.9 reactors at around 0.33 mA/cm^2, which was followed by the 100C:0WBS_0.7 reactors producing peak current around 0.19 mA/cm^2. The current production in duplicate reactors of each applied voltage is provided Appendix B. On the other hand, 0.3 V applied reactors no appreciable current was observed (<0.05 mA/cm^2 throughout operation).

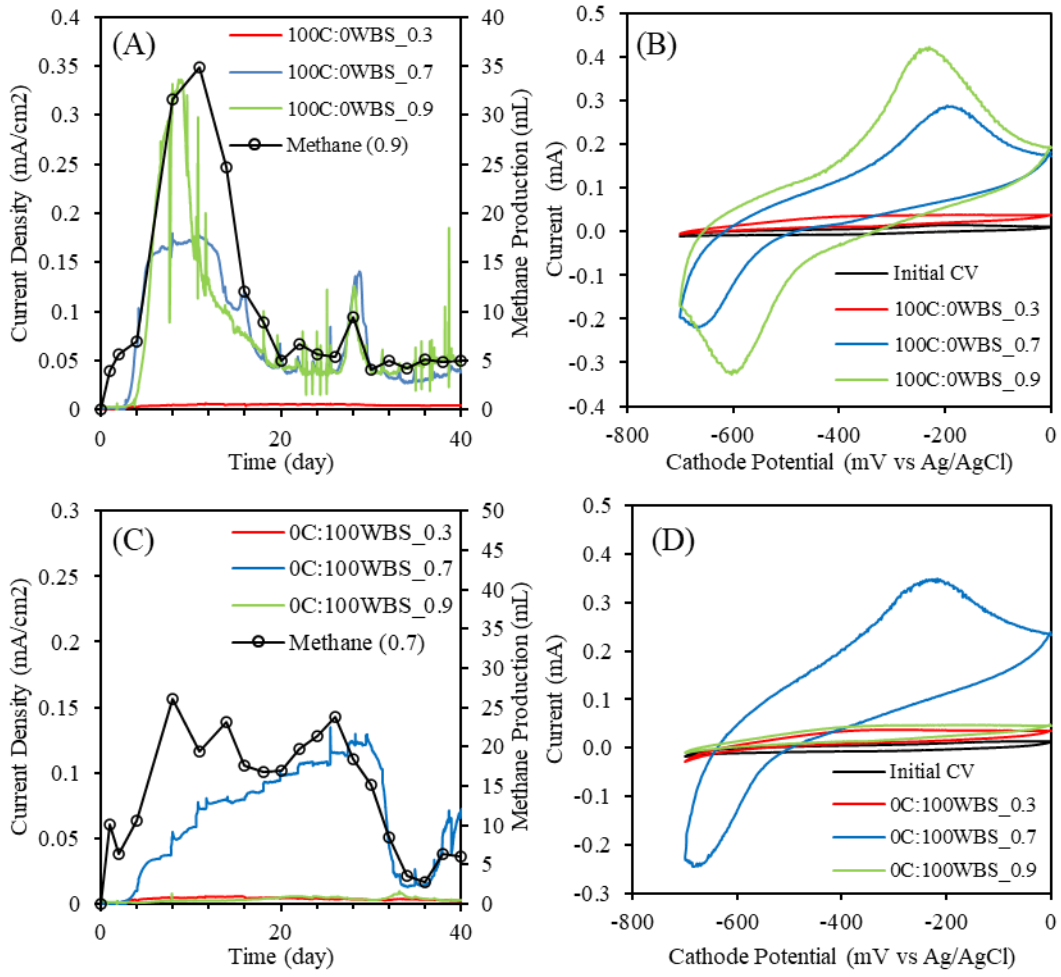

Figure 4.3 A) Current density and methane production of 100C:0W reactors, B) CV profiles of 100C:0W reactors, C) Current density and methane production of 0C:100W reactors, and D) CV profiles of 0C:100W reactors

During AD-MEC reactor operation current was monitored continuously and while methane production was measured manually periodically during the operation. When bioelectrochemical reactor operation, *i.e* applied voltage in AD-MEC system, was the major factor in enhancing methane production there was a good correlation between methane production and current density graphs as given in Figure 4.3. For example, in the case of 100C:0WBS_0.9, where the highest enhancement in methane with 100C:0WBS feed was recorded, there was a clear correlation between the methane production and current density as shown in Figure 4.3A. The peak current

around 0.33 mA/cm^2 was recorded at around day 8 and methane production was peaked around day 11 (Figure 4.3A). On the other hand, for 0C:100WBS feed, where AD-MEC reactor operation did not provide a significant improvement in the performance no such correlation was present. The highest enhancement among 0C:100WBS was recorded in the case of 0.3 V application, yet even with the 0C:100WBS_0.3 reactors no appreciable current production (< 0.005 mA/cm^2) was observed (Figure 4.3C). Contrary to 0.3 V applied reactors, there is a correlation between methane production and current density in 0.7 V applied reactors. However, regardless the highest methane production was recorded at 0.3 V application with 100WBS.

Further, CV of cathodic biofilms at the beginning and the end of operation was performed to evaluate the electrochemical activity of cathodic biofilms (Hua et al., 2019). The cathodic peaks observed in the voltammogram in the CV experiment for 100C:0WBS reactors (Figure 4.3A) also provide evidence that there was a biofilm formation over the electrodes with application of 0.7 V and 0.9 V and the graph shows a correlation with the current density profiles and methane generation in these reactors. Current density and CV profiles clarify that if there is no current produced within the reactors it cannot form a biofilm over the electrodes. 100C:0WBS_0.3 reactors had no current generation over the study period, also CV shows no indication of biofilm formation over the cathode indicated by the absence of reduction peaks. For example, in 100C:0WBS_0.9 reactors the highest peak in current profiles was attained and also the clearest cathodic peak was recorded in the CV profile of its cathodes. All other CV profiles are given in Appendix C. Cathodic peaks observed in the CV of 70C:30WBS reactors provide evidence that there was a biofilm formation over the electrodes with applied voltage of 0.7 V and 0.9 V. Even though the scales were different there was a cathodic reduction peak in both duplicate reactors at these applied voltages. Cathodic peaks of 30C:70WBS reactors provide evidence of biofilm formation over the electrodes in 0.7 and 0.9 V likewise in 100C:0WBS and 70C:30WBS reactors.

4.1.2 Part 2: AD-MEC Operation with Bioelectrodes (Impact of Bioelectrode)

Methane Production

Using bioelectrodes with 0.7 V increased the cumulative methane production by 48% with respect to conventional AD (136 ± 11.1 mL) (Figure 4.4A). For 70C:30WBS reactors, average cumulative methane production in 70C:30WBS_Bare_0.7 was averaged at 183 ± 16.4 mL while the production in 70C:30WBS_Bio_0.7 was averaged 219 ± 0.5 mL CH_4 (Figure 4.4B). Bioelectrode reactors produced around 20% more methane than bare electrode reactors with 70C:30WBS feed. Usage of biofilm formed electrodes has significant impact on the VS removal efficiency amongst 100C:0WBS and 70C:30WBS reactors. VS removal efficiency were 17% and 21% for bare 100C:0WBS and 70C:30WBS, respectively. Due to the biofilm formed electrode usage, removal efficiency of 100C:0WBS increased to 23% and 28% percent which makes around 6 to 7% percent increased removal efficiency on VS basis.

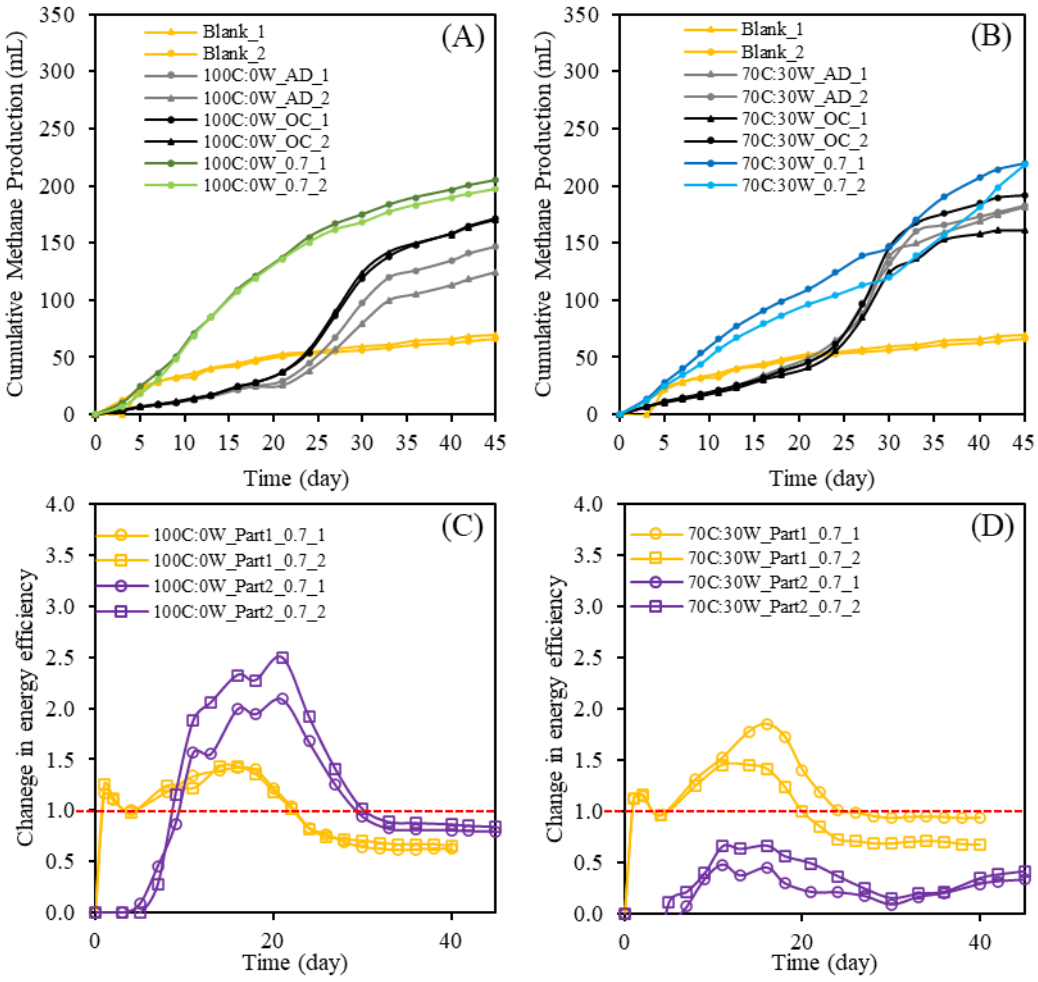

Figure 4.4 A) Cumulative methane production in 100C:0W_Bio reactors, B) Cumulative methane production in 0C:100W_Bio reactors, C) Change in energy recovery efficiency in 100C:0W_0.7 reactors, and D) Change in energy recovery efficiency in 70C:30W reactors (Duplicate reactors are shown by the same color, and indicated as 1 to 2)

Based on the modified Gompertz model fitting (Appendix F), in the Part 2, with the usage of already developed bioelectrodes (even after long wait period), methane production rate at of 100C:0WBS_0.7 increased from 5.0 mL/d to 8.2 mL/d and there was around 78% reduction in lag time in comparison to AD control. However, no such increase was recorded with 70C:30WBS feed, only a significant decrease

(~90%) was recorded in the lag time when AD-MEC with bioelectrodes were operated (Table 4.4).

Table 4.4 Kinetic parameters calculated from the fitting with the modified Gompertz model of Part 2 reactors

Feed Mixing Ratio	Reactor	P_∞ (mL)	R_m (mL/d)	λ (d)	R^2
100C:0WBS	AD	183.2	5.0	13.5	0.981
	OC	198.1 (8)	7.4 (48)	14.7 (-)	0.987
	0.7	201.0 (10)	8.2 (64)	3.0 (78)	0.998
70C:30WBS	AD	263.2	6.7	12.1	0.981
	OC	265.3 (1)	6.8 (1)	12.7 (-)	0.976
	0.7	290.4 (10)	5.1 (-)	1.2 (90)	0.983

Current density profiles of reactors in Part 2 are given in Figure 4.6. After day 25, most of the methane production was completed in 100C:0WBS reactors (Figure 4.4A) and this was corresponding to the drop in the current as given in Figure 4.5A.

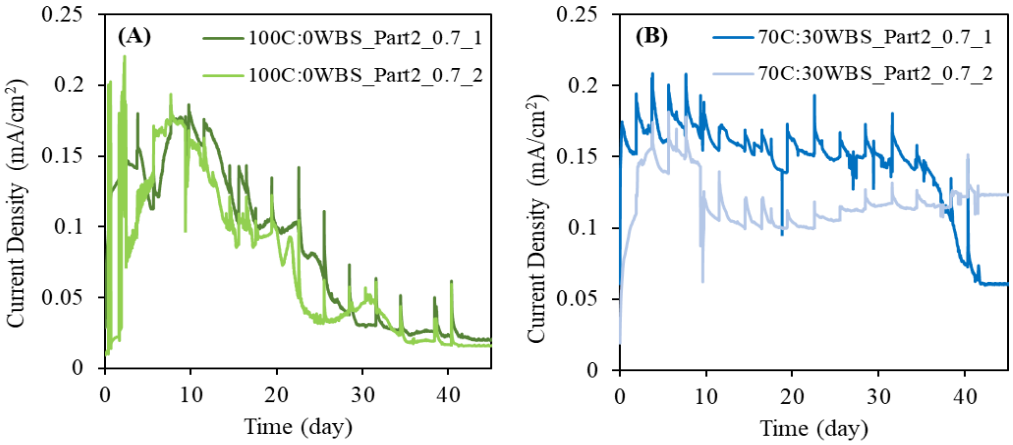

Figure 4.5 Current density graphs of reactors in Part 2

(Duplicate reactors are shown by the same color, and indicated as 1 to 2)

On day 40 current started to drop 70C:30WBS_Bio_0.7_1 reactor also methane production started to plateau on day 40 reactor (Figure 4.4B and Figure 4.5B). As seen in Figure 4.4B, the increase in methane production in one of the duplicates, however, lasted even after 45 days. Similarly, no drop was observed in the current density graph of this duplicate reactor (light blue color, Figure 4.5B).

Change in energy recovery efficieny

Energy recovery efficiency calculations showed that the usage of bioelectrodes shows more efficient system when it compared with the bare versions of the same electrode for 100C:0WBS reactors (Figure 4.4C). According to the calculations held on (Eq. 3.4) change in energy efficiency value will be stated as 1 if the system is same as in conventional AD. If the number calculated is greater than 1 than the AD-MEC system is energy positive. With bioelectrodes in the AD-MEC system, results showed promising outcomes with an increase in energy recovery efficiencies compared to the conventional AD when C used as the substrate. However, no such improvement was recorded with 70C:30WBS, as current production was stable in in AD-MEC reactors of Part 2.

4.2 Set 2: Effect of Bioelectrodes and Feed Pre-treatment on Methane Production from WBS in AD-MEC Systems

Comparatively lower performance of the WBS reactors in Set 1 showed that, using different voltages on WBS fed AD-MEC systems does not have significant effect on methane production with SS mesh cathodes. Hence, to determine whether there will be any enhancement in the performance, the effects of using bioelectrodes and pretreatment of WBS on AD-MEC system was investigated in this set. Experimental design of Set 2 is provided in Table 3.11 and a schematic is given in Figure 3.8.

The impact of feed pretreatment

In this part, feed pretreatment was applied to WBS to increase the hydrolysis rate and sCOD content of the feed. In the literature, there are a number of pretreatment methods applied to sludge samples (Bao et al., 2020; H. Hou et al., 2020; J. Liu et al., 2016). The objective here was to choose the mildest treatment methods to avoid the release of toxic compounds to the solution. Therefore, for pretreatment three different methods were used: autoclaving, alkali treatment and heat treatment. The details of the methods are given in Table 3.4.

In order to choose the most effective pretreatment method, sCOD analysis was conducted for pretreated WBS samples and the results were compared with the raw WBS sample (Table 4.5). Based on the measurements, autoclaving provided highest increase in sCOD. The sCOD concentration in autoclaved WBS was around 3 times higher than sCOD concentration in raw WBS sample.

Table 4.4 sCOD concentrations of WBS samples after different feed pretreatment applications

Sample	**sCOD (mg/L)**
WBS	2508.75 ± 30
Autoclaved WBS	7827.5 ± 470
30 min hWBS*	3434 ± 28
1hr hWBS	4029 ± 82
30 min aWBS**	3097.5 ± 193
1hr aWBS	3265.5 ± 68

*hWBS: Heat treated WBS
**aWBS: Alkali treated WBS

Autoclave choosen as the pretreatment method since increase in sCOD was higher among all methods. Pretreated WBS named as pWBS throughout all parts of the Set 2. Characterization of the pWBS is given in Table 4.6.

Table 4.5 Characterization of the pWBS (Part 2)

Parameter	pWBS at Run 1	pWBS at Run 2
pH	6.39	6.45
TS (%)	3.08 ± 0.01	2.4 ± 0.02
VS (%)	1.84 ± 0.002	1.4 ± 0.01
VS (% of TS)	0.59 ± 0.01	0.58 ± 0.02
COD (mg/L)	57,894 ± 1,285	54,118 ± 2,895
sCOD (mg/L)	7827.5 ± 470	6845.5 ± 610

4.2.1 Part 1: Biofilm formation

Experimental design is given in Table 3.10. During fed-batch operation, each time the Gr reactors were fed within 42 days of operation, the SS mesh reactors were also fed in the same way. When the current density (mA/cm^2) drops below 0.08, the new cycle is started with feeding the reactors with acetic acid. While activity was observed in Gr reactors apparent with currrent generation, no similar activity was observed in SS mesh reactors and the current level is quite low (Figure 4.6). In Set 1 experiments there was no current generation with SS mesh with WBS feed and here again there was no stable current production with SS mesh cathode with filtered WBS feed. Hence, in the light of the data obtained from two different sets, using SS mesh as the electrode material is not suitable for biofilm formation in WBS fed system. SS mesh is a material where hydrogen evolotion reaction can take place on the surface, hence it is used as cathode in MECs for hydrogen production (Kas and Yilmazel, 2022). Yet, the evolved hydrogen may inhibit biofilm attachment in WBS

fed systems. Therefore, graphite electrodes were used as cathode in the rest of the experiments of this set.

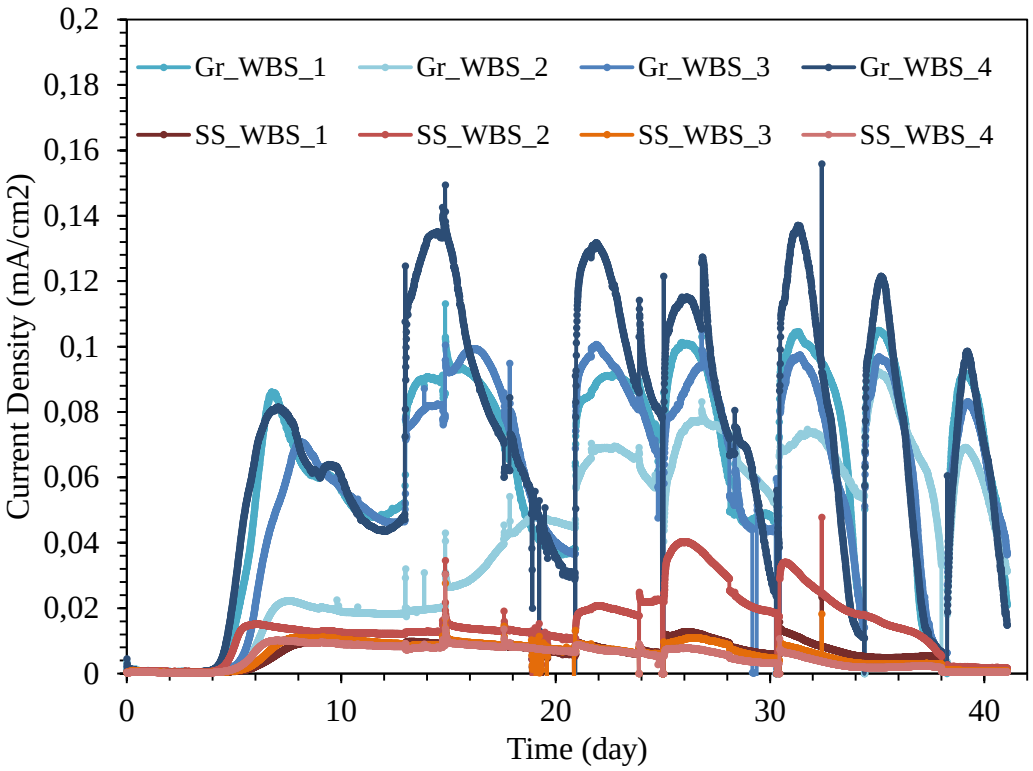

Figure 4.6 Current density profiles of Gr_WBS and SS_WBS reactors (Replicate reactors are shown by the same color, and indicated as 1 to 2)

In order to observe the effect of feed difference on bioelectrodes, acetate was chosen as the second feed since it is not complex and suitable for consumption of most electro-active microorganisms. Acetate fed MECs serve as a positive control in the experiments. Gr_WBS reactors, which were operated together with SS_WBS reactors, continued to be operated without shutdown after 4 Gr_Ace reactors were started (Figure 4.7 and Figure 4.8). Once acetate fed reactors were also added to the experimental design, these reactors were operated for about 40 days . The aim of this

was to achieve the same current density values the bioelectrodes intended to be transported to the AD-MEC part.

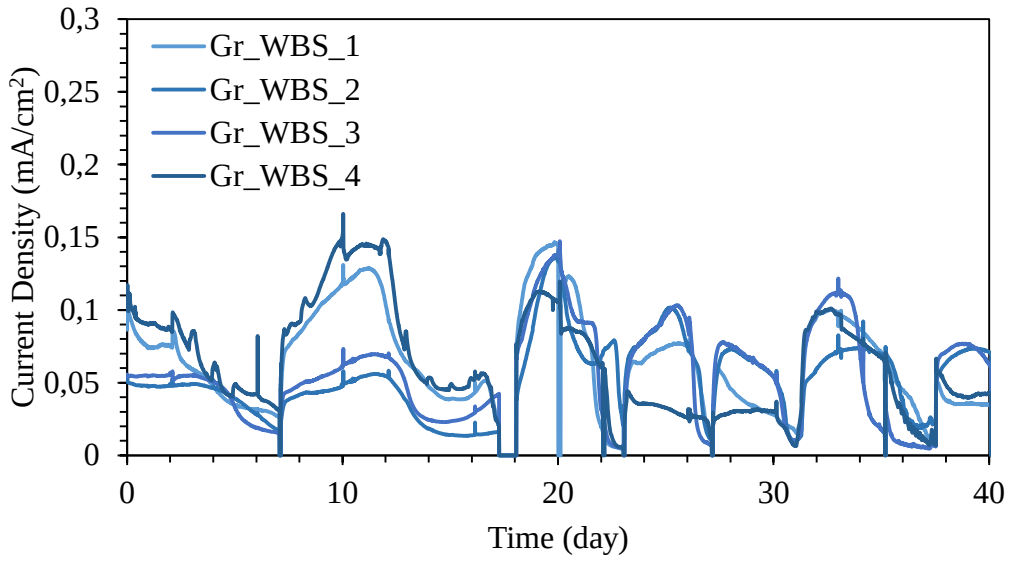

Figure 4.7 Current density profiles of Gr_WBS reactors

(Replicate reactors are shown by the same color, and indicated as 1 to 2)

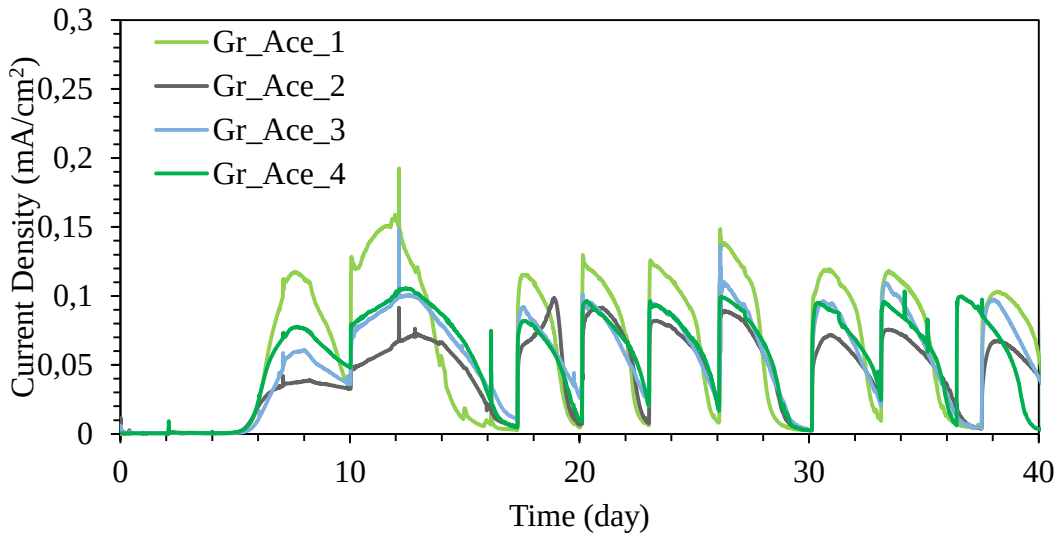

Figure 4.8 Current density profiles of Gr_Ace

(Replicate reactors are shown by the same color, and indicated as 1 to 4)

In order to make sure there were biofilm formation over the electrodes for each substrate, CV analysis was held on (Figure 4.9). Due to the increased number of reactors, one reactor of each feed is selected as the control for CV analysis.

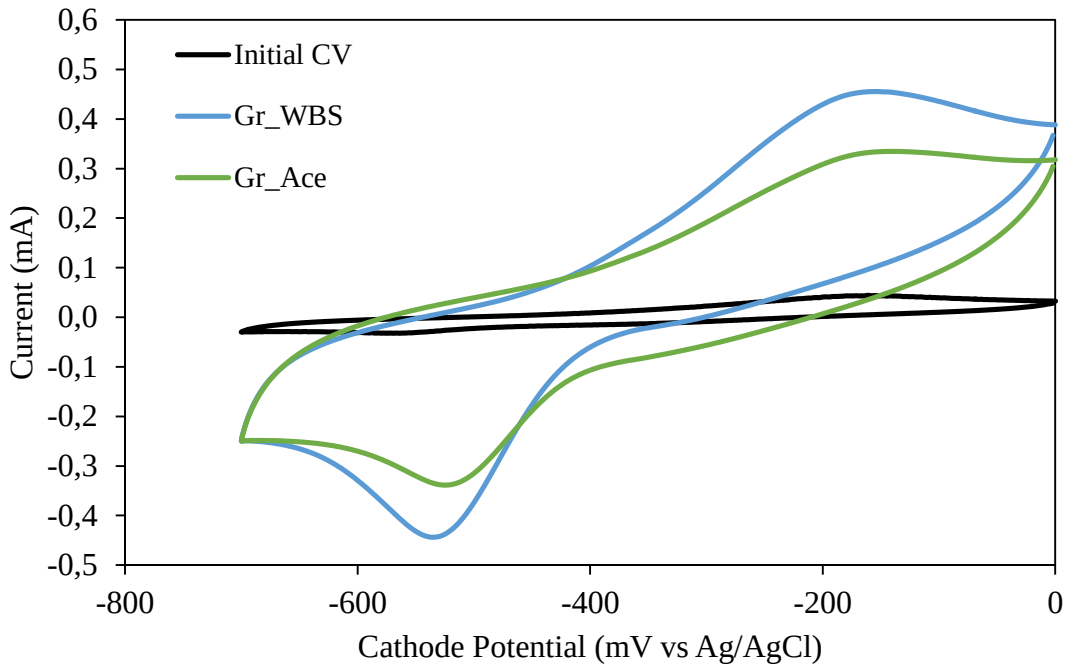

Figure 4.9 CV profiles of Gr_WBS and Gr_Ace reactors at the end of biofilm formation (Part 1)

4.2.2 Part 2: AD-MEC operation

The experimental design of Part 2 is provided in Table 3.11 and briefly described in Figure 3.8. In this part, the objective was to compare the methane production performance of AD-MEC reactors and determine the relative importance of the use of bioelectrodes and feed pretreatment. There were in total two experimental runs in this part and the results will be presented for each run separately.

4.2.2.1 Run 1: Impact of Bioelectrodes and Pre-treatment

Methane Production

The cumulative methane production of the reactors in Run 1 is given in Figure 4.10. The highest cumulative methane production of 228.8 ± 0.7 mL was recorded in pWBS_0.7 reactors, while the lowest cumulative methane production was recorded in AD reactors with 199.6 ± 4.9 mL. This is corresponding to around 15% increase in cumulative methane production in AD-MEC reactor fed with pretreated WBS and operated at applied voltage of 0.7 V with respect to the conventional AD. The increase in cumulative methane production in pWBS_0.7 reactors with respect to the pAD controls is around 6.4%. The percentage difference in cumulative methane production between pAD and pWBS_0.7 were almost the same as the percentage difference between the AD control and Bare_0.7 reactors. In the case of Bare_0.7 reactors, which were fed with the raw WBS and housed bare electrodes, cumulative methane production averaged at 211.1 ± 0.1 mL, which corresponds to a 5.8% increase with respect to the AD. Hence, it can be concluded that AD-MEC operation at 0.7 V slightly increased methane production (~ 6%) over AD with the WBS feed independent of presence of pretreatment.

The impact of bioelectrodes and providing external surface area via placing electrodes into the reactors was assessed by operation of OC controls and bioelectrode reactors. OC reactors with bioelectrodes (WBS_Bio_OC, Ace_Bio_OC) produced similar amount of methane around 199 mL, while AD and OC controls produced around 197 mL during the 15 days of reactor operation (Figure 4.10). In both AD and OC reactors regardless of pre-colonization of electrodes similar methane productions were recorded. This can be interpreted as low impact of providing external surface area for biomass attachment in methane production. In the literature, positive impacts of OC reactors have been reported and this may be due to higher surface area/volume ratio used in other studies. It has been demonstrated that the addition of electrodes to anaerobic digesters results in an improvement in the efficacy of the digestion process. This is due to the fact that electrodes offer an

increased surface area for the adhesion and retention of microbes (de Vrieze et al., 2014). To summarize, there was no significant change in cumulative methane production in bioelectrode inserted OC reactors in comparison to AD.

Addition of 0.7 V to the bioelectrodes housing AD-MEC reactors increased the cumulative methane slightly. There was 206.8 ± 3.2 mL methene production in WBS_Bio_0.7 and 205.3 ± 1.6 mL in Ace_Bio_0.7 reactors. This corresponds to around 4% increase with respect to their respective OC controls. Clearly, substrate used during biofilm formation (Part 1) also did not lead to a change in the cumulative methane production in the Run 1. Filtered WBS and acetate were used to form bioelectrodes, yet both bioelectrode reactors produced similar amounts of methane regardless of the substrate.

If only pretreatment impact is to be analyzed, comparison of AD and pAD reactors is required. The cumulative methane in AD reactors were averaged at 199.6 ± 4.9 mL, while pAD reactors produced 215.0 ± 9.3 mL of methane. The difference between AD and pAD in the cumulative methane production is around 7.5%.

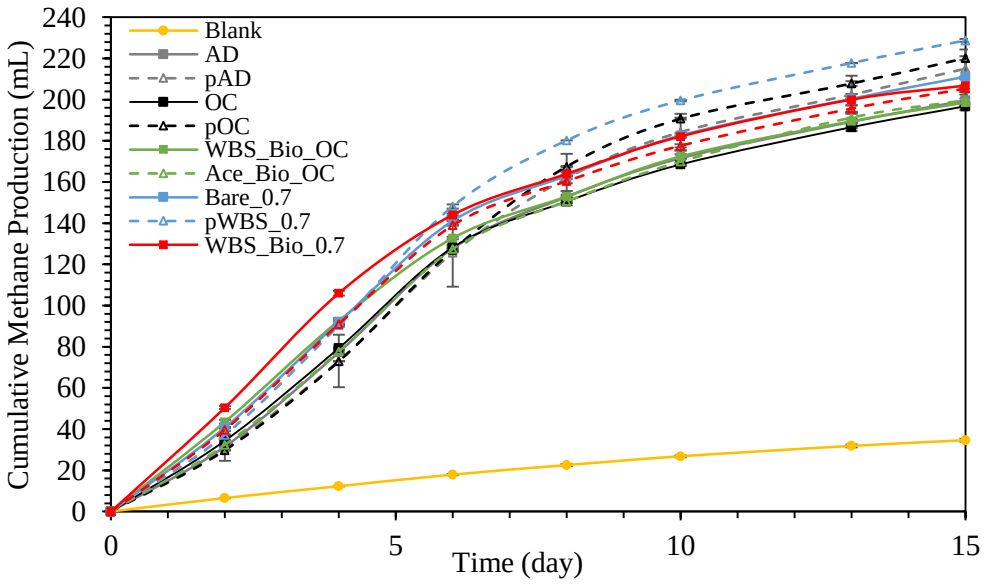

Figure 4.10 Cumulative methane production in reactors in Run 1 (Error bars may be smaller than symbol size)

The modified Gompertz equation (Eq.3.3) was used to fit the methane production data in each reactor (Table 4.7). Based on Gompertz fitting (All fitting graphs given in Appendix G) reactor performances can be compared based on increase in the methane production rate and decrease in the lag phase. With the implementation bioelectrodes, there was always an improvement in the lag phase. Here, there was a difference among different feeds used during acclimation phase of electrodes. For example, among OC reactors where no voltage was applied bioelectrodes developed with filtered WBS showed 74% decrease in lag phase, while bioelectrodes developed with acetate showed only 10% decrease in lag phase in comparison to AD. When they were directly inserted into the reactors without any previous colonization step as in OC reactors, the decrease in lag phase was around 18%. Additionally, when voltage was applied acetate acclimated electrodes decreased the lag time by 34%, while WBS fed bioelectrodes decreased the lag time by 74%. On the other hand, when there was no previous colonization step, *i.e.*, biofilm formation part, a 37% decrease in lag phase was attained. This may imply that the choice of the substrate in Part 1 affects the start-up time of the reactors. It is better to use the same feed during both Part 1 and Part 2 rather than starting-up the reactors with a simple substrate such as acetate. The reason can be explained by the fact that the primary substrate is effective in shaping the electro-active biofilm on the electrodes and the secondary substrate is less significant because the first settlers resist on the electrode surface as detailed in a recent work (Harnisch & Korth, 2021). In their study, Harnish and Korth (2021) studied the impact of changing substrates on microbial community on the electrodes and reported that the microorganism that first colonized on the electrode occupies the surface and hence forms most of the biofilm community.

For all pWBS fed reactors, there was a slight increase in the lag time. Among pWBS fed reactors there was a decrease in lag time with AD-MEC operation (pWBS_0.7) in comparison to pAD. The decrease was around 18%.

Methane production rate (R_m) was also compared; around 8% increase was recorded with WBS_Bio_0.7 reactors, while 4% increase was recorded in Ace_Bio_0.7 and Bare_0.7 reactors in comparison to AD. These results, support the finding about

biofilm formation substrate; if colonization is to be done then it should be performed with the same substrate. The highest increase in the rate was attained with the pWBS_0.7 reactor, which provided around 16% increase in the methane production rate in comparison to AD. When the increase in methane production rate of pWBS_0.7 reactor is calculated with respect to pAD, there was around 12% increase. This increase is 3 times more than the increase attained by Bare_0.7 when compared to AD. Based on these results, even though the differences are not high it may be concluded that the benefit of using AD-MEC over AD depends on the complexity of the substrate. The impact of sole pretreatment in the methane production rate can be determined by comparison of pAD and AD rates, the increase in pAD was around 4%, similar to the increase attained by Bare_0.7.

Table 4.6 Gompertz Results of Run 1

Run Number	**Reactor**	**P**	**R**	**λ (d)**	**R^2**
Run 1	AD	199	25	0.9	0.998
	OC	196 (-)	24 (-)	0.7 (18)	0.997
	WBS_Bio_OC	197 (-)	24 (-)	0.3 (63)	0.995
	Ace_Bio_OC	201 (1)	24 (-)	0.8 (10)	0.997
	WBS_Bio_0.7	204 (3)	27 (8)	0.2 (74)	0.993
	Ace_Bio_0.7	203 (2)	26 (4)	0.6 (34)	0.996
	Bare_0.7	209 (5)	26 (4)	0.6 (37)	0.996
	pAD	218 (10)	26 (4)	1.1(-)	0.999
	pOC	224 (13)(3)	27 (8)(4)	1.2 (-)(-)	0.999
	pWBS_0.7	228 (15)(5)	29 (16)(12)	0.9 (-)(18)	0.998

*The number in parenthesis indicates the percentage increase in $\mathbf{P}_{\infty}$ and, $\mathbf{R_m}$ and decrease in $\boldsymbol{\lambda}$ with respect to: (1) AD; (2) pAD; (-) indicates no enhancement.

Methane production in the reactors were normalized per VS added on a net basis as in Set 1 (Figure 4.11). Among reactors, the highest yield of 426.7 ± 1.6 mL CH_4/g VS_{added} was attained in pWBS_0.7 reactors corresponding to a 13% increase with respect to the yield (377.3 ± 11.1 mL CH_4/g VS_{added}) attained in AD controls. Yields recorded in OC, Ace_Bio_OC and WBS_Bio_OC reactors were similar with AD at an average by 2% difference. Hence, the enhancement may be attributed to voltage application only in the case of 0.7 V applied reactors, since there was an 8% increase in Bare_0.7 reactors with respect to the yield attained in AD control and its corresponding OC control had lower yield.

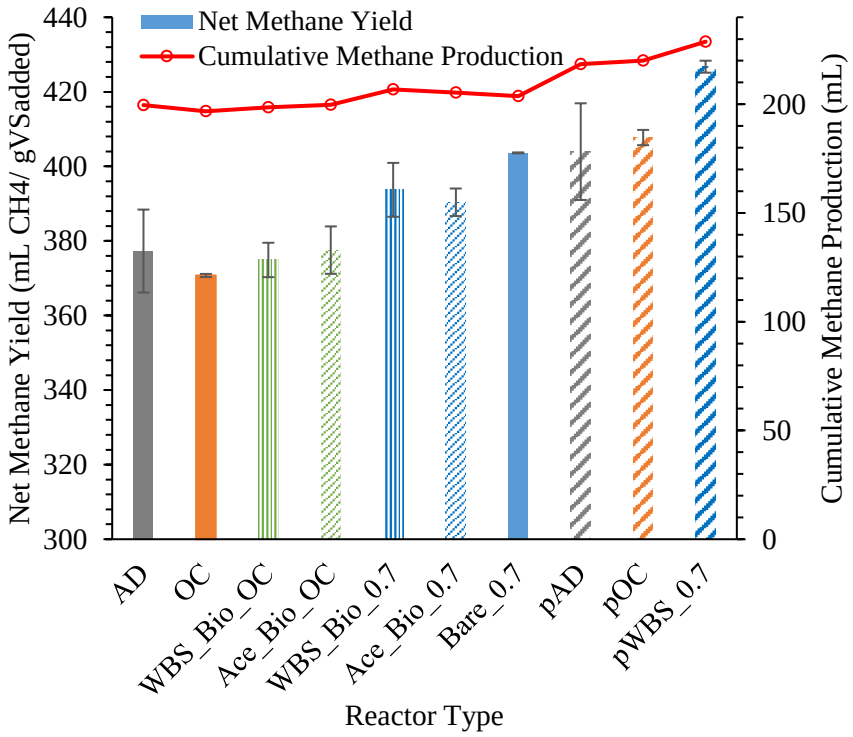

Figure 4.11 Methane yield and cumulative methane production in Run 1

Clearly, in terms of the yield of methane, pWBS feed provided a minor advantage. With pWBS, when yields were analyzed, it was clear that all reactors showed a higher biomethane yield than raw WBS fed reactors, pWBS_0.7 showed an increase compared to the AD (13%). Yet, the difference (~5%) between pWBS_0.7 and pAD controls was similar to the difference on yield basis of Bare_0.7 and AD reactors

which were fed with the raw WBS. Additionally, there were no significant impact of bioelectrodes on methane production. AD and different OC reactors had similar methane yields, while Bare_0.7 increased the methane yield by 8% in comparison to AD. This clarifies that, regardless of the feed pretreatment when WBS is used as feed, implementation of MEC into AD system at an applied voltage of 0.7 V provide a slight positive impact on methane production yield ranging between 5-8% in comparison to conventional AD.

An examination of the relevant literature revealed that WBS combination has been tested in field limitedly (Table 4.3). Without the same reactor structure, materials, and reactor operational circumstances, it is not feasible to directly compare the performance indicators in AD-MEC systems (Logan et al., 2019). However, AD-MEC system performance may be measured using normalized improvement on yield basis. Comparable experiments obtained varying rates of improvement depending on operational variations, such as electrode type and applied voltage (Table 2.1 and 2.2). Different electrode configurations and voltages were reported to boost cumulative methane generation. Methane yields have been reported in a wide variety of studies but comparing them can be challenging since most of them utilize various units, such as volume of methane per COD removed, volume of methane per VSS removed, and volume of methane per VS removed (Table 4.3). Yet, in the majority of these studies, a traditional AD reactor was also operated, and Table 4.3 provides a comparison of the yield gains according to the AD reactors.

According to the literature review stated in Chapter 2, research studies that uses WAS as the main substrate, it is evident that the results are diverse and that no correlation with the applied voltage could be observed. As an example, several voltages (0.3–1.5 V) were used to examine the effect of electrical stimulation on the anaerobic digestion of WAS, and the results indicated that 0.9 V had a considerable inhibitory effect on methane generation, while 0.6 V resulted in the highest methane output (Feng et al., 2015). In Set 1 of this thesis, with the implementation of 0.3 V 43% percent increase on yield basis achieved within WBS fed reactors. With 0.7 V the increase is even lower.

Current Production and Electrochemical Activity

The oxidation of organic compounds and the transfer of electrons from the cathode to the anode as a result of the activity of exoelectrogenic microorganisms are responsible for the production of current in AD-MEC reactors (Kas and Yilmazel, 2022). During the operation of the AD-MEC reactor, the current was monitored continually and primarily, whilst the generation of methane was measured manually periodically during the operation. Current density profiles of AD-MEC reactors at Run 1 are given in Figure 4.12. There was a good replication of the duplicate reactors, and the highest peak current was attained at Ace_Bio_0.7 reactors at around 0.10 mA/cm^2, which was followed by the pWBS_0.7 reactors producing peak current around 0.08 mA/cm^2 (Figure 4.12). On the other hand, Bare and WBS_Bio_0.7 reactors reach up to 0.05mA/cm^2 at max throughout the operation time.

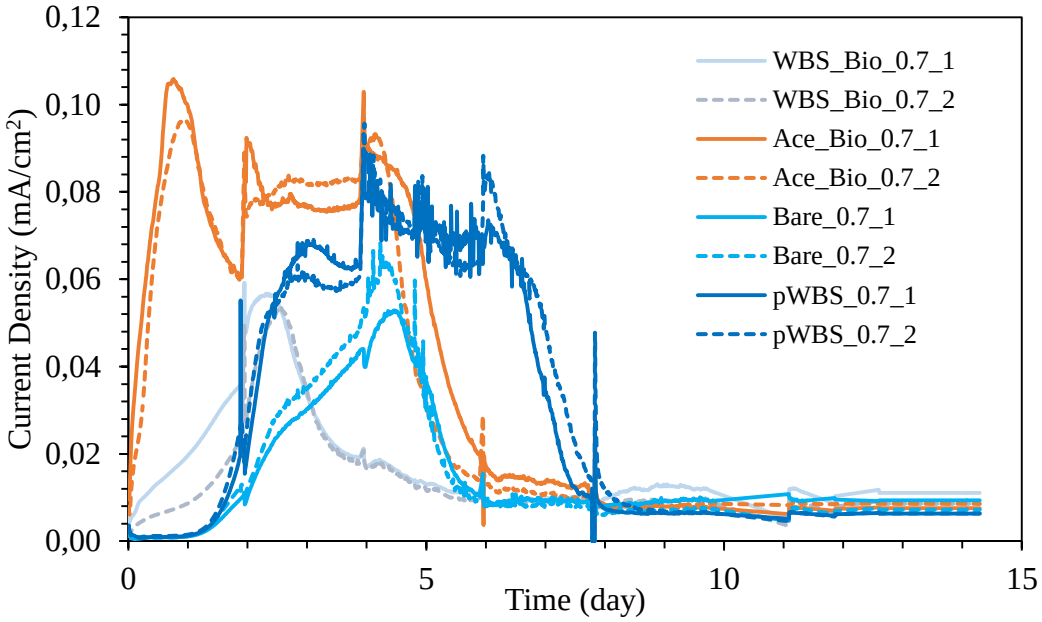

Figure 4.12 Current density profiles of the reactors in Run 1

(Duplicate reactors are shown by the same color, and indicated as 1 and 2)

There was a strong link between the graphs of methane production and current density when the operation of the bioelectrochemical reactor—that is, the voltage that was applied in the AD-MEC system was the primary factor in improving

methane production. For example, in the case of Bare_0.7, where the highest enhancement in methane among the raw WBS fed reactors was recorded, there was a clear correlation between the methane production and current density as shown in Figure 4.13. The peak current around 0.05 mA/cm^2 was recorded at around day 4 and methane production was peaked around day 6 (Figure 4.13).

Ace_Bio_0.7 and WBS_Bio_0.7 reactors with bioelectrodes started to produce current faster than reactors with bare electrodes due to presence of bioelectrodes. According to the current density values, although Ace_Bio_0.7 reactors have almost double the peak values of WBS_Bio_0.7 and Bare_0.7 reactors (Figure 4.13), there is no significant difference between the reactors in terms of methane production. Graph of current density and methane production of Ace_Bio_0.7 reactors showed that, unlike Bare_0.7 reactors, the methane equivalent of the current value produced could not be seen (Figure 4.13). This may be due to the fact that the exoelectrogens over the acetate fed bioelectrodes consume the supplied carbon source faster which results in faster and higher peaks in terms of current density.

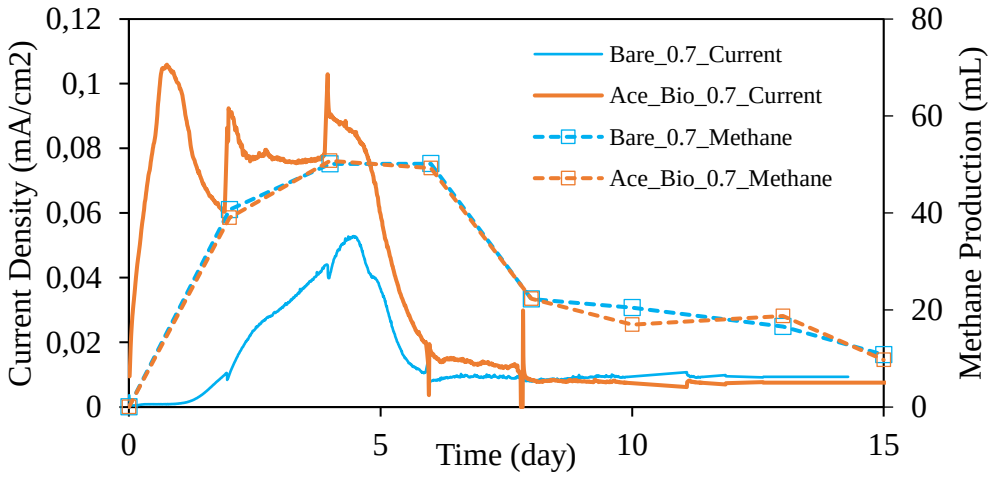

Figure 4.13 Current density and methane production graph of Bare_0.7 and Ace_Bio_0.7 reactors

According to the CV analysis after the end of reactor operation (Figure 4.14), Ace_Bio and WBS_Bio reactors still maintain the biofilm formation over the electrodes. CV analysis showed that, WBS_Bio reactors operated nearly 100 days and still have attached microorganisms over the electrode. On the other hand, despite the higher current density observed in Ace_Bio_0.7 reactors, cathodic peak observed within CV analysis was lower than WBS_Bio_0.7 and Bare_0.7 reactors.

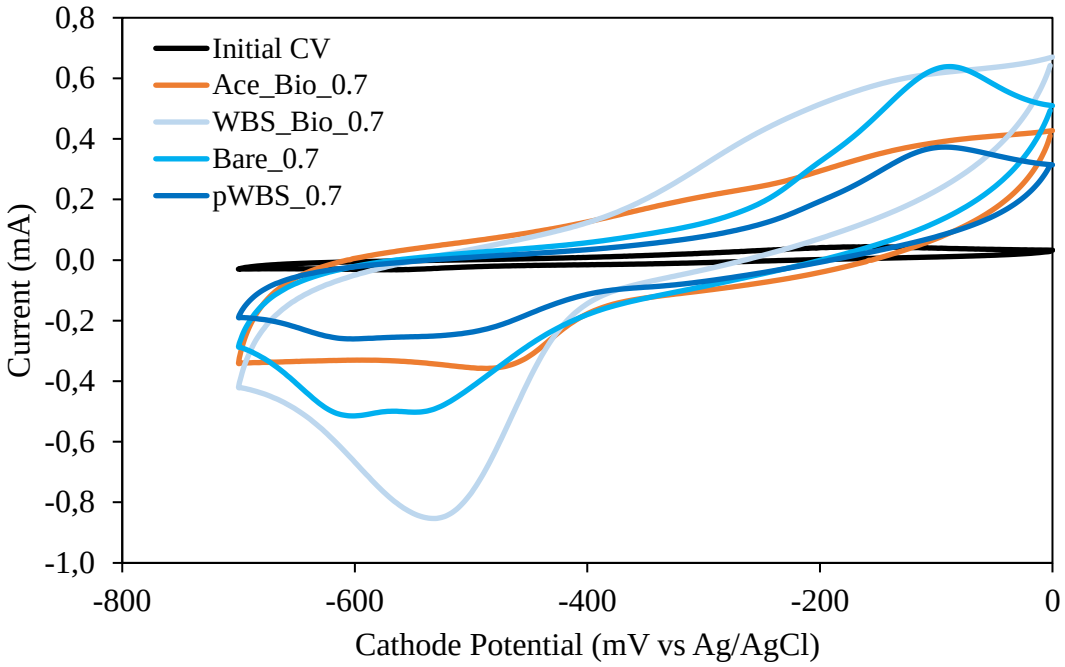

Figure 4.14 CV profiles of the reactors in Run 1

4.2.2.2 Run 2: Impact of Applied Voltage

According to Run 1, the impact of using bioelectrodes is negligible on methane production basis, despite it has beneficial effects like decreased lag time and increased methane production rate with applied voltage of 0.7 V. In the literature with this type of feed highest methane production was mostly observed with applied voltages on the range of 0.3-0.6 V (Table 2.2). Based on literature search, for Run 2, 0.3 V and 0.5 V were chosen as the applied voltage with graphite cathode as described in Figure 3.8

Methane Production

Cumulative methane production graph is provided in Figure 4.15 for Run 2 reactors. 27% increase in methane production was achieved with WBS_0.5 (171.0 ± 8.8 mL CH_4) reactors with respect to AD (134.7 ± 3.09 mL CH_4). Addition of 0.3 V to the reactors increased the cumulative methane slightly. There was 138.3 ± 4.54 mL methene production in WBS_0.3 reactors. This corresponds to around 3% increase with respect to their respective AD controls. If only pretreatment impact is to be analyzed, comparison of AD and pAD reactors is sufficient. The cumulative methane in pAD reactors were averaged at 158.6 ± 0.4 mL, which makes 18% percent increase with respect to AD reactors.

For pWBS_0.3 reactors, average cumulative methane production was recorded as 193.3 ± 6.3 mL CH_4 while the production in pAD was averaged 158.6 ± 0.4 mL CH_4 which indicates 22% increase when it compared with the pAD and 43% increase with respect to AD reactors. Yet, feeding of pWBS with the implementation of 0.5 V does not have a high impact like 0.3 V and produced similar methane amounts with pAD. In fact, at 0.5 V there was a decreased rate until around day 15 in both WBS_0.5 and pWBS_0.5 reactors. Yet, eventually both reactors produced higher methane than AD control.

In terms of the yield of methane, WBS_0.5 reactors had 31% increased methane yield compared with the AD. Highest methane yield achieved with the pWBS_0.3 which is 403.7 ± 15 mL CH_4/g VS_{added}. Despite this, there was only a 3% difference between the yields produced in the AD and the WBS 0.3 reactors (Figure 4.16).

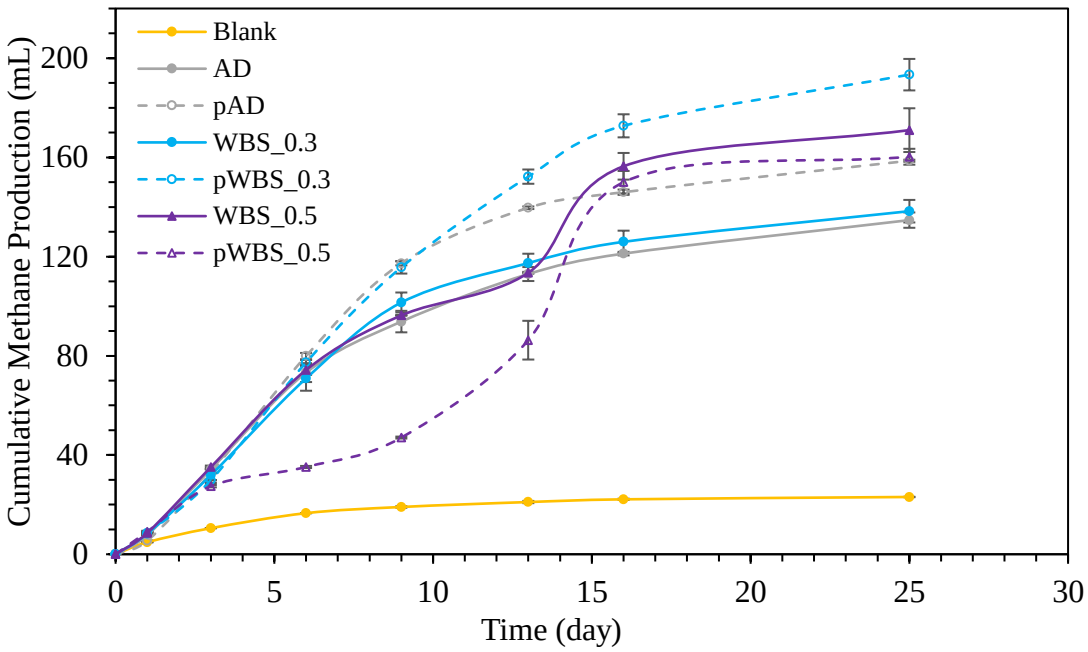

Figure 4.15 Cumulative methane production in reactors in Run 2

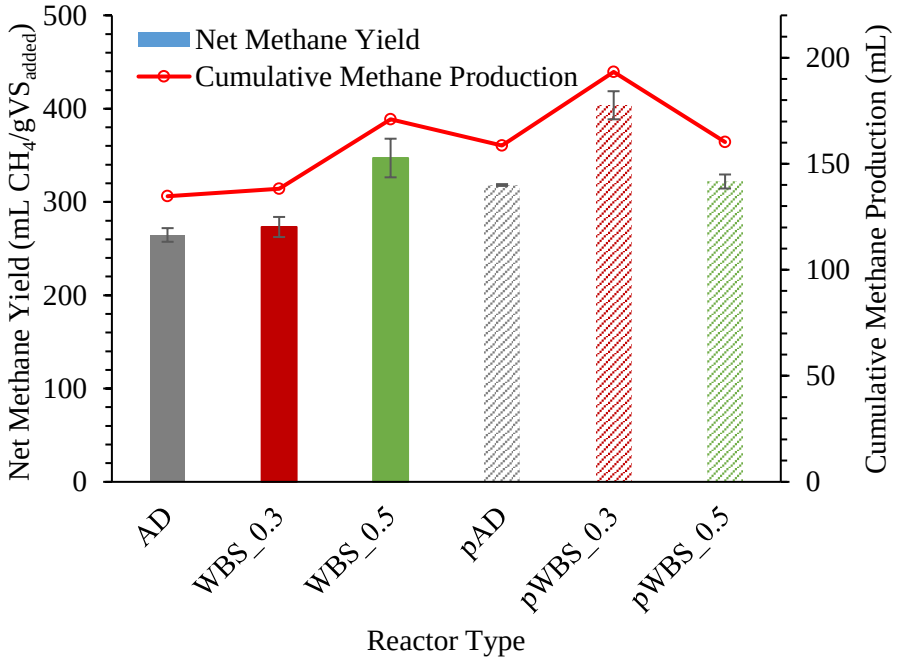

Figure 4.16 Methane yield and cumulative methane production in Run 2

Comparison of lag time and rate were performed based on the modified Gompertz model fitting in Run 2 (Table 4.7). In pWBS_0.5 reactors lag time was increased and methane production rate was decreased, which indicates that, there might be an inhibitory effect of using 0.5 V with pWBS feed.

Effect of pretreated substrate feed shows positive outcomes in terms of rate and also potential. pAD reactors have 20% increased methane potential and 31% increased methane production rate with respect to AD reactors. Additionally, pWBS_0.3 reactors showed 50% and 25% increased methane potential with respect to AD and pAD reactors, while having increased lag time with respect to both reactors. All Gompertz fitting graphs of reactors in Run 2 given in Appendix H.

Table 4.7 Gompertz Results of Run 2

Run Number	**Reactor**	**P**	**R_m**	**λ (d)**	**R^2**
Run 2	AD	129	13	0.6	0.993
	WBS_0.3	134 (4)	14 (8)	0.8 (-)	0.997
	WBS_0.5	176 (36)	11 (-)	0.4 (25)	0.979
	pAD	155 (20)	17 (31)	1.2 (-)	0.998
	pWBS_0.3	194 (50)(25)	15 (15)(-)	1.3 (-)(-)	0.998
	pWBS_0.5	188 (46)(33)	10 (-)(-)	2.8 (-)(-)	0.951

*The number in parenthesis indicates the percentage increase in $\mathbf{P}_\infty$ and, $\mathbf{R_m}$ and decrease in **λ** with respect to: (1) AD; (2) pAD; (-) indicates no enhancement.

Current Production and Electrochemical Activity

Current density profiles of AD-MEC reactors at Run 2 are given in Figure 4.17. Despite highest methane achieved over the pWBS_0.3 reactors current densities of these reactors were stayed below 0.005 mA/cm^2 throughout the operation period. Despite the fact that, both 0.5 V applied reactors showed similar pattern with respect to each other and reach around 0.04 mA/cm^2 the current density attained over 0.5 V applied reactors were less than the current density achieved in reactors at Run1.

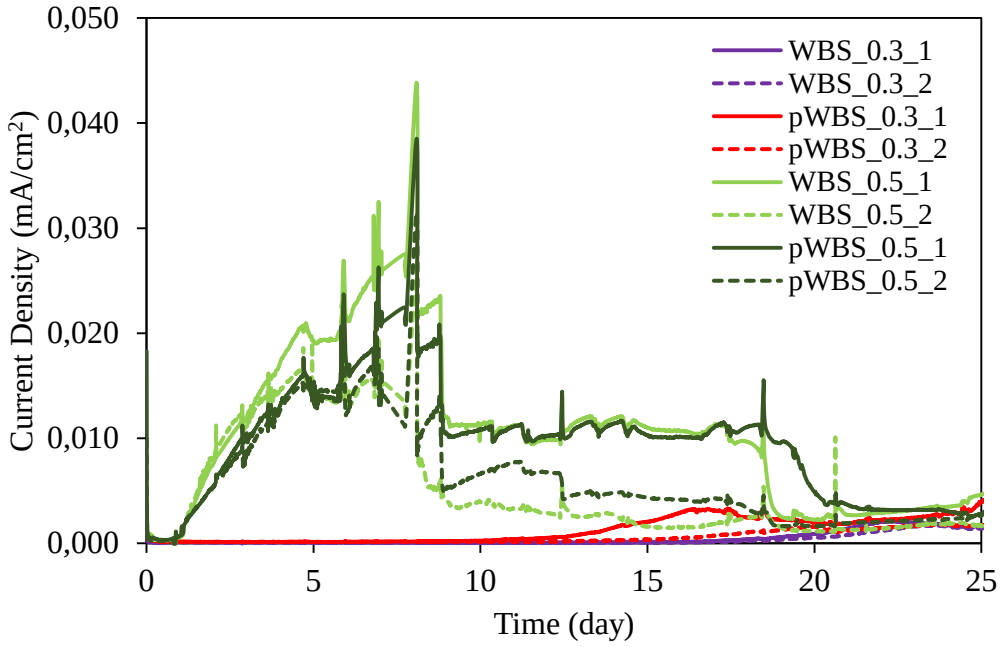

Figure 4.17 Current density profiles of the reactors in Run 2

(Duplicate reactors are shown by the same color, and indicated as 1 and 2)

CV analysis was performed so that it can be determined whether a biofilm was formed over the electrodes despite the low current density profiles that were being produced by the 0.3 V applied reactors (Figure 4.18). There were no cathodic peaks obtained within the 0.3 V applied reactors similar to Set 1. Hence, the increased methane production may stem from the synergistic impact of voltage addition to feed pretreatment.

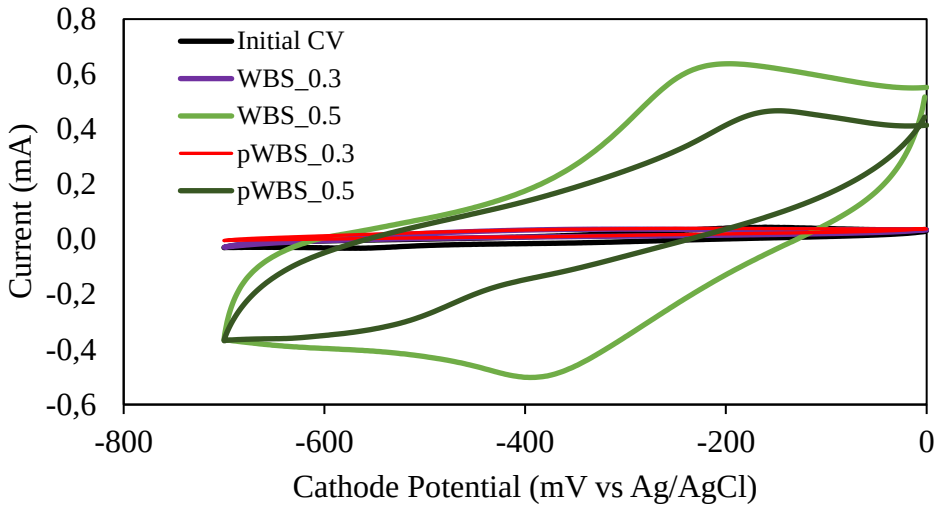

Figure 4.18 CV profiles of reactors in Run 2

In the case of current production and relation with methane production despite highest methane yield and production achieved within pWBS_0.3 reactors, there were no correlation between the production of methane and current density (Figure 4.19). Current density of the pWBS_0.3 reactors were always below 0.01 mA/cm^2 Figure 4.19.

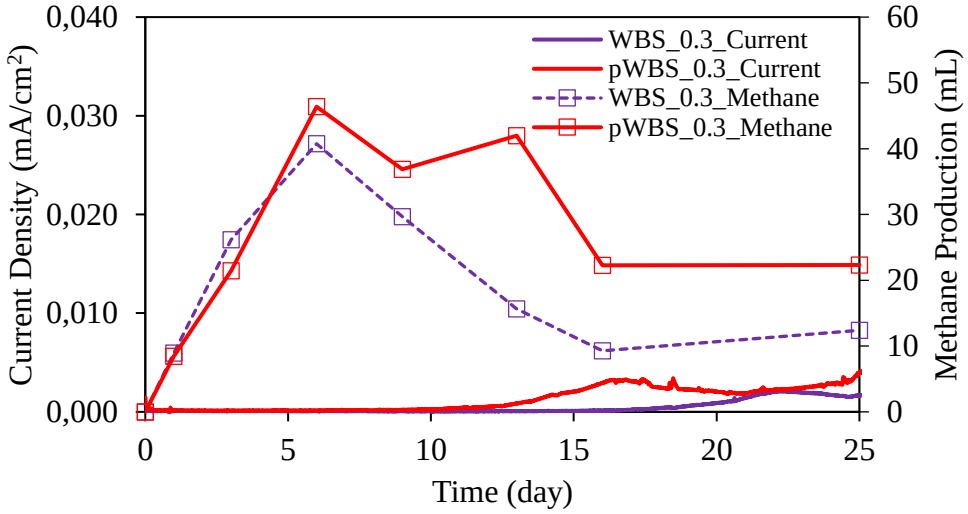

Figure 4.19 Current density vs methane production graph of 0.3V applied reactor in Run 2

In the case of 0.5 V applied reactors, which are pWBS_0.5 and WBS_0.5, methane production and current density correlations were different than each other (Figure 4.20). WBS_0.5 reactors showed better patterns when it compared with the 0.3 V applied reactors since the increasing pattern on current density was similar with the methane production pattern as well. However, for pWBS_0.5 reactors there were no correlation between the peaks of current density and methane production.

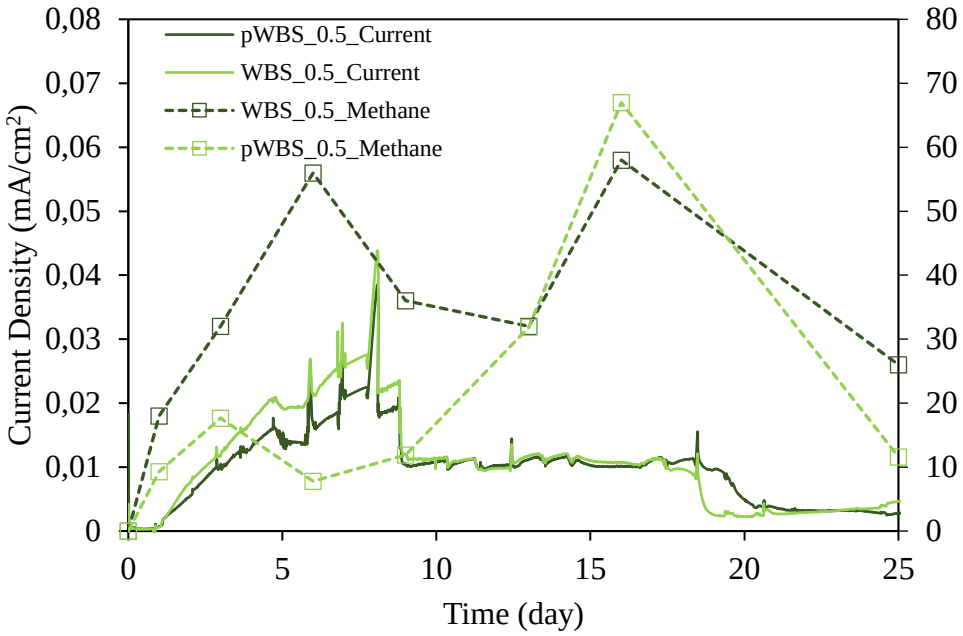

Figure 4.20 Current density vs. methane production graph of 0.5 applied reactor at Run 2

CHAPTER 5

CONCLUSIONS

This thesis study was focused on methane production potential in AD-MEC integrated systems with changing process conditions such as applied voltage, electrode material and substrate type. In this experimental work, important results have been obtained regarding the use of biofilm formed electrodes, effect of voltage on two different substrates used in this study (C and WBS). In summary the following conclusions can be drawn:

- Among different waste mixing ratios of 100C:0WBS, 70C:0WBS, 30C:70WBS and 0C:100WBS the highest improvement was attained with sole manure reactor (100C:0WBS) in AD-MEC systems. With the use of SS mesh as cathode and graphite plate as anode, solely cattle manure fed AD-MEC system showed 70% percent increase in methane yield with respect to conventional AD reactor.
- Results showed that, there was no significant effect of applied voltage on methane production in the WBS dominant reactors with SS mesh cathode which may be related to biofilm formation.
- Highest methane improvement with solely WBS fed system achieved within 0.3 V applied reactors despite this increase is not correlated with the implementation of MEC into AD system.
- The use of bioelectrodes with 100C:0W at 0.7 V applied voltage increased the methane yield by 63% in compared to the bare electrodes when SS mesh cathode and graphite anodes were used in AD-MECs.
- Unlike manure feed, using bioelectrodes with WBS feed showed no advantage over bare electrodes with applied voltage of 0.7 V with graphite electrodes.

- AD-MEC reactors fed with WBS showed similar performance enhancement compared to corresponding AD controls, regardless of the feed pretreatment.
- The highest improvement with WBS feed was attained with 0.3 V application yet no significant current generation was recorded. Also, there was no good cathodic peak in CV analysis. Hence, it may be concluded that the low voltage application to WBS feed MECs may synergistically amplify the effect of feed pretreatment and thus increase methane production.

When the results of the two sets are considered together, the two feeds tested herein provide completely different experimental results and therefore each system should be optimized based on the feed for methane production in AD-MEC systems.

CHAPTER 6

RECOMMENDATIONS

In AD-MEC integrated systems, the interaction between the electrode, the microbial community and the applied voltage occurs through a series of complex reactions. For this reason, each system must be optimized primarily according to the feed type. There are multiple factors such as applied voltage, electrode material that play a significant role in methane production performance of AD-MEC integrated systems. In this study, multiple of these factors were investigated for two different feed types. Below topics may further be investigated in future studies:

- Optimization of process conditions such as applied voltage, electrode type, feed type should be conducted for each case and statistical experimental design may reduce the number of trials.
- In this study experiments were conducted in small scale (< 200 mL) batch reactors. Based on the information provided here larger scale reactors (> 2000 mL) may be operated at a batch mode and then on continuous mode for better assessment of the process conditions.
- Considering the complexity of the integrated AD-MEC system, a more enlightening reactor design with sensor-based live monitoring approaches can be considered in order to better understand the processes operational conditions on the performance of the system.

REFERENCES

Ahn, Y., Im, S., & Chung, J. W. (2017). Optimizing the operating temperature for microbial electrolysis cell treating sewage sludge. *International Journal of Hydrogen Energy*, *42*(45), 27784–27791. https://doi.org/10.1016/j.ijhydene.2017.05.139

Angelidaki, I., Karakashev, D., Batstone, D. J., Plugge, C. M., & Stams, A. J. M. (2011). Biomethanation and its potential. In *Methods in Enzymology* (Vol. 494, pp. 327–351). Academic Press Inc. https://doi.org/10.1016/B978-0-12-385112-3.00016-0

Anukam, A., Mohammadi, A., Naqvi, M., & Granström, K. (2019). A review of the chemistry of anaerobic digestion: Methods of accelerating and optimizing process efficiency. In *Processes* (Vol. 7, Issue 8, pp. 1–19). MDPI AG. https://doi.org/10.3390/PR7080504

Arelli, V., Juntupally, S., Begum, S., & Anupoju, G. R. (2022). Solid state anaerobic digestion of organic waste for the generation of biogas and bio manure. In *Advanced Organic Waste Management: Sustainable Practices and Approaches* (pp. 247–277). Elsevier. https://doi.org/10.1016/B978-0-323-85792-5.00023-X

Asztalos, J. R., & Kim, Y. (2015). Enhanced digestion of waste activated sludge using microbial electrolysis cells at ambient temperature. *Water Research*, *87*, 503–512. https://doi.org/10.1016/j.watres.2015.05.045

Baek, G., Kim, J., Kim, J., & Lee, C. (2020). Individual and combined effects of magnetite addition and external voltage application on anaerobic digestion of dairy wastewater. *Bioresource Technology*, *297*. https://doi.org/10.1016/j.biortech.2019.122443

Baek, G., Kim, J., Lee, S., & Lee, C. (2017). Development of biocathode during repeated cycles of bioelectrochemical conversion of carbon dioxide to methane. *Bioresource Technology*, *241*, 1201–1207. https://doi.org/10.1016/j.biortech.2017.06.125

Bao, H., Yang, H., Zhang, H., Liu, Y., Su, H., & Shen, M. (2020). Improving methane productivity of waste activated sludge by ultrasound and alkali pretreatment in microbial electrolysis cell and anaerobic digestion coupled system. *Environmental Research*, *180*. https://doi.org/10.1016/j.envres.2019.108863

Blasco-Gómez, R., Batlle-Vilanova, P., Villano, M., Balaguer, M. D., Colprim, J., & Puig, S. (2017). On the edge of research and technological application: A critical review of electromethanogenesis. In *International Journal of Molecular Sciences* (Vol. 18, Issue 4). MDPI AG. https://doi.org/10.3390/ijms18040874

Bo, T., Zhu, X., Zhang, L., Tao, Y., He, X., Li, D., & Yan, Z. (2014). A new upgraded biogas production process: Coupling microbial electrolysis cell and anaerobic digestion in single-chamber, barrel-shape stainless steel reactor. *Electrochemistry Communications*, *45*, 67–70. https://doi.org/10.1016/j.elecom.2014.05.026

Bora, A., Mohanrasu, K., Angelin Swetha, T., Ananthi, V., Sindhu, R., Chi, N. T. L., Pugazhendhi, A., Arun, A., & Mathimani, T. (2022). Microbial electrolysis cell (MEC): Reactor configurations, recent advances and strategies in biohydrogen production. *Fuel*, *328*. https://doi.org/10.1016/j.fuel.2022.125269

Cai, W., Liu, W., Yang, C., Wang, L., Liang, B., Thangavel, S., Guo, Z., & Wang, A. (2016). Biocathodic Methanogenic Community in an Integrated Anaerobic Digestion and Microbial Electrolysis System for Enhancement of Methane Production from Waste Sludge. *ACS Sustainable Chemistry and Engineering*, *4*(9), 4913–4921. https://doi.org/10.1021/acssuschemeng.6b01221

Call, D., & Logan, B. E. (2008). Hydrogen production in a single chamber microbial electrolysis cell lacking a membrane. *Environmental Science and Technology*, *42*(9), 3401–3406. https://doi.org/10.1021/es8001822

Cerrillo, M., Viñas, M., & Bonmatí, A. (2018). Anaerobic digestion and electromethanogenic microbial electrolysis cell integrated system: Increased stability and recovery of ammonia and methane. *Renewable Energy*, *120*, 178–189. https://doi.org/10.1016/j.renene.2017.12.062

Chen, Y., Yu, B., Yin, C., Zhang, C., Dai, X., Yuan, H., & Zhu, N. (2016). Biostimulation by direct voltage to enhance anaerobic digestion of waste activated sludge. *RSC Advances*, *6*(2), 1581–1588. https://doi.org/10.1039/c5ra24134k

Cheng, S., Xing, D., Call, D. F., & Logan, B. E. (2009a). Direct biological conversion of electrical current into methane by electromethanogenesis. *Environmental Science and Technology*, *43*(10), 3953–3958. https://doi.org/10.1021/es803531g

Cheng, S., Xing, D., Call, D. F., & Logan, B. E. (2009b). Direct biological conversion of electrical current into methane by electromethanogenesis. *Environmental Science and Technology*, *43*(10), 3953–3958. https://doi.org/10.1021/es803531g

Choi, K. S., Kondaveeti, S., & Min, B. (2017). Bioelectrochemical methane (CH4) production in anaerobic digestion at different supplemental voltages. *Bioresource Technology*, *245*(September), 826–832. https://doi.org/10.1016/j.biortech.2017.09.057

Clauwaert, P., Tolêdo, R., van der Ha, D., Crab, R., Verstraete, W., Hu, H., Udert, K. M., & Rabaey, K. (2008). Combining biocatalyzed electrolysis with anaerobic digestion. *Water Science and Technology*, *57*(4), 575–579. https://doi.org/10.2166/wst.2008.084

Cusick, R. D., Bryan, B., Parker, D. S., Merrill, M. D., Mehanna, M., Kiely, P. D., Liu, G., & Logan, B. E. (2011). Performance of a pilot-scale continuous flow microbial electrolysis cell fed winery wastewater. *Applied Microbiology and Biotechnology*, *89*(6), 2053–2063. https://doi.org/10.1007/s00253-011-3130-9

Dattatraya Saratale, G., Rajesh Banu, J., Nastro, R. A., Kadier, A., Ashokkumar, V., Lay, C. H., Jung, J. H., Seung Shin, H., Ganesh Saratale, R., & Chandrasekhar, K. (2022). Bioelectrochemical systems in aid of sustainable biorefineries for the production of value-added products and resource recovery from wastewater: A critical review and future perspectives. In *Bioresource Technology* (Vol. 359). Elsevier Ltd. https://doi.org/10.1016/j.biortech.2022.127435

de Vrieze, J., Gildemyn, S., Arends, J. B. A., Vanwonterghem, I., Verbeken, K., Boon, N., Verstraete, W., Tyson, G. W., Hennebel, T., & Rabaey, K. (2014). Biomass retention on electrodes rather than electrical current enhances stability in anaerobic digestion. *Water Research*, *54*, 211–221. https://doi.org/10.1016/j.watres.2014.01.044

Ding, A., Yang, Y., Sun, G., & Wu, D. (2015). Impact of applied voltage on methane generation and microbial activities in an anaerobic microbial electrolysis cell (MEC). *Chemical Engineering Journal*, *283*, 260–265. https://doi.org/10.1016/j.cej.2015.07.054

Dou, Z., Dykstra, C. M., & Pavlostathis, S. G. (2018). Bioelectrochemically assisted anaerobic digestion system for biogas upgrading and enhanced methane production. *Science of the Total Environment*, *633*, 1012–1021. https://doi.org/10.1016/j.scitotenv.2018.03.255

Elgrishi, N., Rountree, K. J., McCarthy, B. D., Rountree, E. S., Eisenhart, T. T., & Dempsey, J. L. (2018). A Practical Beginner's Guide to Cyclic Voltammetry. *Journal of Chemical Education*, *95*(2), 197–206. https://doi.org/10.1021/acs.jchemed.7b00361

Escapa, A., Mateos, R., Martínez, E. J., & Blanes, J. (2016). Microbial electrolysis cells: An emerging technology for wastewater treatment and energy recovery. from laboratory to pilot plant and beyond. In *Renewable and Sustainable Energy Reviews* (Vol. 55, pp. 942–956). Elsevier Ltd. https://doi.org/10.1016/j.rser.2015.11.029

Feng, Q., Song, Y. C., & Bae, B. U. (2016). Influence of applied voltage on the performance of bioelectrochemical anaerobic digestion of sewage sludge and planktonic microbial communities at ambient temperature. *Bioresource Technology*, *220*, 500–508. https://doi.org/10.1016/j.biortech.2016.08.085

Feng, Y., Zhang, Y., Chen, S., & Quan, X. (2015). Enhanced production of methane from waste activated sludge by the combination of high-solid anaerobic digestion and microbial electrolysis cell with iron-graphite electrode. *Chemical Engineering Journal*, *259*, 787–794. https://doi.org/10.1016/j.cej.2014.08.048

Flores-Rodriguez, C., Nagendranatha Reddy, C., & Min, B. (2019). Enhanced methane production from acetate intermediate by bioelectrochemical anaerobic digestion at optimal applied voltages. *Biomass and Bioenergy*, *127*. https://doi.org/10.1016/j.biombioe.2019.105261

Gajaraj, S., Huang, Y., Zheng, P., & Hu, Z. (2017). Methane production improvement and associated methanogenic assemblages in bioelectrochemically assisted anaerobic digestion. *Biochemical Engineering Journal*, *117*, 105–112. https://doi.org/10.1016/j.bej.2016.11.003

Gao, Y., Sun, D., Dang, Y., Lei, Y., Ji, J., Lv, T., Bian, R., Xiao, Z., Yan, L., & Holmes, D. E. (2017). Enhancing biomethanogenic treatment of fresh incineration leachate using single chambered microbial electrolysis cells. *Bioresource Technology*, *231*, 129–137. https://doi.org/10.1016/j.biortech.2017.02.024

Gray, N. F. (2004). *Biology of wastewater treatment*. Imperial College Press.

Guo, X., Liu, J., & Xiao, B. (2013). Bioelectrochemical enhancement of hydrogen and methane production from the anaerobic digestion of sewage sludge in single-chamber membrane-free microbial electrolysis cells. *International Journal of Hydrogen Energy*, *38*(3), 1342–1347. https://doi.org/10.1016/j.ijhydene.2012.11.087

Hagos, K., Liu, C., & Lu, X. (2018). Effect of endogenous hydrogen utilization on improved methane production in an integrated microbial electrolysis cell and anaerobic digestion: Employing catalyzed stainless steel mesh cathode. *Chinese Journal of Chemical Engineering*, *26*(3), 574–582. https://doi.org/10.1016/j.cjche.2017.08.005

Harnisch, F., & Korth, B. (2021a). First settlers persist. *Joule*, *5*(6), 1316–1319. https://doi.org/10.1016/j.joule.2021.05.022

Harnisch, F., & Korth, B. (2021b). First settlers persist. *Joule*, *5*(6), 1316–1319. https://doi.org/10.1016/j.joule.2021.05.022

Hassanein, A., Witarsa, F., Guo, X., Yong, L., Lansing, S., & Qiu, L. (2017). Next generation digestion: Complementing anaerobic digestion (AD) with a novel microbial electrolysis cell (MEC) design. *International Journal of Hydrogen Energy*, *42*(48), 28681–28689. https://doi.org/10.1016/j.ijhydene.2017.10.003

Hassanein, A., Witarsa, F., Lansing, S., Qiu, L., & Liang, Y. (2020). Bio-electrochemical enhancement of hydrogen and methane production in a combined anaerobic digester (AD) and microbial electrolysis cell (MEC) from dairy manure. *Sustainability (Switzerland)*, *12*(20), 1–12. https://doi.org/10.3390/su12208491

Hou, H., Li, Z., Liu, B., Liang, S., Xiao, K., Zhu, Q., Hu, S., Yang, J., & Hu, J. (2020). Biogas and phosphorus recovery from waste activated sludge with protocatechuic acid enhanced Fenton pretreatment, anaerobic digestion and microbial electrolysis cell. *Science of the Total Environment*, *704*. https://doi.org/10.1016/j.scitotenv.2019.135274

Hou, Y., Zhang, R., Luo, H., Liu, G., Kim, Y., Yu, S., & Zeng, J. (2015). Microbial electrolysis cell with spiral wound electrode for wastewater treatment and methane production. *Process Biochemistry*, *50*(7), 1103–1109. https://doi.org/10.1016/j.procbio.2015.04.001

Hua, T., Li, S., Li, F., Ondon, B. S., Liu, Y., & Wang, H. (2019). Degradation performance and microbial community analysis of microbial electrolysis cells for erythromycin wastewater treatment. *Biochemical Engineering Journal*, *146*, 1–9. https://doi.org/10.1016/j.bej.2019.02.008

Huang, Q., Liu, Y., & Dhar, B. R. (2022). A critical review of microbial electrolysis cells coupled with anaerobic digester for enhanced biomethane recovery from high-strength feedstocks. *Critical Reviews in Environmental Science and Technology*, *52*(1), 50–89. https://doi.org/10.1080/10643389.2020.1813065

Jain, S., Jain, S., Wolf, I. T., Lee, J., & Tong, Y. W. (2015). A comprehensive review on operating parameters and different pretreatment methodologies for anaerobic digestion of municipal solid waste. In *Renewable and Sustainable Energy Reviews* (Vol. 52, pp. 142–154). Elsevier Ltd. https://doi.org/10.1016/j.rser.2015.07.091

Jiao, Y., Yuan, Y., He, C., Liu, L., Pan, X., & Li, P. (2022). Enrichment culture combined with microbial electrochemical enhanced low-temperature anaerobic digestion of cow dung. *Bioresource Technology*, *360*. https://doi.org/10.1016/j.biortech.2022.127636

Jin, X., Zhang, Y., Li, X., Zhao, N., & Angelidaki, I. (2017). Microbial Electrolytic Capture, Separation and Regeneration of CO2 for Biogas Upgrading. *Environmental Science and Technology*, *51*(16), 9371–9378. https://doi.org/10.1021/acs.est.7b01574

Joicy, A., Seo, H., Lee, M. E., Song, Y. C., Jeong, Y. W., & Ahn, Y. (2022). Influence of applied voltage and conductive material in DIET promotion for

methane generation. *International Journal of Hydrogen Energy*, *47*(18), 10228–10238. https://doi.org/10.1016/j.ijhydene.2022.01.075

Kadier, A., Simayi, Y., Abdeshahian, P., Azman, N. F., Chandrasekhar, K., & Kalil, M. S. (2016). A comprehensive review of microbial electrolysis cells (MEC) reactor designs and configurations for sustainable hydrogen gas production. In *Alexandria Engineering Journal* (Vol. 55, Issue 1, pp. 427–443). Elsevier B.V. https://doi.org/10.1016/j.aej.2015.10.008

Kamusoko, R., Jingura, R. M., Chikwambi, Z., & Parawira, W. (2022). Biogas: microbiological research to enhance efficiency and regulation. In *Handbook of Biofuels* (pp. 485–497). Elsevier. https://doi.org/10.1016/b978-0-12-822810-4.00025-7

Kargi, F., Catalkaya, E. C., & Uzuncar, S. (2011). Hydrogen gas production from waste anaerobic sludge by electrohydrolysis: Effects of applied DC voltage. *International Journal of Hydrogen Energy*, *36*(3), 2049–2056. https://doi.org/10.1016/j.ijhydene.2010.11.087

Karthikeyan, R., Cheng, K. Y., Selvam, A., Bose, A., & Wong, J. W. C. (2017). Bioelectrohydrogenesis and inhibition of methanogenic activity in microbial electrolysis cells - A review. In *Biotechnology Advances* (Vol. 35, Issue 6, pp. 758–771). Elsevier Inc. https://doi.org/10.1016/j.biotechadv.2017.07.004

Kas, A., & Yilmazel, Y. D. (2022). High current density via direct electron transfer by hyperthermophilic archaeon, Geoglobus acetivorans, in microbial electrolysis cells operated at 80 °C. *Bioelectrochemistry*, *145*. https://doi.org/10.1016/j.bioelechem.2022.108072

Kim, T., Choi, W., Shin, H. C., Choi, J. Y., Kim, J. M., Park, M. S., & Yoon, W. S. (2020). Applications of voltammetry in lithium ion battery research. In *Journal of Electrochemical Science and Technology* (Vol. 11, Issue 1). https://doi.org/10.33961/jecst.2019.00619

Kirkegaard, R. H., McIlroy, S. J., Kristensen, J. M., Nierychlo, M., Karst, S. M., Dueholm, M. S., Albertsen, M., & Nielsen, P. H. (2017). The impact of immigration on microbial community composition in full-scale anaerobic digesters. *Scientific Reports*, *7*(1). https://doi.org/10.1038/s41598-017-09303-0

Kokko, M., Epple, S., Gescher, J., & Kerzenmacher, S. (2018). Effects of wastewater constituents and operational conditions on the composition and dynamics of anodic microbial communities in bioelectrochemical systems. In *Bioresource Technology* (Vol. 258, pp. 376–389). Elsevier Ltd. https://doi.org/10.1016/j.biortech.2018.01.090

Lee, B., Park, J. G., Shin, W. B., Tian, D. J., & Jun, H. B. (2017). Microbial communities change in an anaerobic digestion after application of microbial electrolysis cells. *Bioresource Technology*, *234*, 273–280. https://doi.org/10.1016/j.biortech.2017.02.022

Li, P., Li, W., Sun, M., Xu, X., Zhang, B., & Sun, Y. (2019). Evaluation of biochemical methane potential and kinetics on the anaerobic digestion of vegetable crop residues. *Energies*, *12*(1). https://doi.org/10.3390/en12010026

Li, X., Zeng, C., Lu, Y., Liu, G., Luo, H., & Zhang, R. (2019). Development of methanogens within cathodic biofilm in the single-chamber microbial electrolysis cell. *Bioresource Technology*, *274*, 403–409. https://doi.org/10.1016/j.biortech.2018.12.002

Li, Y., Zhang, Y., Liu, Y., Zhao, Z., Zhao, Z., Liu, S., Zhao, H., & Quan, X. (2016). Enhancement of anaerobic methanogenesis at a short hydraulic retention time via bioelectrochemical enrichment of hydrogenotrophic methanogens. *Bioresource Technology*, *218*, 505–511. https://doi.org/10.1016/j.biortech.2016.06.112

Liu, D., Zhang, L., Chen, S., Buisman, C., & ter Heijne, A. (2016). Bioelectrochemical enhancement of methane production in low temperature

anaerobic digestion at 10 °C. *Water Research*, *99*, 281–287. https://doi.org/10.1016/j.watres.2016.04.020

Liu, J., Yu, D., Zhang, J., Yang, M., Wang, Y., Wei, Y., & Tong, J. (2016). Rheological properties of sewage sludge during enhanced anaerobic digestion with microwave-H2O2 pretreatment. *Water Research*, *98*, 98–108. https://doi.org/10.1016/j.watres.2016.03.073

Liu, W., Cai, W., Guo, Z., Wang, L., Yang, C., Varrone, C., & Wang, A. (2016). Microbial electrolysis contribution to anaerobic digestion of waste activated sludge, leading to accelerated methane production. *Renewable Energy*, *91*, 334–339. https://doi.org/10.1016/j.renene.2016.01.082

Liu, Y., Li, Y., Gan, R., Jia, H., Yong, X., Yong, Y. C., Wu, X., Wei, P., & Zhou, J. (2020). Enhanced biogas production from swine manure anaerobic digestion via in-situ formed graphene in electromethanogenesis system. *Chemical Engineering Journal*, *389*. https://doi.org/10.1016/j.cej.2020.124510

Logan, B. E. (2008). Microbial Fuel Cells. In *Microbial Fuel Cells*. https://doi.org/10.1002/9780470258590

Logan, B. E., Call, D., Cheng, S., Hamelers, H. V. M., Sleutels, T. H. J. A., Jeremiasse, A. W., & Rozendal, R. A. (2008). Microbial electrolysis cells for high yield hydrogen gas production from organic matter. In *Environmental Science and Technology* (Vol. 42, Issue 23, pp. 8630–8640). https://doi.org/10.1021/es801553z

Logan, B. E., Hamelers, B., Rozendal, R., Schröder, U., Keller, J., Freguia, S., Aelterman, P., Verstraete, W., & Rabaey, K. (2006). Microbial fuel cells: Methodology and technology. In *Environmental Science and Technology* (Vol. 40, Issue 17, pp. 5181–5192). https://doi.org/10.1021/es0605016

Logan, B. E., Rossi, R., Ragab, A., & Saikaly, P. E. (2019). Electroactive microorganisms in bioelectrochemical systems. In *Nature Reviews*

Microbiology (Vol. 17, Issue 5, pp. 307–319). Nature Publishing Group. https://doi.org/10.1038/s41579-019-0173-x

Luo, H., Liu, G., Zhang, R., Bai, Y., Fu, S., & Hou, Y. (2014). Heavy metal recovery combined with H2 production from artificial acid mine drainage using the microbial electrolysis cell. *Journal of Hazardous Materials*, *270*, 153–159. https://doi.org/10.1016/j.jhazmat.2014.01.050

Moreno, R., San-Martín, M. I., Escapa, A., & Morán, A. (2016). Domestic wastewater treatment in parallel with methane production in a microbial electrolysis cell. *Renewable Energy*, *93*, 442–448. https://doi.org/10.1016/j.renene.2016.02.083

Nagarajan, S., Jones, R. J., Oram, L., Massanet-Nicolau, J., & Guwy, A. (2022). Intensification of Acidogenic Fermentation for the Production of Biohydrogen and Volatile Fatty Acids—A Perspective. In *Fermentation* (Vol. 8, Issue 7). MDPI. https://doi.org/10.3390/fermentation8070325

Nancharaiah, Y. v., Venkata Mohan, S., & Lens, P. N. L. (2015). Metals removal and recovery in bioelectrochemical systems: A review. In *Bioresource Technology* (Vol. 195, pp. 102–114). Elsevier Ltd. https://doi.org/10.1016/j.biortech.2015.06.058

Park, J. G., Lee, B., Park, H. R., & Jun, H. B. (2019). Long-term evaluation of methane production in a bio-electrochemical anaerobic digestion reactor according to the organic loading rate. *Bioresource Technology*, *273*, 478–486. https://doi.org/10.1016/j.biortech.2018.11.021

Rader, G. K., & Logan, B. E. (2010). Multi-electrode continuous flow microbial electrolysis cell for biogas production from acetate. *International Journal of Hydrogen Energy*, *35*(17), 8848–8854. https://doi.org/10.1016/j.ijhydene.2010.06.033

Raj, T., Chandrasekhar, K., Kumar, A. N., Sharma, P., Pandey, A., Jang, M., Jeon, B. H., Varjani, S., & Kim, S. H. (2022). Recycling of cathode material from

spent lithium-ion batteries: Challenges and future perspectives. *Journal of Hazardous Materials*, *429*. https://doi.org/10.1016/j.jhazmat.2022.128312

Rozendal, R. A., Hamelers, H. V. M., Euverink, G. J. W., Metz, S. J., & Buisman, C. J. N. (2006). Principle and perspectives of hydrogen production through biocatalyzed electrolysis. *International Journal of Hydrogen Energy*, *31*(12), 1632–1640. https://doi.org/10.1016/j.ijhydene.2005.12.006

Sugnaux, M., Happe, M., Cachelin, C. P., Gasperini, A., Blatter, M., & Fischer, F. (2017). Cathode deposits favor methane generation in microbial electrolysis cell. *Chemical Engineering Journal*, *324*, 228–236. https://doi.org/10.1016/j.cej.2017.05.028

Tartakovsky, B., Mehta, P., Santoyo, G., Roy, C., Frigon, J. C., & Guiot, S. R. (2014). Electrolysis-enhanced co-digestion of switchgrass and cow manure. *Journal of Chemical Technology and Biotechnology*, *89*(10), 1501–1506. https://doi.org/10.1002/jctb.4224

Villano, M., Aulenta, F., Ciucci, C., Ferri, T., Giuliano, A., & Majone, M. (2010). Bioelectrochemical reduction of CO2 to CH4 via direct and indirect extracellular electron transfer by a hydrogenophilic methanogenic culture. *Bioresource Technology*, *101*(9), 3085–3090. https://doi.org/10.1016/j.biortech.2009.12.077

Villano, M., Ralo, C., Zeppilli, M., Aulenta, F., & Majone, M. (2016). Influence of the set anode potential on the performance and internal energy losses of a methane-producing microbial electrolysis cell. *Bioelectrochemistry*, *107*, 1–6. https://doi.org/10.1016/j.bioelechem.2015.07.008

Wagner, R. C., Regan, J. M., Oh, S. E., Zuo, Y., & Logan, B. E. (2009). Hydrogen and methane production from swine wastewater using microbial electrolysis cells. *Water Research*, *43*(5), 1480–1488. https://doi.org/10.1016/j.watres.2008.12.037

Wang, K., Sheng, Y., Cao, H., Yan, K., & Zhang, Y. (2017). Impact of applied current on sulfate-rich wastewater treatment and microbial biodiversity in the cathode chamber of microbial electrolysis cell (MEC) reactor. *Chemical Engineering Journal*, *307*, 150–158. https://doi.org/10.1016/j.cej.2016.07.106

Wang, R., Li, Y., Wang, W., Chen, Y., & Vanrolleghem, P. A. (2015). Effect of high orthophosphate concentration on mesophilic anaerobic sludge digestion and its modeling. *Chemical Engineering Journal*, *260*. https://doi.org/10.1016/j.cej.2014.09.050

Wang, W., Chang, J. S., & Lee, D. J. (2022). Integrating anaerobic digestion with bioelectrochemical system for performance enhancement: A mini review. In *Bioresource Technology* (Vol. 345). Elsevier Ltd. https://doi.org/10.1016/j.biortech.2021.126519

Wei, J., Liang, P., & Huang, X. (2011). Recent progress in electrodes for microbial fuel cells. In *Bioresource Technology* (Vol. 102, Issue 20, pp. 9335–9344). https://doi.org/10.1016/j.biortech.2011.07.019

Xiao, B., Chen, X., Han, Y., Liu, J., & Guo, X. (2018). Bioelectrochemical enhancement of the anaerobic digestion of thermal-alkaline pretreated sludge in microbial electrolysis cells. *Renewable Energy*, *115*, 1177–1183. https://doi.org/10.1016/j.renene.2017.06.043

Xing, T., Yun, S., Li, B., Wang, K., Chen, J., Jia, B., Ke, T., & An, J. (2021a). Coconut-shell-derived bio-based carbon enhanced microbial electrolysis cells for upgrading anaerobic co-digestion of cow manure and aloe peel waste. *Bioresource Technology*, *338*(July), 125520. https://doi.org/10.1016/j.biortech.2021.125520

Xing, T., Yun, S., Li, B., Wang, K., Chen, J., Jia, B., Ke, T., & An, J. (2021b). Coconut-shell-derived bio-based carbon enhanced microbial electrolysis cells for upgrading anaerobic co-digestion of cow manure and aloe peel waste. *Bioresource Technology*, *338*. https://doi.org/10.1016/j.biortech.2021.125520

Yilmazel, Y. D., Zhu, X., Kim, K. Y., Holmes, D. E., & Logan, B. E. (2018). Electrical current generation in microbial electrolysis cells by hyperthermophilic archaea Ferroglobus placidus and Geoglobus ahangari. *Bioelectrochemistry*, *119*, 142–149. https://doi.org/10.1016/j.bioelechem.2017.09.012

Yin, C., Shen, Y., Yuan, R., Zhu, N., Yuan, H., & Lou, Z. (2019). Sludge-based biochar-assisted thermophilic anaerobic digestion of waste-activated sludge in microbial electrolysis cell for methane production. *Bioresource Technology*, *284*, 315–324. https://doi.org/10.1016/j.biortech.2019.03.146

Yin, Q., Zhu, X., Zhan, G., Bo, T., Yang, Y., Tao, Y., He, X., Li, D., & Yan, Z. (2016). Enhanced methane production in an anaerobic digestion and microbial electrolysis cell coupled system with co-cultivation of Geobacter and Methanosarcina. *Journal of Environmental Sciences (China)*, *42*, 210–214. https://doi.org/10.1016/j.jes.2015.07.006

Yu, J., Kim, S., & Kwon, O. S. (2019). Effect of applied voltage and temperature on methane production and microbial community in microbial electrochemical anaerobic digestion systems treating swine manure. *Journal of Industrial Microbiology and Biotechnology*, *46*(7), 911–923. https://doi.org/10.1007/s10295-019-02182-6

Yu, Z., Leng, X., Zhao, S., Ji, J., Zhou, T., Khan, A., Kakde, A., Liu, P., & Li, X. (2018). A review on the applications of microbial electrolysis cells in anaerobic digestion. *Bioresource Technology*, *255*, 340–348. https://doi.org/10.1016/J.BIORTECH.2018.02.003

Yuan, Y., Cheng, H., Chen, F., Zhang, Y., Xu, X., Huang, C., Chen, C., Liu, W., Ding, C., Li, Z., Chen, T., & Wang, A. (2020). Enhanced methane production by alleviating sulfide inhibition with a microbial electrolysis coupled anaerobic digestion reactor. *Environment International*, *136*. https://doi.org/10.1016/j.envint.2020.105503

Zakaria, B. S., & Dhar, B. R. (2019). Progress towards catalyzing electro-methanogenesis in anaerobic digestion process: Fundamentals, process optimization, design and scale-up considerations. In *Bioresource Technology* (Vol. 289). Elsevier Ltd. https://doi.org/10.1016/j.biortech.2019.121738

Zakaria, B. S., & Dhar, B. R. (2021). Characterization and significance of extracellular polymeric substances, reactive oxygen species, and extracellular electron transfer in methanogenic biocathode. *Scientific Reports*, *11*(1). https://doi.org/10.1038/s41598-021-87118-w

Zhang, Y., & Angelidaki, I. (2014). Microbial electrolysis cells turning to be versatile technology: Recent advances and future challenges. In *Water Research* (Vol. 56, pp. 11–25). Elsevier Ltd. https://doi.org/10.1016/j.watres.2014.02.031

Zhen, G., Zheng, S., Lu, X., Zhu, X., Mei, J., Kobayashi, T., Xu, K., Li, Y. Y., & Zhao, Y. (2018). A comprehensive comparison of five different carbon-based cathode materials in CO2 electromethanogenesis: Long-term performance, cell-electrode contact behaviors and extracellular electron transfer pathways. *Bioresource Technology*, *266*, 382–388. https://doi.org/10.1016/j.biortech.2018.06.101

APPENDICES

A. Supplementary information for the SMA procedure

Density of the HAc = 1.05 kg/L = 1050 mg/mL

$CH_3COOH + 2O_2 \rightarrow 2CO_2 + 2H_2O$

Molar weight of acetic acid is 12+1+1+1+12+16+16+1 = 60 g

60 g acetic acid needs 2·(16+16) = 64 g oxygen COD is 64 g oxygen/60 g acetic acid = 1.07 g oxygen/g acetid acid

COD of the HAc = 1050 mg/mL * 1.07 = 1123.5 mg/mL

Since we are going to have 65 mL of working volume, needed amount of HAc inside the reactor (If the needed COD from HAc will be 3000 mg/L) will be;

1123.5 mg/mL * X = 3000 mg/L * 65 mL

X= 0.174 mL of HAc inside 65 mL

Proposed media ingredients

Ingrediant	Volume (mL)
Acetic Acid	0.18
Media	10
Seed	33.5
DI water	21.32
	65

Expected net methane from Acetic Acid = 3000*0.395*65 = 77 mL methane

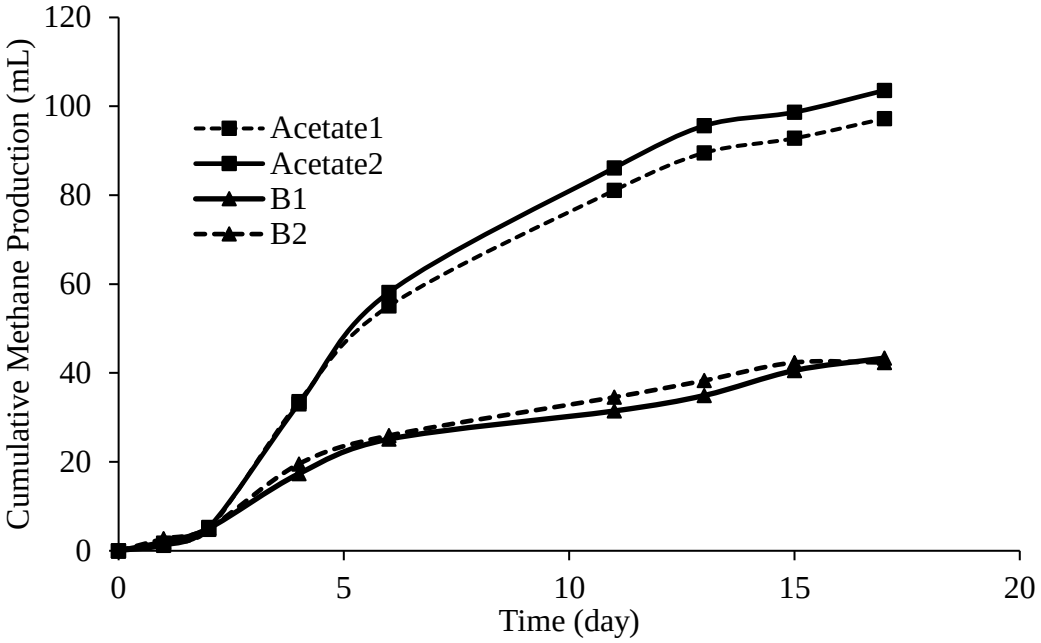

Figure A.1 Cumulative methane production within reactors at SMA test (Duplicate reactors are shown, and indicated as 1 and 2

Date	Blank -_AVG	Ace_AVG	Net Methane
-	0.00	0.00	0.00
1/16/2021	2.35	1.48	-0.88
1/17/2021	5.07	5.01	-0.06
1/19/2021	18.44	33.31	14.88
1/23/2021	25.53	56.60	31.08
1/26/2021	33.00	83.61	50.61
1/29/2021	36.63	92.59	55.96
1/31/2021	41.46	95.74	54.28
2/2/2021	42.86	100.41	57.55

Activity = 100 * Net methane produced / Expected Methane

= 100 * 57.55/77 = 75% activity

B. Current density profiles of the reactors at Set 1-Part 1

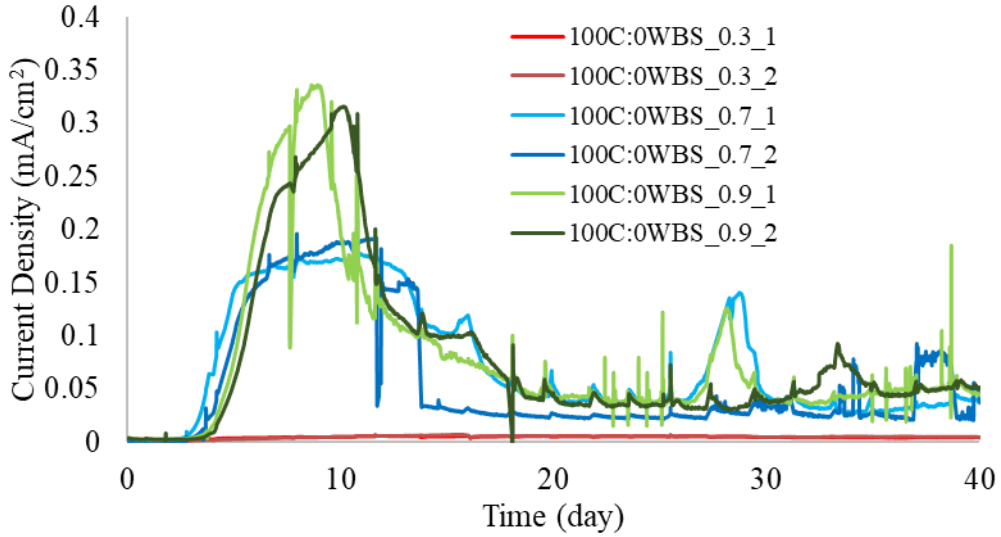

Figure B.1 Current density profiles of the 100C:0WBS reactors (Duplicate reactors are shown by the same color, and indicated as 1 and 2)

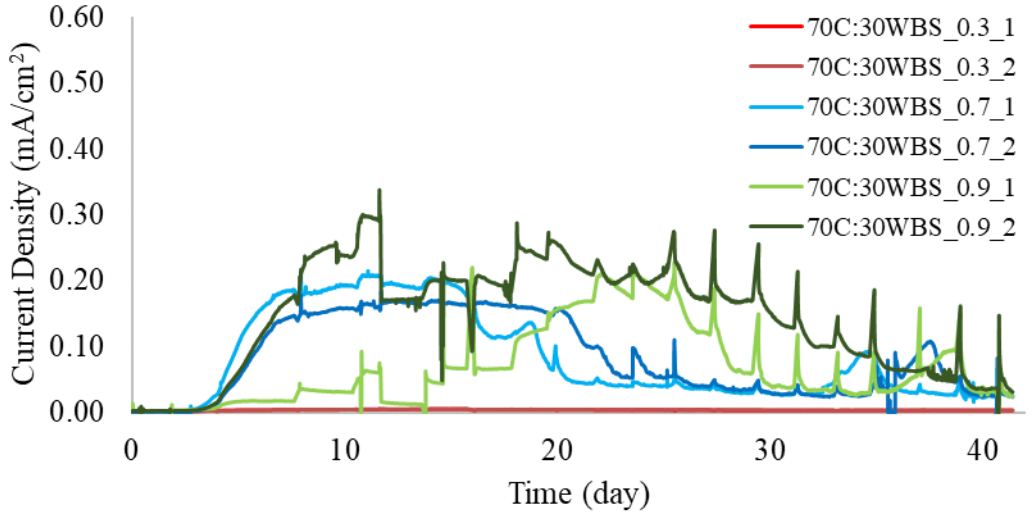

Figure B.2 Current density profiles of the 70C:30WBS reactors ((Duplicate reactors are shown by the same color, and indicated as 1 and 2)

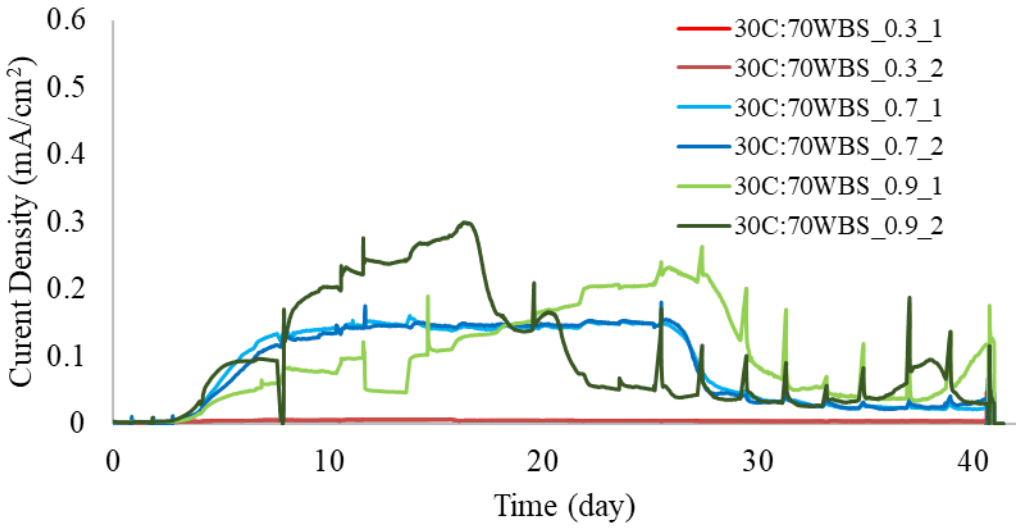

Figure B.3 Current density profiles of the 30C:70WBS reactors ((Duplicate reactors are shown by the same color, and indicated as 1 and 2)

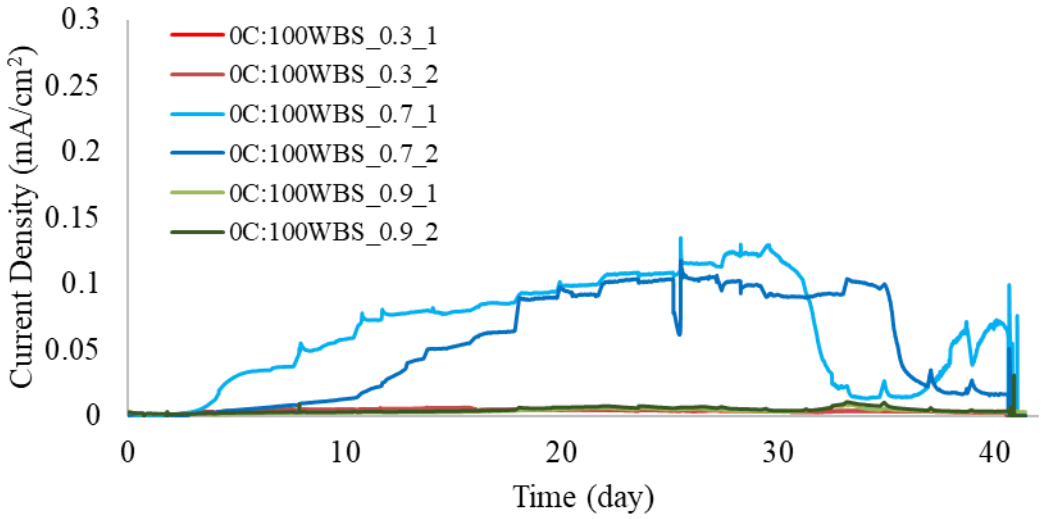

Figure B.4 Current density profiles of the 0C:100WBS reactors ((Duplicate reactors are shown by the same color, and indicated as 1 and 2)

C. CV profiles of the reactors at Set 1-Part 1

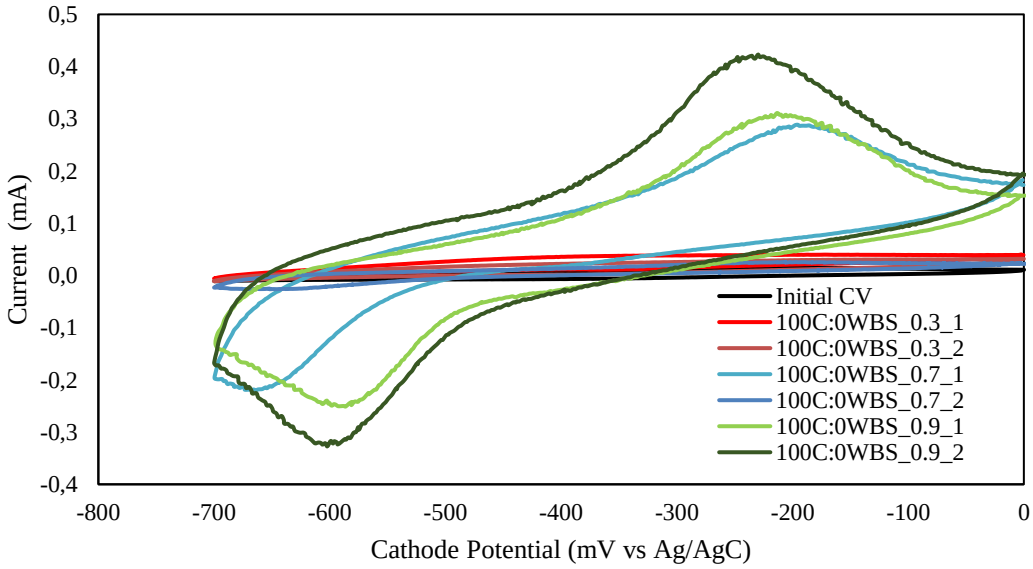

Figure C.1 CV profiles of 100C:0WBS reactors

(Duplicate reactors are shown by the same color, and indicated as 1 to 2)

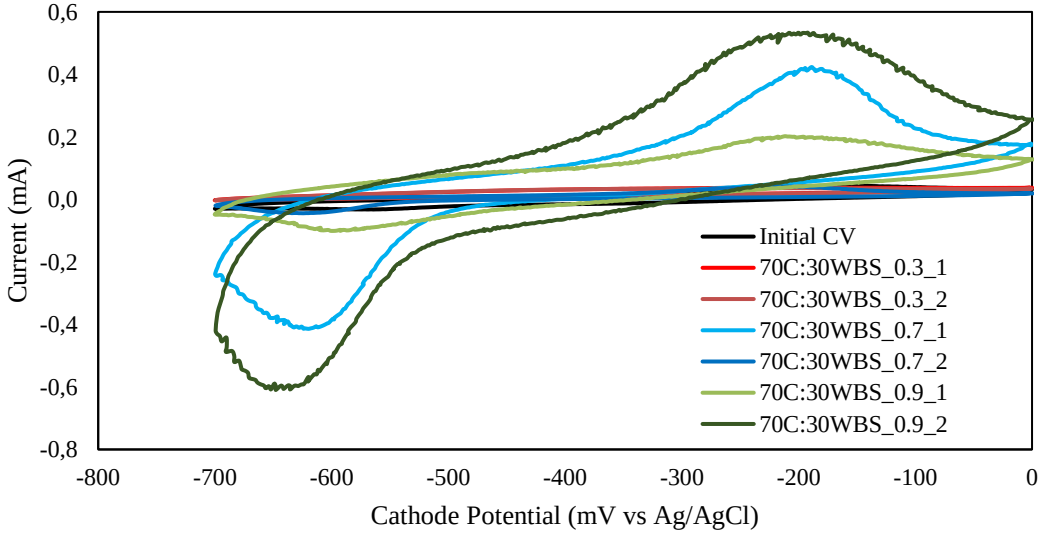

Figure C.2 CV profiles of 70C:100WBS reactors

(Duplicate reactors are shown by the same color, and indicated as 1 to 2)

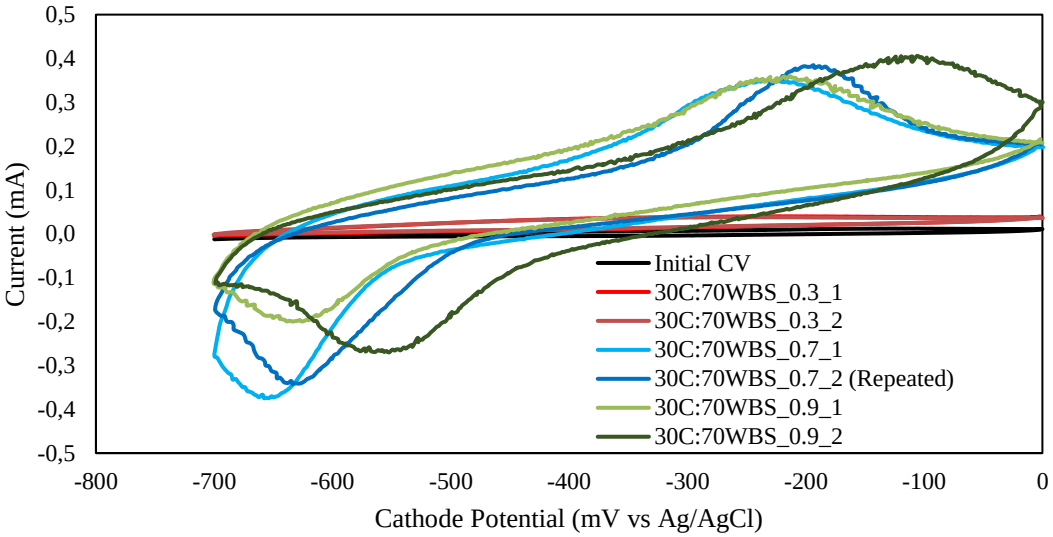

Figure C.3 CV profiles of 30C:70WBS reactors

(Duplicate reactors are shown by the same color, and indicated as 1 to 2)

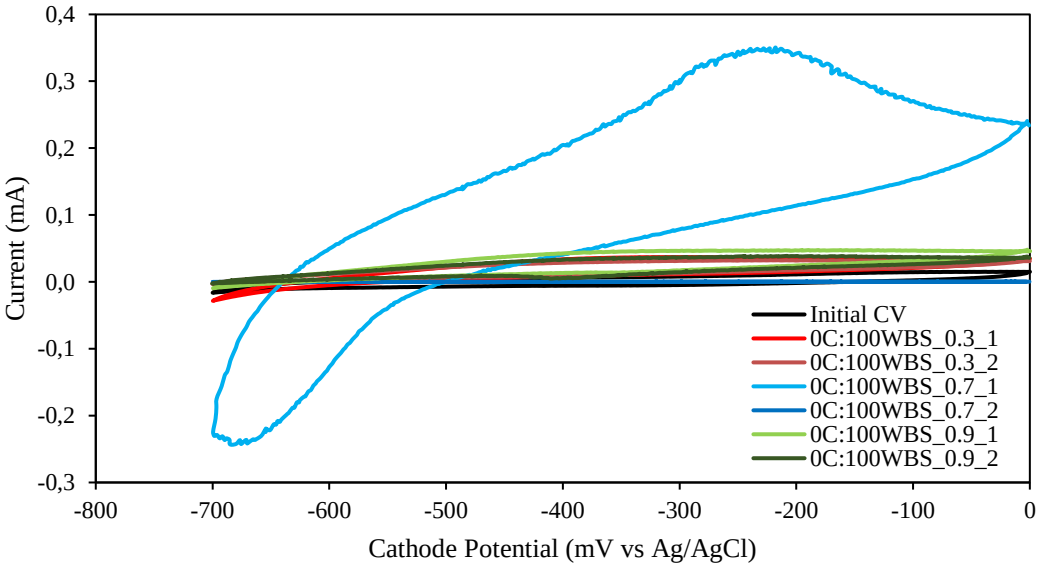

Figure C.4 CV profiles of 0C:100WBS reactors

(Duplicate reactors are shown by the same color, and indicated as 1 to 2)

D. Current density graphs for 100C:0W and 70C:30WBS reactors during reviving procedure

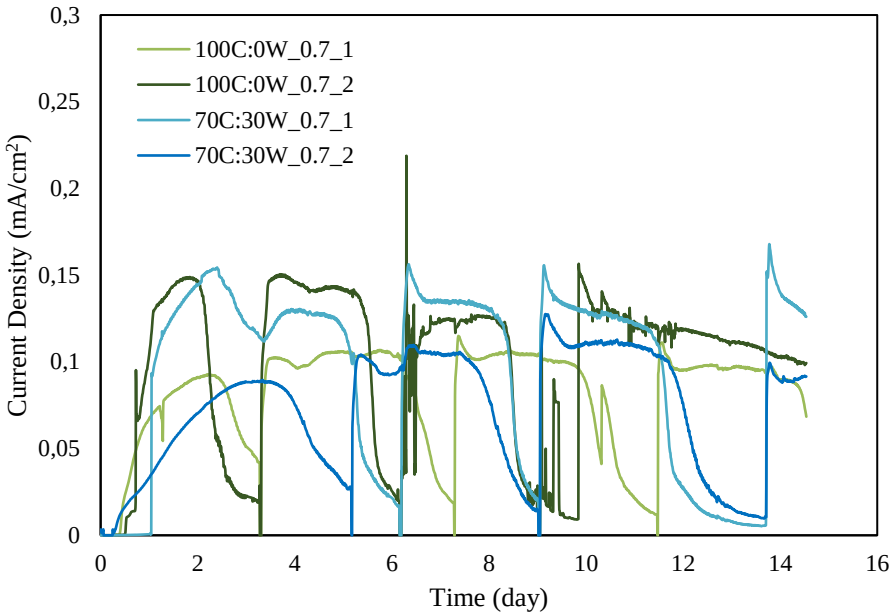

Figure C.1 Current density profiles of the selected reactors on reviving procedure

(Duplicate reactors are shown by the same color, and indicated as 1 and 2; acetate was used as feed)

E. Modified Gompertz Fittings of Cumulative Methane in Set1-Part 1

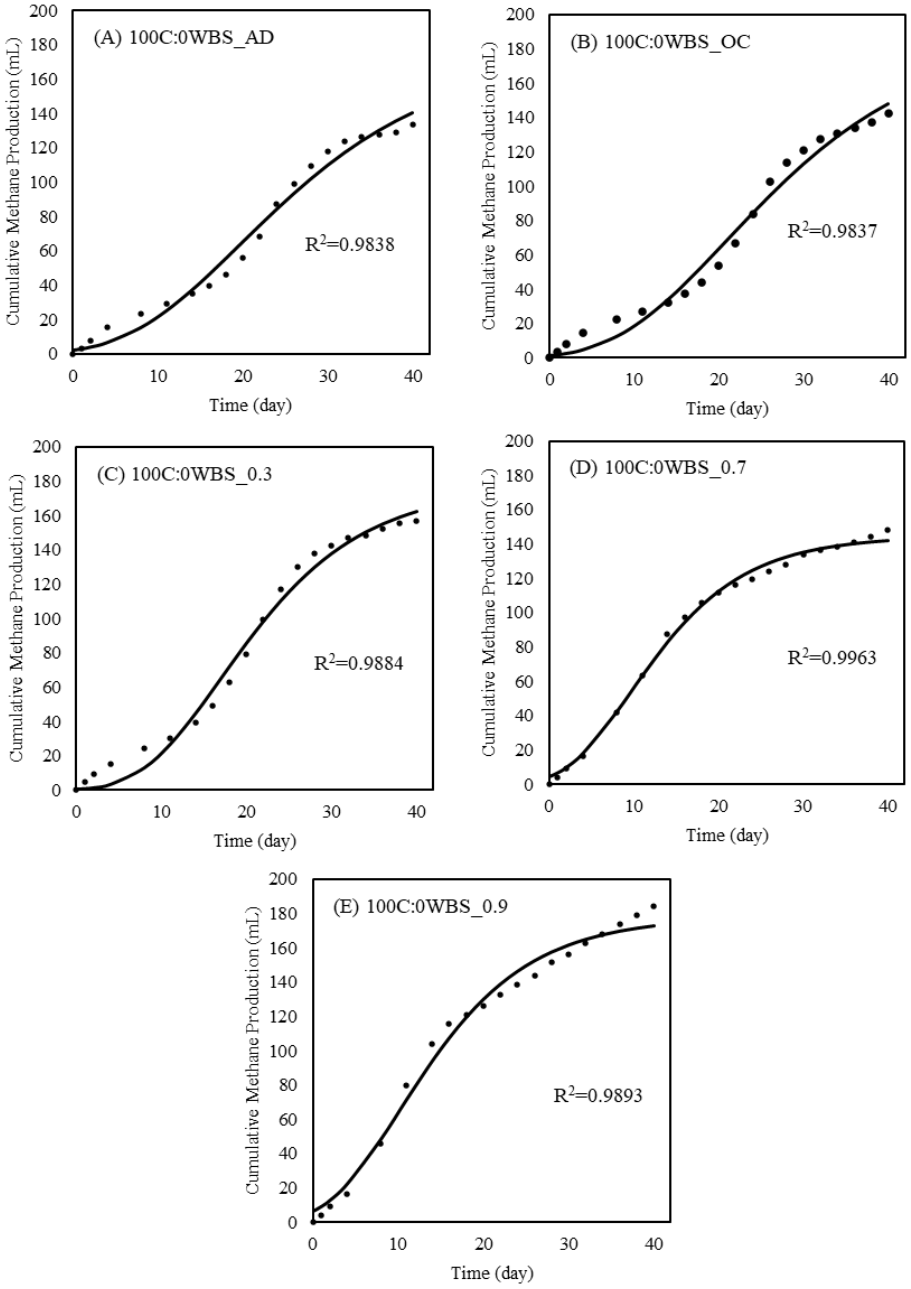

Figure D.1 Modified Gompertz fittings of 100C:0WBS reactors operated at Set 1-Part 1; (A) AD, (B) OC, (C) 0.3, (D) 0.7 and (E) 0.9 (Dots: Experimental Results, Solid Line: Gompertz Fittings)

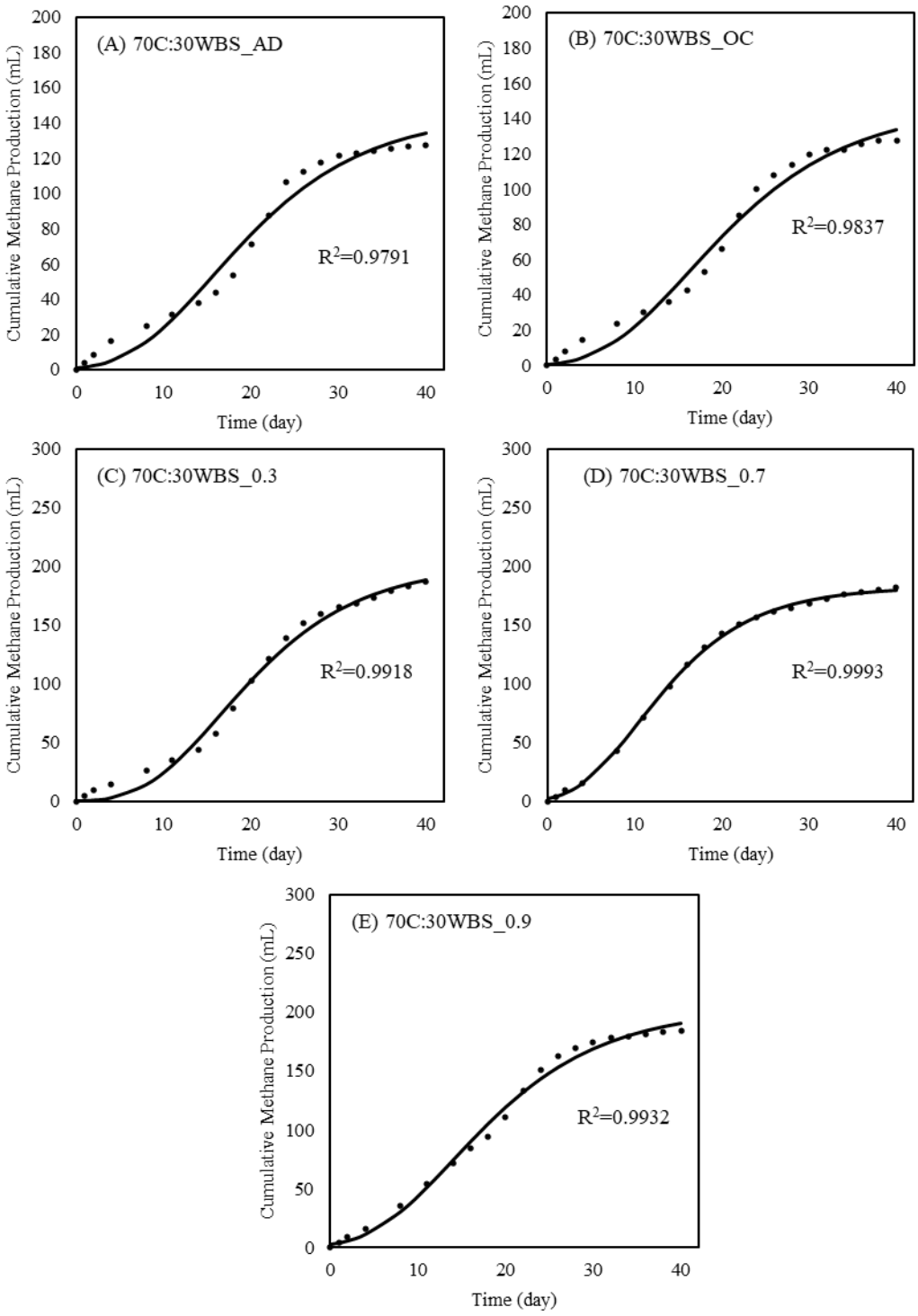

Figure D.2 Modified Gompertz fittings of 70C:30WBS reactors operated at Set 1-Part 1; (A) AD, (B) OC, (C) 0.3, (D) 0.7 and (E) 0.9 (Dots: Experimental Results, Solid Line: Gompertz Fittings)

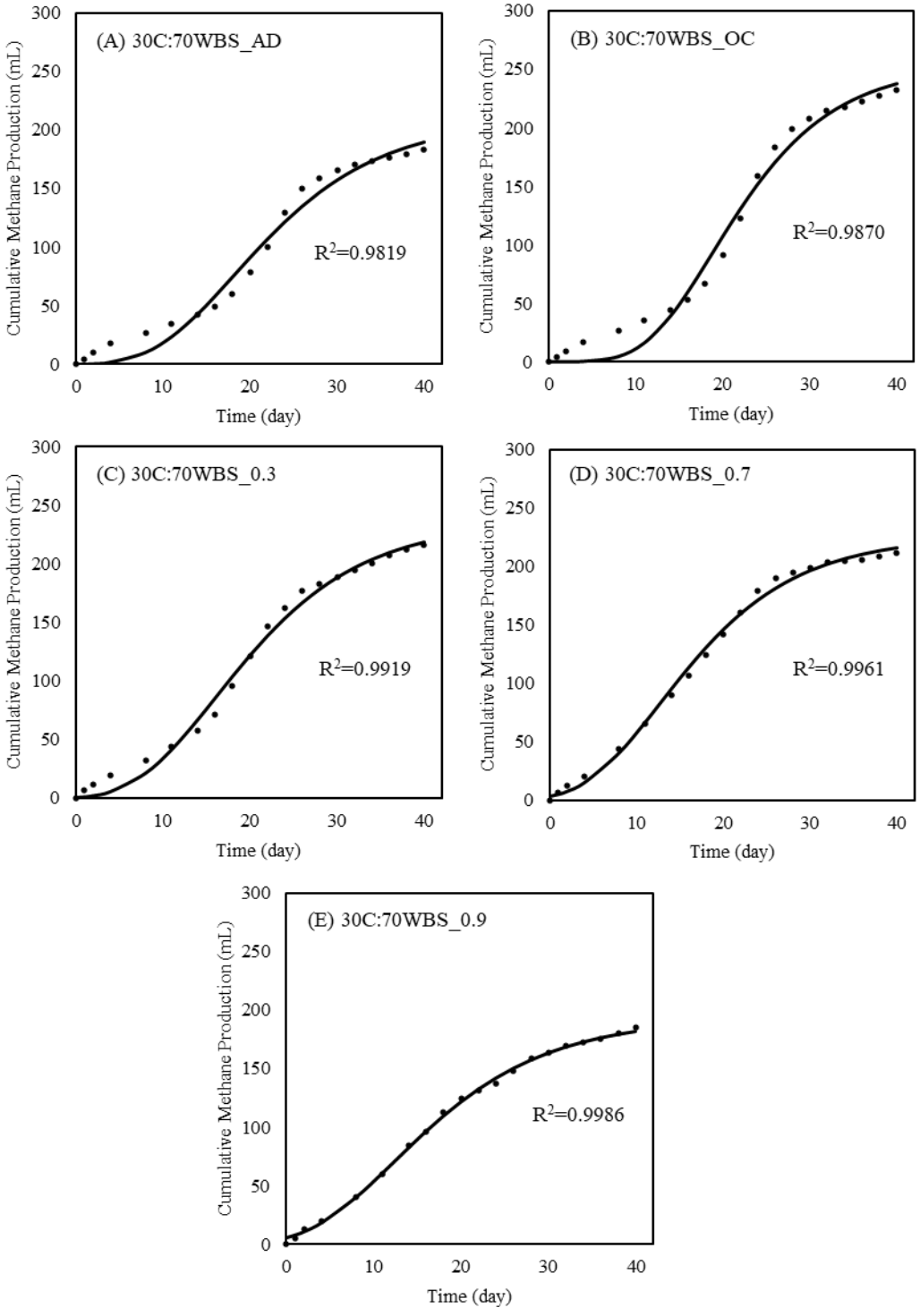

Figure D.3 Modified Gompertz fittings of 30C:70WBS reactors operated at Set 1-Part 1; (A) AD, (B) OC, (C) 0.3, (D) 0.7 and (E) 0.9 (Dots: Experimental Results, Solid Line: Gompertz Fittings)

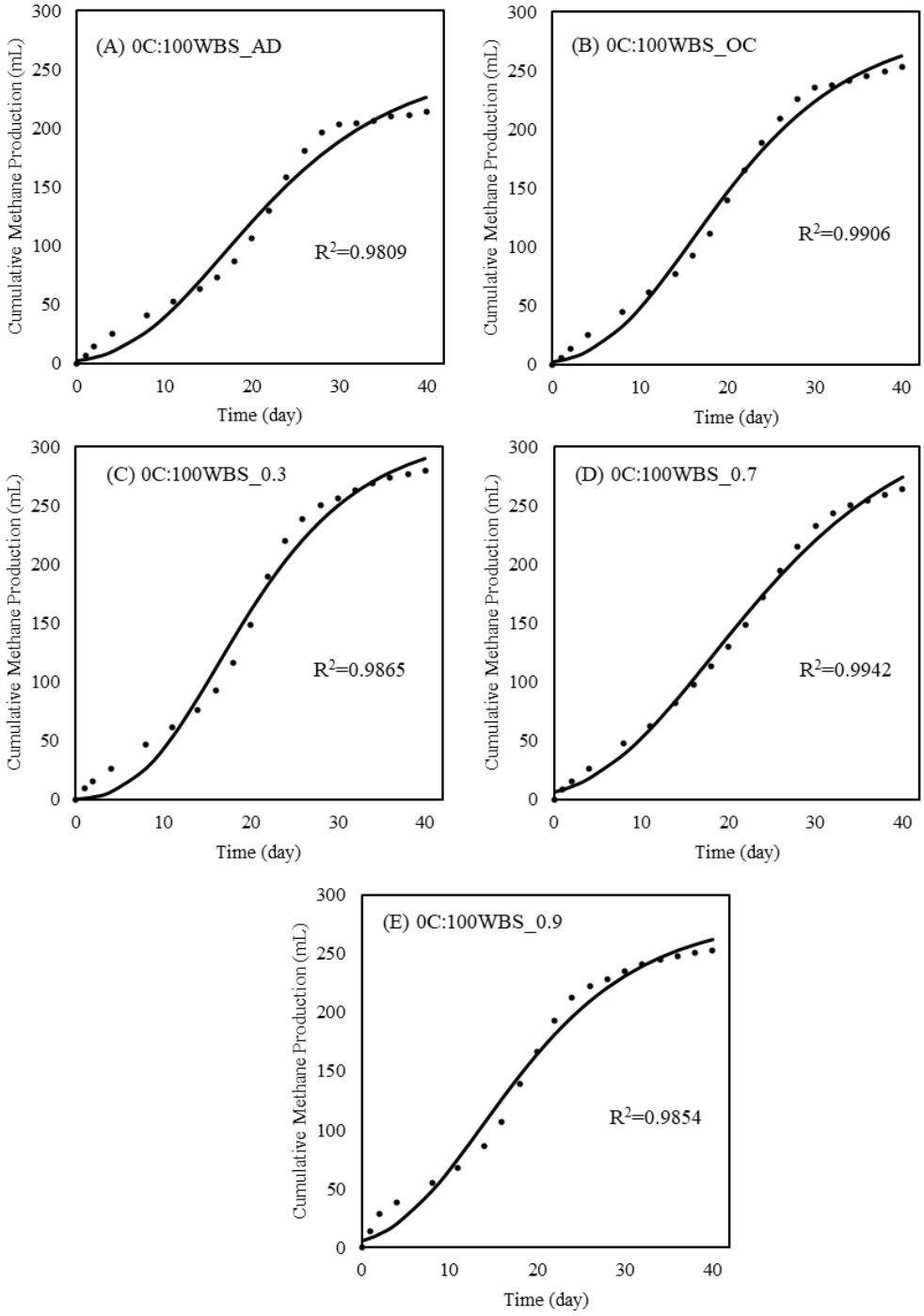

Figure D.4 Modified Gompertz fittings of 0C:100WBS reactors operated at Set 1-Part 1; (A) AD, (B) OC, (C) 0.3, (D) 0.7 and (E) 0.9 (Dots: Experimental Results, Solid Line: Gompertz Fittings)

F. Modified Gompertz Fittings of Cumulative Methane in Set1-Part 2

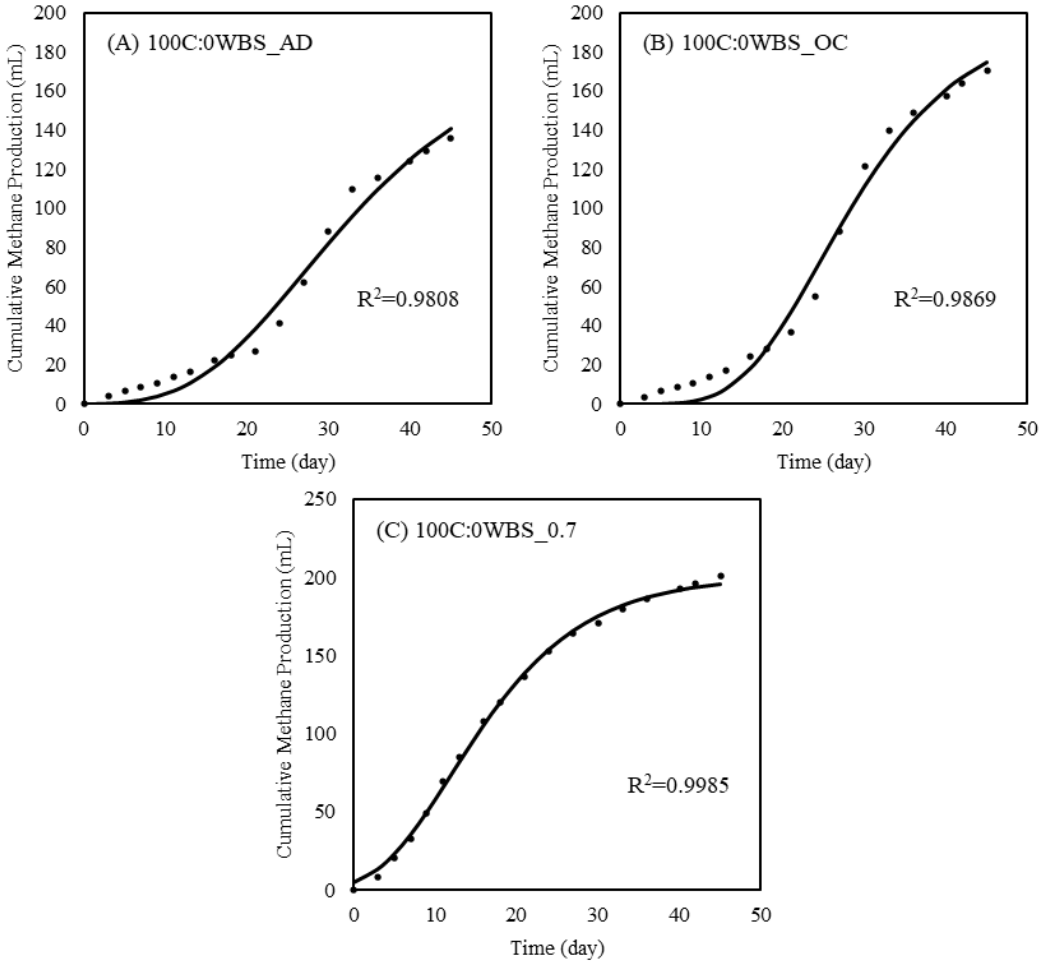

Figure E.1 Modified Gompertz fittings of 100C:0W reactors in Set 1-Part 2; (A) AD, (B) OC and (C) 0.7 (Dots: Experimental Results, Solid Line: Gompertz Fittings)

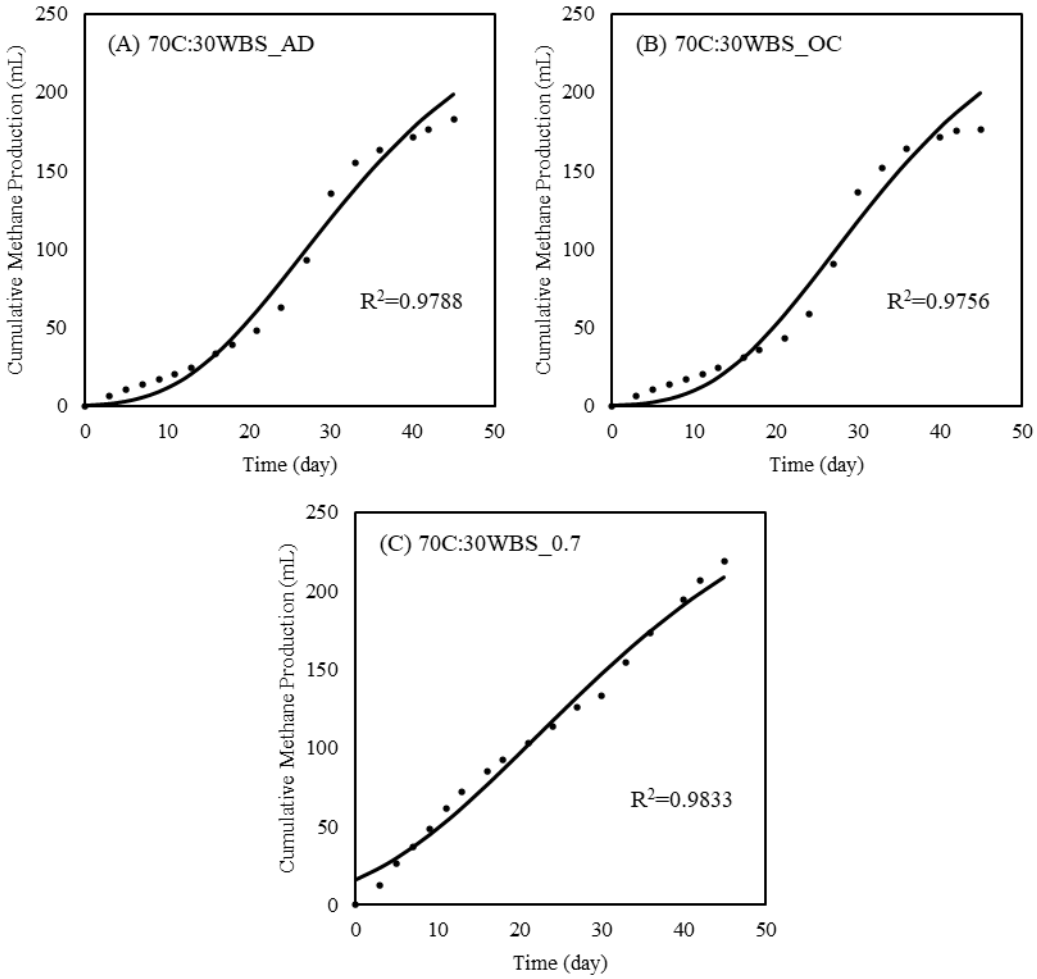

Figure E.2 Modified Gompertz fittings of 70C:30W reactors in Set 1-Part 2; (A) AD, (B) OC and (C) 0.7 (Dots: Experimental Results, Solid Line: Gompertz Fittings)

G. Modified Gompertz Fittings of Cumulative Methane in Set 2-Run 1

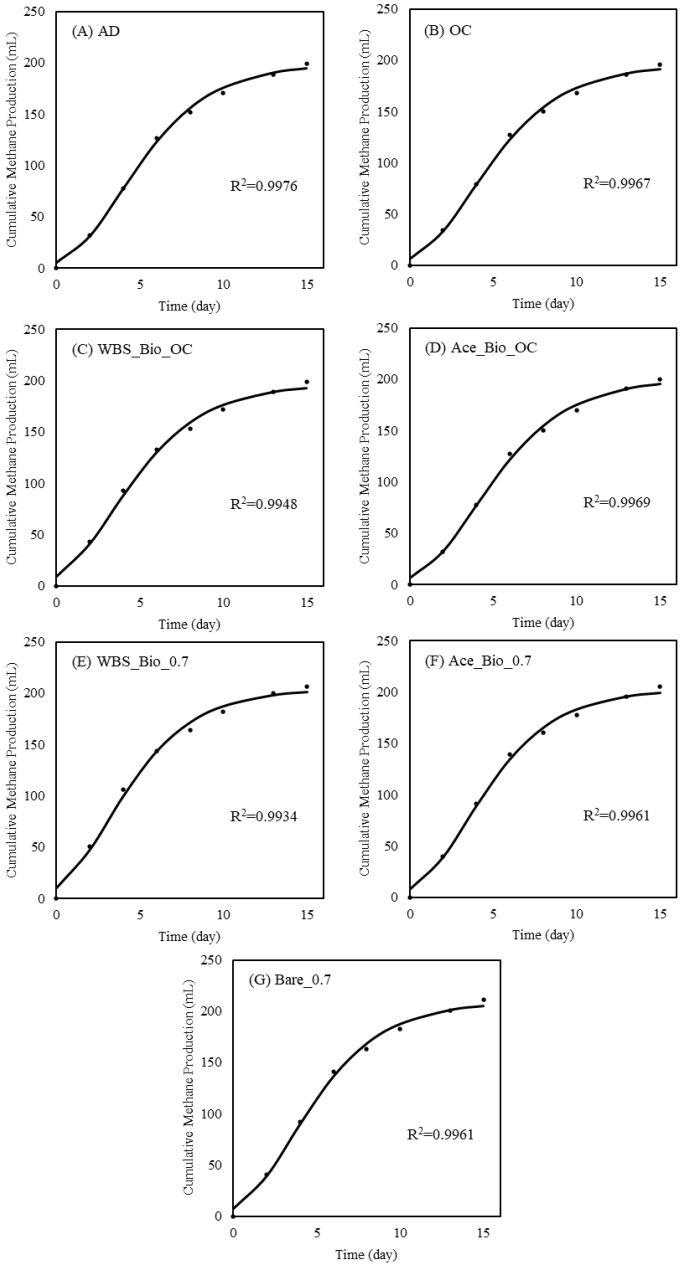

Figure F.1 Modified Gompertz fittings of reactors in Set 2- Run 1; (A) AD, (B) OC, (C) WBS_Bio_OC, (D) Ace_Bio_OC, (E) WBS_Bio_0.7, (F) Ace_Bio_0.7 and (G) Bare_0.7 (Dots: Experimental Results, Solid Line: Gompertz Fittings)

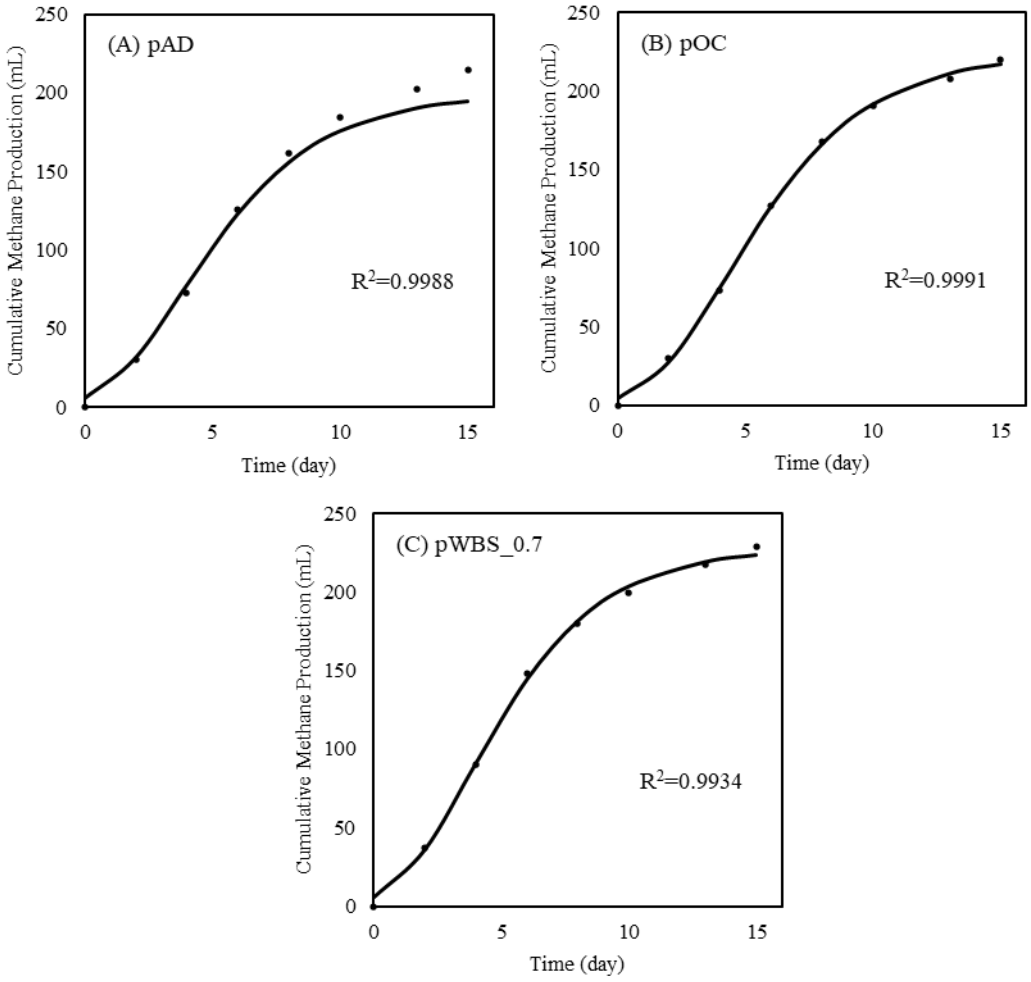

Figure F.2 Modified Gompertz fittings of reactors in Set 2- Run 1; (A) pAD, (B) pOC and (C) pWBS_0.7 (Dots: Experimental Results, Solid Line: Gompertz Fittings)

H. Modified Gompertz Fittings of Cumulative Methane in Set 2-Run 2

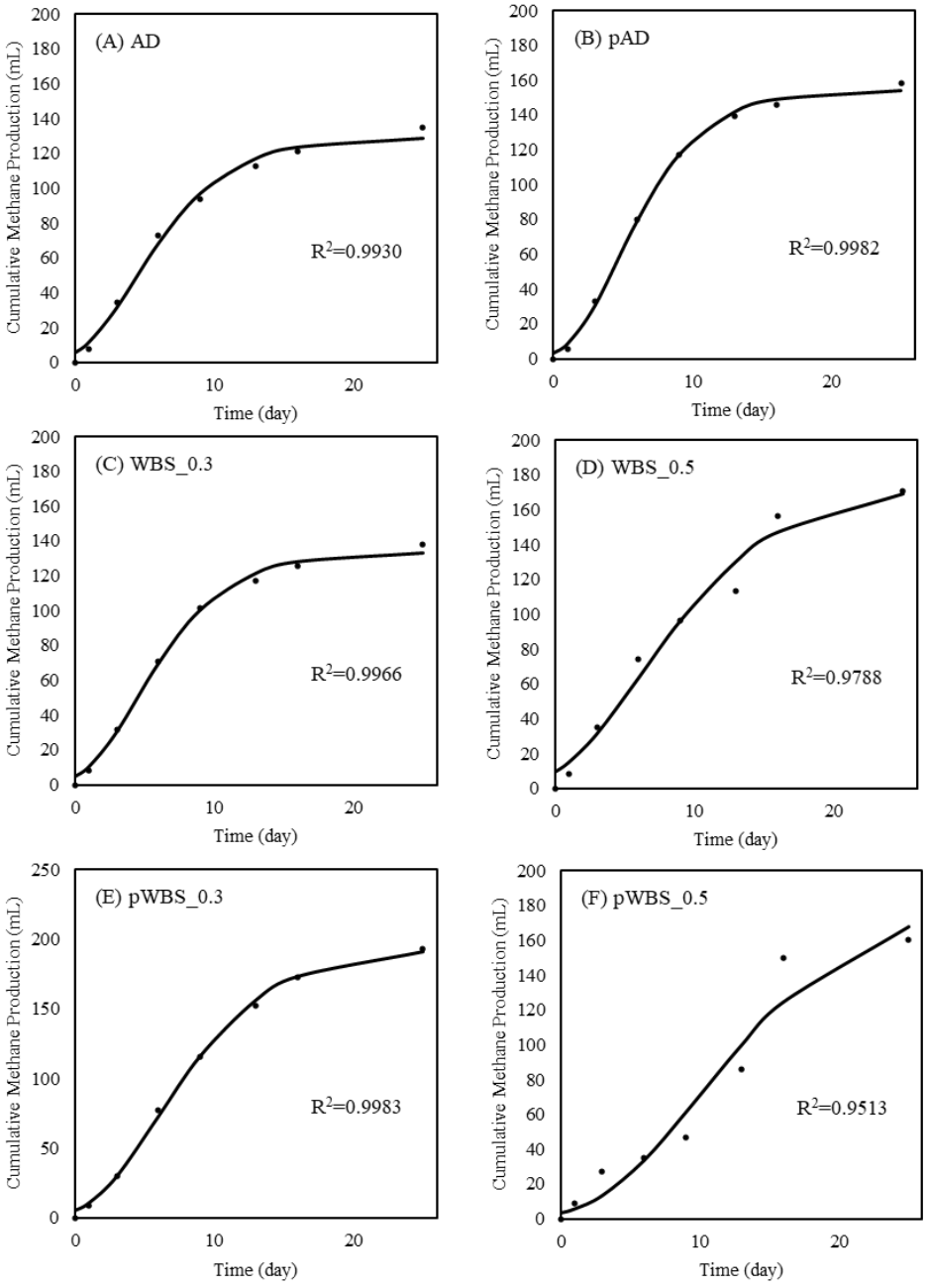

Figure G.1 Modified Gompertz fittings of reactors in Set 2- Run 1; (A) AD, (B) pAD, (C) WBS_0.3, (D) WBS_0.5, (E) pWBS_0.3 and (F) pWBS_0.5 (Dots: Experimental Results, Solid Line: Gompertz Fittings)